Investigation of the role of Paxillin in spindle orientation responses to mechanical stimuli in cultured cells and in the vertebrate embryo

Maria Zheltkova

University of Cyprus

Department of Biological Sciences

June 2020

Research Advisor: Dr. Paris A. Skourides,

Associate Professor

Laboratory of Cell and Developmental Biology

Contents

1. Abbreviations

SO = Spindle Orientation

ECM = Extracellular Matrix

LGN = Leucine-Glycine-Asparagine repeat protein

NuMa = Nuclear Mitotic apparatus protein

RFs = Retraction Fibers

FA = Focal Adhesion

FAK = Focal Adhesion Kinase

SH2/3 = Src Homology domain

Y = Tyrosine

ILK = Integrin-linked Kinase

AJ = Adherens Junction

FN = Fibronectin

DN = Dominant Negative

GFP = Green Fluorescent Protein

RFP = Red Fluorescent Protein

2. Abstract

Mitotic **s**pindle orientation plays an essential role in all multicellular organisms and is involved in diverse processes such as cell fate determination, tissue responses to mechanical stimuli and homeostasis. Given its involvement in such critical processes, the mechanisms responsible for establishing the correct SO, both *in vitro* and *in vivo* have been studied extensively. The determination of SO in space is mainly driven by internal, geometric, and external, mechanical and signaling cues. Previous work from our laboratory proposed that a cortical mechanosensory complex (CMC) forms at the lateral cortex of the mitotic cell, and controls SO responses to external mechanical cues. The CMC is established on force activated integrin β1 and includes well studied FA proteins such as FAK and Src. The full composition of the complex is currently under investigation however, previous work also suggested the involvement of the adaptor proteins p130Cas and Paxillin. Specifically, it was shown that cells lacking p130Cas or Paxillin, display defects in SO with respect to the substrate plane. Although the mechanism which determines SO with respect to the plane of adhesion has not been proven to be the same as the mechanism that determines responses to spatial adhesive cues within that plane, we have proposed that both rely on the CMC. We thus have investigated a possible role for p130Cas and Paxillin in SO responses stemming from the adhesion geometry. We initially used Paxillin and p130Cas null fibroblasts to address the involvement of these proteins in mitotic cell responses to spatial cues that lead to anisotropic force distribution on the cortex. Both Paxillin and p130Cas null fibroblasts display moderate defects, however they fail to fully round up during mitosis maintaining shape anisotropy throughout the process making them a poor choice for this type of study given the intrinsic shape sensing through astral microtubules present in all cells to ensure symmetric division. This asymmetry would invariably mask defects in the majority of cells. We thus went on, to develop a DN for Paxillin to further address its role in SO in HeLa cells which have been extensively used and characterized in this context. Specifically, we autonomously expressed a construct composed of the C-terminus LIM domains of Paxillin (Paxillin C-terminus). The LIM domains have been shown to be necessary and sufficient for FA targeting, while the lack of the LD motifs results in the disruption of the scaffolding functions of the protein. We show that Paxillin C-terminus partially displaces endogenous Paxillin from the FAs of HeLa cells leading to disruption of its scaffolding functions, such as recruitment of FAK and ILK at FAs. Dominant Negative effects however required high levels of expression and investigation using FRAP revealed that this is due to a lower affinity of the Paxillin C-terminus compared to the full length protein for FAs, while super resolution confocal imaging revealed a clear spatial segregation of Paxillin C-terminus and endogenous Paxillin within individual FAs. These data suggest that the ability of the

endogenous protein to interact with other FA proteins through its LD motifs at the N terminus creates stable clusters within FAs which the exogenous Paxillin C terminus fails to disrupt. Although this would suggest a limited DN activity at FAs, which are stable complexes with a long half-life, disruption of Paxillin function at the CMC a far more dynamic complex would be expected to be more robust. In agreement with this we show that the expression of Paxillin C-terminus in HeLa cells elicits defective responses to spatial adhesive cues and suggesting that Paxillin is a member of the CMC and is required for spindle responses to external mechanical stimuli. We go on to examine the role of Paxillin *in vivo* using *Xenopus* embryos focusing on the morphogenesis of the prospective neurectoderm. Expression of Paxillin C-terminus in the animal cap results in severe gastrulation defects, including delayed blastopore closure stemming from defective epiboly and the mechanical linkage of the animal cap to the involuting mesoderm. We show that the defects in epiboly stem from spindle misorientation of the deep cell layer, and that this is secondary to defects Fibronectin fibril formation. Collectively, our results implicate Paxillin in spindle orientation responses to mechanical stimuli suggesting that it's a core member of the CMC while at the same time provide evidence that Paxillin is necessary for FN fibrillogenesis during embryonic development.

3. Introduction

3.1 Mitosis

Mitosis is a process by which a cell segregates its duplicated DNA and divides into two daughter cells, by the formation of the mitotic spindle (Mclntosh, 2016).

3.1.1 Mitotic Spindle

The mitotic spindle is a bipolar, microtubule-based structure that mediates the segregation of parental chromosomes into daughter cells and thereby ensures genomic stability (Walczak and Heald, 2008). This event is conserved in all eukaryotes. Anomalies in chromosome segregation lead to aneuploidy, which results in genomic instability, as well as in cancer (Levine and Holland, 2018).

The presence of several microtubule-based motor proteins and localized regulation of microtubule dynamics are implicated in the assembly and function of the spindle. Once chromosomes are aligned perpendicular to the spindle pole axis, equidistantly from both poles, the movement and separation of sister chromatids to opposite spindle poles occurs, which leads to the formation of two daughter cells that contain exact complements of the parental genetic material (Wittmann et al,2001; Cooper and Hausman, 2007; Dumont and Mitchison, 2009b; Mogilner and Craig, 2010; Cheeseman and Desai, 2008; Alberts et al., 2015).

The mitotic spindle is mainly composed of microtubules which are long polar polymers that contain molecules of tubulin. Each molecule of tubulin is a heterodimer that forms from two 55 kD globular polypeptides, known as a-tubulin and b-tubulin. Microtubules have a cylindrical structure in which 13 linear protofilaments of alternating a- and b-tubulin subunits are packed around a central core. Due to parallel alignment of these protofilaments, microtubules are polar structures in which a plus and a minus-end can easily be distinguished (Wittmann et al,2001; Cheeseman and Desai, 2008; Alberts et al.,2015).

The organization and nucleation center of microtubules is the centrosome. Centrosomes contain a pair of cylindrical structures, known as centrioles, which are surrounded by the Pericentriorial material (PCM). The PCM contains a minor form of tubulin, γ tubulin, and can mediate microtubule nucleation. During interphase, duplication and segregation of the centrosomes occur resulting in two equal daughter centrosomes. Once mitosis begins, these daughter centrosomes move to opposite sides of the nucleus forming the two poles of the spindle (Alberts et al., 2015).

Due to their dynamic instability and polarity, microtubules can mediate the spindle formation. Specifically, each microtubule can alternate between growth and shrinkage phases, due to rapid

GTP hydrolysis. This rapid turnover of microtubules, known as dynamic instability, plays a crucial role in the remodeling of the cytoskeleton. Specifically, the mitotic spindle will organize the chromosomes at the equator of the cell and through its dynamic remodeling it will pull apart the chromatids in order to guide them to the poles and resulting in their split into the two daughter cells. The dynamic instability of microtubules can be modified by the Microtubule Associated Proteins (MAPs), which can interact with them. In agreement with this, drugs including Colchicine and Taxol, that affect microtubule assembly are used in the treatment of cancer (Cooper and Hausman, 2007). Additionally, the polarity of microtubules can act as a track for the several proteins of Dynein and Kinesin superfamilies, which recognize microtubules and move along them. Interestingly, three subpopulations of microtubules are found in the mitotic spindle, the kinetochore microtubules, the interpolar microtubules and the astral microtubules. The kinetochore microtubules bind to chromosomes and the centrosomes and interact with several proteins forming the kinetochore, a complex of proteins that serves as a site for the binding of microtubules to chromosomes. The interpolar microtubules stabilize the bipolarity of the spindle. Finally, the astral microtubules, are extending away from centrosomes into the cytoplasm towards the cell cortex with free minus ends and are implicated in the orientation and positioning of the spindle within the cell, through their capturing on the cell cortex. The role of astral microtubules in the orientation of the spindle is essential, since the use of Nocodazole, a drug which promotes microtubule depolymerization and at low doses the disruption only of astral microtubules, results in spindle misorientation (**Figure 1.1**, Toyoshima and Nishida, 2007; Jeon, 2000; Cooper and Hausman, 2007; Desai and Mitchison, 1997; Mitchison and Kirschner, 1984; Wittmann et al,2001; Cheeseman and Desai, 2008; Alberts et al.,2015).

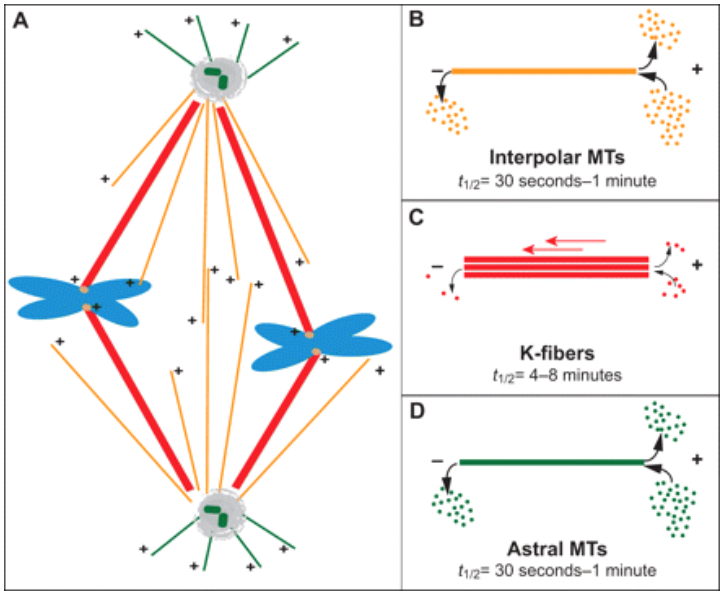

Figure 1.1: Schematic presentation of the three microtubules in the mitotic spindle. The kinetochore microtubules that bind chromosomes, the interpolar microtubules that organize mitotic spindle and the astral microtubules that stabilize the spindle to the plasma membrane are shown in the scheme (Meunier and Vernos, 2012).

3.1.2 Stages of Mitosis

During interphase, chromosomes are not visible, and chromatin appears like a diffused amorphous network. Once the cell enters mitosis, the DNA condenses, resulting in visible chromosomes (Hagstrom and Meyer, 2003).

Mitosis consists of five well-characterized stages: prophase, prometaphase, metaphase, anaphase and telophase, followed by the division of the cytoplasm, known as cytokinesis. Each of them is distinguished by the physical state of the chromosomes and the spindle.

During prophase, the condensation of chromosomes and the movement of the centrosomes into opposite sides of the nucleus occur. This movement initiates spindle formation during late prophase, in which the centrosomes form the two poles of the mitotic spindle. When the nuclear envelope breaks down, allowing the microtubules to bind chromosomes, via kinetochores, a cell has reached the prometaphase. Then during metaphase, chromosomes shuffle back and forth until they align in the center of the spindle, known as the metaphase plate. At anaphase, the sister chromatids split apart and move to opposite poles of the spindle, pulled by the kinetochore microtubules. Also, at this stage, the distance between the two poles increase due to spindle elongation by the interpolar microtubules. Mitosis ends with telophase, in which arrived chromosomes at the poles are released from kinetochore microtubules and decondensed. Additionally, nuclear envelopes are re-forming. Finally, during cytokinesis, the two identical daughter cells are generated by the contraction of the contractile ring, a dynamic structure composed of actin and several structural and regulatory proteins (Alberts et al, 2015; Cooper and Hausman, 2007; Hagstrom and Meyer, 2003; Cheeseman and Desai, 2008; Mitchison and Salmo, 2001).

3.1.3 Spindle Orientation

As mentioned before, the mitotic spindle is implicated in the segregation of the genetic material into the two daughter cells (Walczak and Heald, 2008). Additionally, proper spindle orientation with respect to the geometry adhesion and with respect to the plane of adhesion (**Figure 1.2**) in both embryonic and adult tissues has a crucial role in several processes, such as cell fate in both asymmetric and symmetric divisions, tissue and organ morphogenesis as well as homeostasis. Specifically, in symmetrical dividing cells, like epithelial cells, the spindle should be oriented

in the plane of the tissue, so that both daughter cells abide within the epithelium, thus maintaining the epithelium integrity. During asymmetric divisions, the spindle must align with respect to the polarity axis, ensuring the segregation of cell fate determinants into only one daughter cell, so that it aquires a different fate from the other daughter cell (Bergstarlh et al, 2017; Lu and Johnston; 2013; Williams and Fuchs, 2013). Also, spindle orientation has a crucial role in maintaining tissue structure and generating tissue shape due to control over the positioning of the daughter cells that occurs after the division.

During embryonic development, the orientation of the spindle is essential in embryogenesis, organogenesis, and cell differentiation. Importantly, defects in spindle orientation can contribute to several pathologies, including cancer and microcephaly in adult tissues, as well as failed morphogenesis and organogenesis in embryos (Fish et al, 2006; Quyn et al, 2010; Pease and Tirnauer; 2011; Baena-Lopez et al, 2005; Quesada-Hernández et al, 2010; Lu and Johnston; 2013; Gonzalez, 2007; Knoblich, 2010).

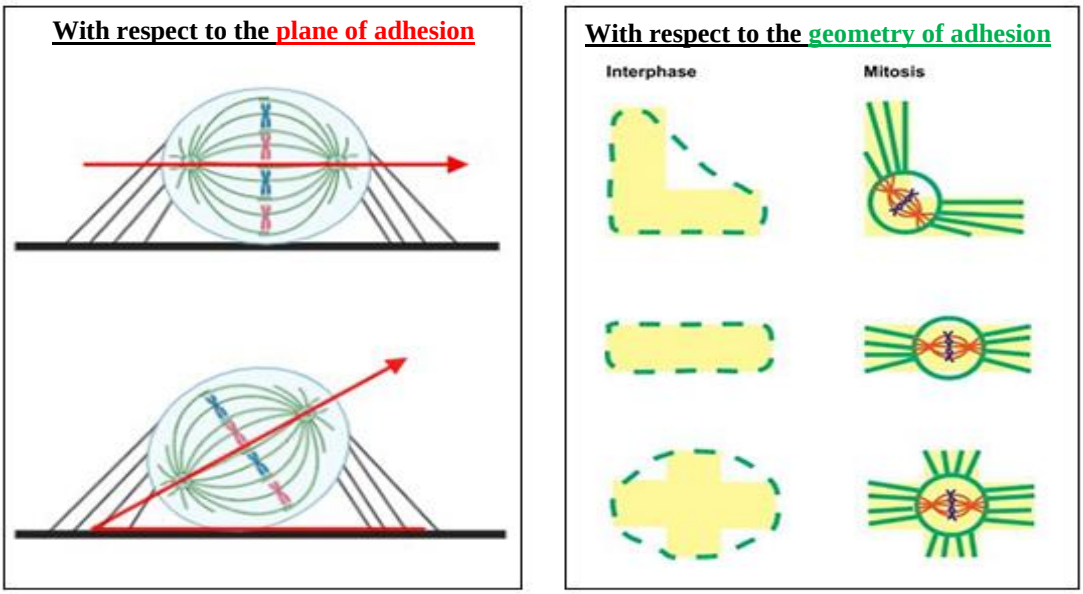

Figure 1.2: Schematic representation of mitotic spindle orientation both with respect to the plane of adhesion (Z axis) and geometry adhesion (XY axis). Cells must orient their spindle with respect to the plane of adhesion so they can remain within the epithelium and attach to their substrate. Concurrently, cells need to orient their spindle with respect to geometry adhesion so both daughter cells have space to spread in and fill the space of the initial mother cell (Left scheme made by online program Biorender, Right scheme adapted from: Nestor-Bergamnn et al., 2014)

3.1.4 Regulation of Spindle Orientation

The mitotic spindle orientation can be regulated by either internal cues due to cell polarity, geometric cues, or external cues, including cell-cell adhesion and cell-ECM adhesion (Hertwig and Hertwig, 1884; Kotak et al., 1991; Mink et al., 2011; Pietro et al., 2016; Nestor-Bergmann et al., 2014).

3.1.4.1 Internal cues

Several studies have shown that specific regulators of cell polarity are implicated in SO. Specifically, the adaptor protein LGN (Leucine-Glycine-Asparagine repeat protein) and the Gai subunits of heterotrimeric G proteins are shown to be involved in SO, by using Drosophila embryonic neuroblasts. Additionally, they can interact with the adaptor NuMa (Nuclear Mitotic apparatus protein) resulting in the recruitment of the motor protein Dynein to the cell cortex. Indeed, in most animal cell types the conserved complex Gai/LGN/NuMa was implicated in the spindle positioning and orientation by capturing the astral microtubules at the cortex and recruiting there the motor protein Dynein (Shaefer et al., 2000; Yu et al., 2000).

Gai/LGN/NuMa Complex

The Gai/LGN/NuMa complex is an evolutionarily conserved complex composed of the G protein Gai, LGN, and NuMa in mammalian cells and Gai, Pins, and Mud in Drosophila. This complex has fundamental functions in spindle movements and dynamics of SO in different tissues (Morin et al, 2007; Peyre et al, 2011; Lechler and Fuchs, 2005; Schaefer et al, 2000; Yu et al, 2000). During mitosis, this complex is found at the cortex of cells in a polarized fashion, localized at the spindle capture sites where it captures the spindle through the recruitment of the minus-end microtubule interacting motor protein Dynein. Once Dynein is recruited, it moves along the astral microtubules generating pulling forces on the spindle poles and thus controlling the orientation, centering and positioning of the spindle. In agreement with this, the localization of the complex acts as a determinant as to where the site of highest force concentration is and thus the axis the spindle must orient along (Kotak et al, 2012).

Interactions of the members of Gai/LGN/NuMa Complex

Once Gai protein binds to the plasma membrane through myristylation, the α subunit of Gai, when its GDP bound, interacts with the GoLoco motifs of LGN (Leucine-Glycine-Asparagine repeat protein). This interaction leads to a conformational change of LGN, which enables the N-terminal tetracopeptide repeats (TPR) to interact with the C-terminus of NuMA. Up next NuMa binds to the motor protein Dynein, which captures the astral microtubules and generates pulling forces by moving towards their minus end (**Figure 1.3** , Willard et al, 2004; Kotak et al,2012; Bowman et al, 2006; Zheng et al, 2010; Zheng et al, 2013; Peyre et al, 2011). The proper localization of the Gai/LGN/NuMa complex is controlled by distinct spindle-pole and chromosome-derived signals. Specifically, during metaphase LGN and NuMa appear as two cortical crescents overlying each spindle pole, that result from a chromosome derived RanGTP gradient that delays the complex formation in the vicinity of chromosomes and thus maintaining the axis of the spindle (Kiyomitsu and Cheeseman, 2012; Bergstralh et al, 2013). Additionally, the spindle pole localized kinase Plk1 negatively mediates dynein localization by controlling the interaction of dynein-dynactin, NuMa, and LGN. When the spindle is not centered, then the Dynein/Dynactin complex accumulates to the side of the cell where the spindle is closer to the cortex and then generates pulling forces, followed by spindle repositioning (Tame et al, 2014; Kiyomitsu and Cheeseman, 2012). Furthermore, additional polarity proteins, including Afadin and Dlg, mediate the localization of LGN and NuMa at the lateral and apical cortex, respectively. In addition, the polarity protein aPKC, inhibits the localization of the LGN at the apical cortex in MDCK cells (Carminati et al,2016; Johnston et al, 2009; Zheng et al., 2010).

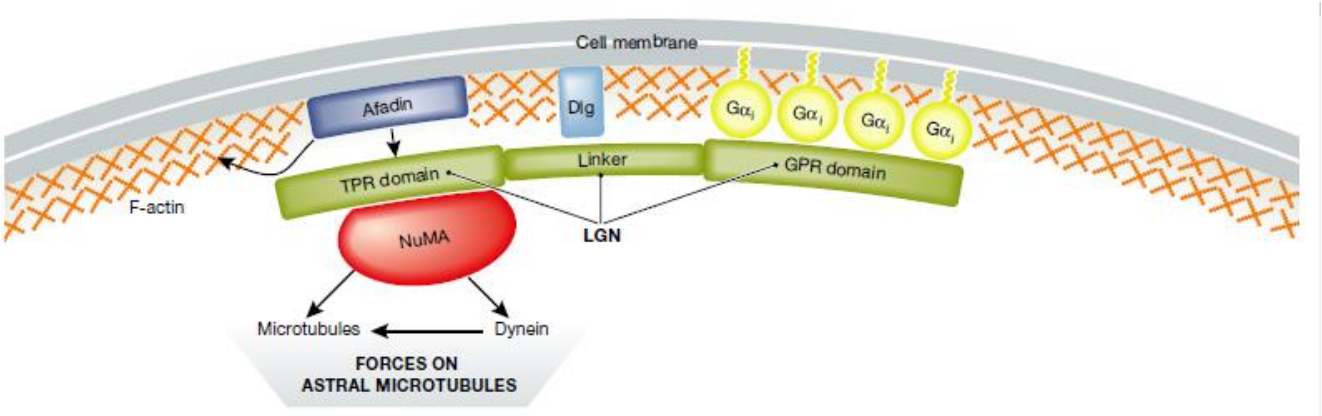

Figure 1.3: Schematic representation of the interactions between Gai, LGN, NuMa, and Dynein (Pietro et al, 2016)

3.1.4.2 Geometric cues

In 1884, Oscar Hertwig, by using *Xenopus* embryos, was first to propose that cells place their spindle at the center of their protoplasmic mass and parallel to their longest axis (Hertwig and Hertwig, 1884). Thus, it was suggested that cells orient their spindle parallel to the long axis of interphase. Subsequently, when single-celled sea urchin zygotes were pushed into chambers of various shapes, causing them to adapt their geometry, their subsequent divisions were parallel to their long axis. However, some of them did not divide along the longest axis, but along the longest axis of symmetry, proposing that the geometry of the cell can be read by the length of the astral microtubules, where the longer microtubules represent the greater force along where the spindle will have to orient (Mink et al, 2011). Thus, the mitotic spindle can be placed at the geometric center of the cell by the shape-sensing mechanisms that involve pulling or pushing forces due to the length of astral microtubules (O'Connell and Wang, 2000; Grill and Hyman, 2005; Mink et al., 2011). Interestingly, since force can change cell geometry and thus the orientation of spindle can be regulated by this change, it was shown that cells can also orient their spindle with a shape-independent force sensing mechanism, by using elliptical micropatterning and applied unidirectional stretch, and hence separate shape and force (Fink et al., 2011). In addition, after applying unidirectional stretch on the epithelium, cells always oriented their spindle along the axis of stretch, independently of their shape (Hart et al., 2017).

3.1.4.3 External cues

Several studies have proposed that adhesion-related forces can regulate SO in single cells. Indeed, when cells were seeded on micropatterns with a specific shape to promote the adaptation of the shape, their spindles were oriented along the long axis of the pattern, while when unidirectional stretch was applied to cells without promoting the cells to acquire a long axis, their spindles were oriented along the applied stretch (Thery et al., 2005; Fink et al., 2011). Thus suggesting, that the adhesive contacts of the cell with its external environment are implicated in SO due to mechanical forces that the external environment exerts on the cell (Vogel and Sheetz, 2006). Importantly, when a cell rounds up during mitosis, Retraction Fibers, which are actin filament-based tubes, anchor the cell to the extracellular matrix, reflecting the adhesive pattern of the cell to its substrate during interphase. Therefore, RFs may be implicated in the orientation of the mitotic spindle by exerting pulling forces onto the cell cortex (Thery et al., 2005; Thery et al., 2007; Fink et al., 2011). Specifically, by using adhesive micro-patterns and laser ablation to cut the longer RFs, cells were shown to re-orient their spindles along the second major force vector and the remaining longer RFs. This was confirmed by measuring forces associated with RFs using beads and optical tweezers. In agreement with this, subcortical

actin filaments were observed at the sites of RFs, suggesting that they may act as a link between force sensing and SO by biasing the region of the cortex where microtubules will attach. Once localized at the RFs, the actin filaments recruit microtubule motors that will pull astral microtubules and eventually will orient mitotic spindle (Thery et al., 2005; Fink et al., 2011; Kwon et al., 2015).

Recent studies in Zebrafish and Drosophila melanogaster implicated force in the regulation of mitotic spindle in epithelial tissues. Specifically, the orientation of spindle in zebrafish embryos was shown to be regulated by the pattern of tension across the tissue, while in Drosophila, cells of the epithelium of the wing imaginal disc orient their spindles due to a global pattern of mechanical forces (Campinho et al., 2013; Mao et al., 2013; Mao et al., 2011; LeGoff et al., 2013).

Interestingly, several studies identified an integrin-dependent mechanism for regulation of SO (Thery et al., 2005; Toyoshima and Nishida, 2007). In β1-integrin knockout mice, basal epidermal cells display random spindle orientation and defects in polar localization of LGN, NuMa, and aPKC (Lechler and Fuchs, 2005). In Drosophila follicular cells, it was shown that the interaction of integrin with the ECM activates integrin signaling cascade resulting in the regulation of spindle orientation (Fernandez-Minan et al., 2007). Additionally, a ligand-independent and force-dependent activation of integrin β1 occurs at the lateral cortex of mitotic cells where the spindle captures sites are, which corresponds to where the longest RFs terminate, resulting in the recruitment of FA proteins such as FAK, Src and p130Cas and the formation of the Cortical Mechanosensory Cortex (CMC) (**Figure 1.4**). The CMC then can regulate spindle orientation in response to external forces. Indeed, when blocking the activation of β1 integrin and disrupting its polar localization at the cell lateral cortex, spindle misorientation occurs, even when adhesion of cells is β1 independent (Petridou and Skourides, 2016; Anastasiou et al., 2020).

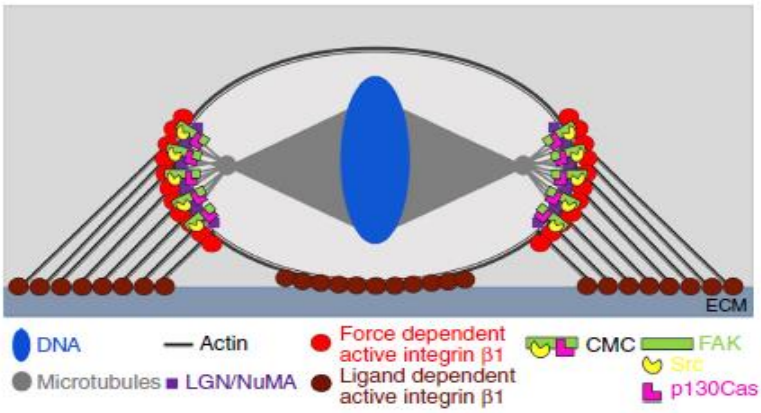

Figure 1.4: Schematic representation of β1 lateral activation and formation of CMC (Petridou and Skourides, 2016)

3.2 Focal Adhesions

Focal Adhesions are multiprotein complexes where transmembrane integrin receptors link the actin cytoskeleton with the extracellular matrix (ECM), mediating interactions of the cell with its extracellular environment. (Shemesh et al, 2005; Berrier and Yamada, 2007). These highly dynamic flat linear structures are formed at the cell periphery after the interaction of integrins with extracellular matrix ligands. This interaction leads to integrin clustering and activation, which is followed by the hierarchical recruitment of several structural and signal transduction proteins, such as Talin, Vinculin, Paxillin and Zyxin (**Figure 1.5**, Miyamoto et al., 1995; Abercrombie and Dunn, 1975).

Before maturation, many proteins are recruited to smaller adhesion sites, which are known as focal complexes and are controlled by Rac (Rac Family Small GTPase 2) and Cdc42 (Cell division cycle 42 protein) (Hotchin and Hall, 1995; Petit and Thiery, 2000). Maturation of focal complexes into more stable and large structures, known as Focal Adhesions, is promoted by Rho activity, followed by the recruitment of more proteins to FAs (Hotchin and Hall, 1995; Ridley and Hall, 1992). The dynamics and turnover of FAs are controlled by tyrosine kinases targeted at the sites, two of the major ones being FAK and Src. Accumulation of other proteins, with an SH2 domain, is promoted by tyrosine phosphorylation within FAs (Mayer et al, 1995). The stabilization of these complexes is controlled by the recruitment of Tensin and Zyxin.

Focal Adhesions are essential for cell migration. The process in which new FAs are forming at the anterior and old FAs are dissociating at the rear of the cell has high significance in cell movement (Webb et al., 2002). FAs can behave differently in response to force because of their mechanosensitive properties, and hence they can control cell migration. Exertion of force at the FAs promotes their elongation, while upon reduction of force they dissociate (Shemesh et al., 2005).

Interaction of cells with the extracellular matrix is essential for many biological processes including tissue formation, cell survival and embryogenesis (Petit and Thiery, 2000; Zaidel-Bar et al. 2004). Disruption of the FAs complex has been shown to associate with several human diseases, such as malignant diseases and Kindler syndrome (Wu, 2007).

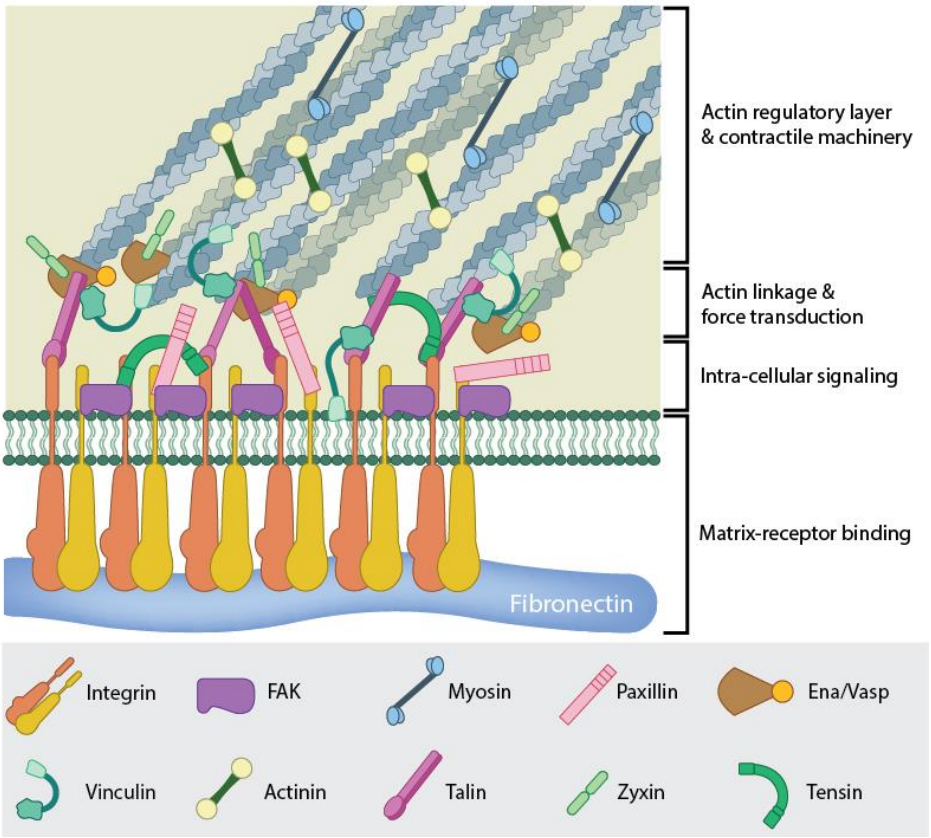

Figure 1.5: Focal Adhesion Complex. Focal Adhesions are multi-protein structures that exploit transmembrane integrin receptors to link the extracellular matrix with the actin cytoskeleton. Integrin activation promotes focal adhesion formation and recruitment of several proteins to these sites, such as Vinculin, Paxillin and FAK (Adapted from: <https://www.mechanobio.info/what-is-mechanosignaling/what-is-the-extracellular-matrix-and-the-basal-lamina/what-are-focal-adhesions/what-are-mature-focal-adhesions-composed-of/> [Accessed 1 June 2020]).

3.3 Integrins

Integrins are heterodimer transmembrane glycoprotein receptors involved in cell adhesion to the extracellular matrix. They consist of two subunits, α and β, which are linked non-covalently. The major β subunit is integrin β1, since it can form heterodimers with almost all α subunits (Hynes, 2002; Petit and Thiery, 2000).

Integrins contain three domains, a large extracellular domain which binds extracellular ligands, a single transmembrane domain which promotes the conformation responsible for ECM binding by stabilizing the dimer, and the small cytoplasmic domain which is linked to several structural and signaling intracellular proteins as well as the actin cytoskeleton (Hynes, 2002; Humphries and Newham, 1998; Hynes, 1992; Zaidel-Bar et al., 2007a; Springer and Wang, 2004; Arnaout et al., 2005). Many extracellular matrix proteins, including fibronectin and collagen, are ligands for integrins. For example, α5β1 is the major fibronectin receptor, while α1β1 is a collagen receptor (Hynes, 2002).

Upon activation and clustering of integrins at the cell surface FAs are formed, with several proteins getting recruited to these sites, such as Vinculin, Talin, Paxillin and FAK. At FAs, integrins provide as adhesion links between the extracellular environment and the actin cytoskeleton (Geiger et al, 2001; Berrier and Yamada, 2007). Also, integrins are involved in the control of intracellular signaling pathways that control cell migration, cell proliferation, cell survival and orientation of the mitotic spindle (Hynes, 2002; Schwartz et al., 1995; Petridou and Skourides, 2016). The following section describes the core focal adhesion proteins in more detail.

3.4 Paxillin

Paxillin is a 68kD multi-domain protein, a member of the FA complex. It acts as an adaptor or scaffold protein, because of its multiple docking sites for other proteins and its lack of enzymatic activity (Schaller, 2001). Paxillin is a member of a protein family that is comprised of three other additional members: Leupaxin, PaxB, and Hic-5 (Schaller, 2001).

3.4.1 Structural characteristics of Paxillin and its interaction with binding partners

Paxillin contains several different motifs, including the LD motifs, the LIM domains and the SH3- and SH2- binding sites, which mediate interactions with its binding partners. Specifically, within the N-terminus there are five LD motifs, that interact with several proteins in response to cell signaling, and proline-rich SH-3 binding domains (Brown et al., 1998a, Tumbarello et al., 2002; **Figure 1.6**). The LD motifs are comprised of binding sites for Vinculin, FAK and other FA proteins. Specifically, FAK interacts with the LD2 and LD4 motifs, Vinculin interacts

with the LD1, LD2 and LD4 motifs, while ILK interacts with the LD1 motif of Paxillin. Proteins that interact with the LD motifs contain the Paxillin Binding Subdomain (PBS), a domain that is present both within the tail of Vinculin and the FAT domain of FAK (Brown and Turner, 2004; Nikolopoulos et al, 2000). In addition, Paxillin has four LIM domains at the C-terminus, that mediate its targeting to FAs. Specifically, it has been shown that LIM3 and LIM4 bind to Kindlin-2 that eventually targets Paxillin to nanscent and mature FAs (López-Colomé et al., 2017., Theodosiou et al., 2015, Zhu et al., 2019). In addition, it has been shown that the phosphorylation of LIM domains accelerates the localization of Paxillin to FAs (Brown et al., 1998b). Importantly, throughout Paxillin serine/threonine and tyrosine phosphorylation sites are distributed (Brown et al., 1998a).

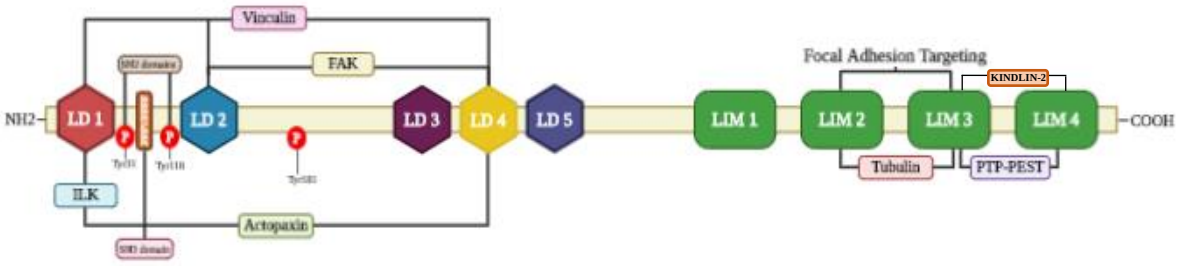

Figure 1.6: Paxillin domains and sites of interactions with major binding partners (Scheme made by online program Biorender)

3.4.2 Functional characteristics of Paxillin

Paxillin is implicated in coordinating downstream signaling for the regulation of cell spreading and motility, by the recruitment of several signaling molecules (Schaller, 2001). In addition, Paxillin has a crucial role in the regulation of cell migration through its involvement in growth factor and integrin signaling pathways (Brown and Turner, 2004). To regulate cell migration, Paxillin must first localize at FAs where it will interact with FA proteins such as Vinculin and FAK, and then become phosphorylated at its major phosphorylation residues Tyr31 and Tyr 118, by the FAK/Src complex (Bellis et.al, 1995; Schaller et al, 1995; Brown and Turner, 2004). The Y31F/Y118F mutant of Paxillin, which cannot get phosphorylated at the specific tyrosine residues, has been shown to block cell migration, indicating that phosphorylation of these residues is essential for this process (Zaidel-Bar et al., 2007). Additionally, Paxillin was found to be critically involved in the embryonic development, since Paxillin knockout in mice leads to embryonic death at day E9.5 and phenotypically it resembles the Fibronectin knockout, proposing that Paxillin is essential for transducing signals from fibronectin receptors during

development. Additionally, fibroblasts derived from these mice show increased size of focal adhesions, decreased turnover and reduced rates of cell migration (Hagel et al., 2002). Finally, evidence shows that the interaction of Paxillin with FAK, another major protein of FAs, is not only important for localization of FAK at FAs, but it is also critical for proper spindle orientation. The FAK – L1034S point mutant, that cannot interact with Paxillin, has been shown to be unable to rescue SO defects (Petridou and Skourides, 2014). Additionally, use of morpholino that downregulates Paxillin results in SO defects with respect to the plane of adhesion (Petridou and Skourides, 2014). These data suggest that Paxillin is a member of the CMC, however its role in spindle responses to adhesion geometry or responses to mechanical stimuli have not been investigated.

3.5 FAK

FAK is a 125 kD highly conserved focal adhesion protein (Corsi et al, 2006). It is classified as a cytoplasmic non-receptor tyrosine kinase, which is implicated in many fundamental cellular processes, including cell proliferation, signaling pathways and oncogenesis (Schaller et al., 1992; Cherrier et al, 2014; Miranti and Brugge, 2002; Parsons, 2003; Schlaepfer et al., 2004).
FAK is comprised of three main domains, a FAT domain at the C-terminus, a FERM domain and proline-rich regions at the N-terminus, and a kinase domain between the FERM and FAT domains, which gives the protein its catalytic kinase activity. The focal adhesion targeting (FAT) domain mediates the interaction with Paxillin for targeting FAK at FAs, while the FERM domain and proline-rich regions, provide docking sites for several proteins (Hildebrand et al., 1993).
Once FAK localizes at FAs upon integrin activation, it becomes auto phosphorylated on Tyr397, which in turn is recognized by the SH2 domain of Src, another tyrosine kinase (Parsons, 2003, Schaller et al., 1994). Assembly of the FAK-Src complex leads to FAK phosphorylation on additional tyrosine sites, specifically Tyr576 and Tyr577, leading to increased FAK kinase activity. This event is required for the phosphorylation of downstream protein targets, such as Paxillin and p130Cas (Hanks et al., 2003, Schaller et al., 1999; Calalb et al., 1995). Other sites of FAK, such as Y861 and Y925, become phosphorylated by Src, providing binding sites for Grb2 (Growth factor receptor-bound protein 2), followed by the recruitment of dynamin which will contribute to the disassembly of FAs (Deramaudt et al., 2011).
Furthermore, FAK has a crucial role in normal adhesion and migration of many cell types both *in vitro* and *in vivo* (Ilic et al., 1995, Mitra et al., 2005). In vitro experiments in FAK null fibroblasts showed an increased presence of immature focal adhesions and reduced turnover

rates in comparison with control cells. Additionally, these fibroblasts failed to spread and migrate because of their disorganized cortical cytoskeleton, since they displayed a rounder shape in comparison with controls (Ilic et al., 1995, Schwock et al., 2009).

Additionally, in vivo experiments have revealed the involvement of FAK in embryonic development. Experiments on FAK deficient mice demonstrated that lack of FAK leads to embryonic death at day E8.5. These embryos initiate gastrulation normally, but exhibit abnormalities in the following stages and do not survive beyond the end of neurulation. Abnormalities such as defective notochord formation and defective heart development are a result of a defect in mesodermal tissue migration (Ilic et al., 1995). Under normal conditions, during gastrulation FAK expression increases and is detected in the mesoderm, the marginal zone ectoderm and cells of the blastocoel roof, while at later stages is detected at intersomitic junctions, in the neural plate, in the brain and several cranial nerves (Fonar et al., 2011, Hens and DeSimone, 1995). Use of antisense inhibition of FAK expression (Fonar et al., 2011) or DN constructs of FAK (Kragtorp and Miller, 2006, Petridou et al., 2013, Stylianou and Skourides, 2009) revealed a significant role of FAK in neurulation, axial elongation and somitogenesis in *Xenopus* and *Zebrafish* embryos. Defects in epiboly, radial intercalation, and blastopore closure occurred when using FF, a dominant-negative of FAK, in *Xenopus* embryos, revealing the involvement of FAK in early morphogenetic events (Petridou et al., 2013). In agreement with this, published data implicated FAK in the tension-dependent organization of collectively migrating mesendoderm (Bjerke et al., 2014).

Finally, FAK is essential in SO. Recent published reports propose that FAK is necessary for the transduction of external forces in order to orient the mitotic spindle (Petridou and Skourides, 2014). FAK is suggested to act as a mechanosensor and it is part of the Cortical Mechanosensory Cortex (CMC), along with p130Cas an Src. The CMC is formed downstream of integrin β1 ligand independent and force dependent activation at the lateral cortex of mitotic cells and promotes SO in respond to external cues (Petridou and Skourides, 2016). FAK is the sole member of the CMC in addition to integrin β1 which has clearly been shown to be necessary for both spindle orientation with respect to the plane of adhesion as well as spindle orientation responses to adhesion geometry and force vectors on the cell cortex.

3.6 p130Cas

p130Cas is a 130 kD protein, a member of focal adhesions. It does not exhibit any enzymatic activity, but it contains multiple binding sites for other proteins, thus it is classified as an adaptor or scaffold protein. p130Cas can either interact directly with other proteins via its several domains or mediate protein-protein interactions. It contains an N-terminal SH3 domain, with which it interacts with FAK, several proline-rich and serine-rich regions, a cluster of 15 repetitive YXXP motifs known as the substrate domain (SD) and a C-terminal domain which contains the binding motif to Src SH2 domain (Sakai et al., 1994; Burnham et al.,1996; Harte et al., 1996; Mayer et al., 1995). The SD is the main site of tyrosine phosphorylation and when phosphorylated it acts as a binding site for Crk (CT10 Regulator of Kinase) and Nck (non-catalytic region of tyrosine kinase adaptor protein 1) (Sakai et al., 1994; Schlaepfer et al., 1997). The SH3 domain of p130Cas, through association with FAK, and the YDVY motif, through association with Src, can lead to the recruitment of p130Cas at FAs. Additionally, a recently published report proposed that localization of p130Cas at FAs also results from the interaction of the Cas family homology domain (CCHD) and the LD1 motif of Paxillin (Zhang et al, 2017).

The targeting of p130Cas at FAs is crucial for its tyrosine phosphorylation. Once p130Cas gets phosphorylated, it can regulate several processes, including cell spreading, cell migration, cell survival and cell proliferation, through its involvement in many signaling pathways (Honda et al., 1999; Almeida et al., 2000; Oktay et al., 1999). In agreement with that, knockout fibroblasts that lack p130Cas, display defects in cell migration on fibronectin (Honda et al., 1999; Honda et al., 1998).

In the context of SO, p130Cas interacts with Src and FAK, forming the Cortical Mechanosensory Complex at the lateral cortex of mitotic cells upon activation of integrin β1. Interestingly, Cas null fibroblasts that lack p130Cas, exhibit SO defects with respect to the plane of adhesion unlike Cas reconstituted cells. Expression of the CasΔSH3 mutant, which cannot bind to FAK, fails to rescue the SO phenotype suggesting that the FAK-p130Cas interaction is necessary in this process. In addition, the re-introduction of the Cas 15F mutant, that cannot be phosphorylated in the 15 YXXP motifs, cannot rescue this defect. A similar outcome is present upon the expression of the Y397F FAK mutant in FAK null cells, which cannot bind to Src, fails to rescue SO defects. These data suggest that the presence of p130Cas and the direct interaction between the members of CMC are implicated in proper spindle orientation in adherent cells and vertebrate epithelia, however its involvement in spindle responses to spatial adhesive cues has not yet been investigated (Petridou and Skourides, 2016).

3.7 Vinculin

Vinculin is a 117 kD structural protein that localizes at FAs (Geiger, 1979). Vinculin is comprised of a large globular head domain and a tail region, linked via a proline-rich sequence (Ziegler, 2006). Vinculin adapts an auto-inhibited conformation state when it is unbound, due to interaction of the head domain to the tail domain. Once Vinculin localizes at FAs, it changes into the open conformation state, in which the head domain interacts with the rod domains of the protein Talin, while the tail is bound to actin bundles (Galbraith et al., 2002; Johnson and Craig, 1994; Johnson and Craig, 1995; Chen et al, 2005). The interaction with both Talin and actin together is proposed to be necessary for the full activation of Vinculin, while the interaction with Talin, and probably Paxillin, is required for targeting Vinculin to FAs (Geiger et al, 2001; Zhang et al, 2008; Bakolitsa et al, 2004; Chen et al, 2006). When activated, Vinculin interacts with multiple proteins, such as Paxillin and a-actinin (Turner et al., 1990; Carisey and Ballestrem, 2011).

Importantly, Vinculin is implicated in the transmission of extracellular and intracellular mechanical cues, that are essential for assembly, disassembly and reorganization of FAs that result in polarized cell motility, as well as the assembly and reorganization of the actin cytoskeleton (Carisey et al, 2013; Critchley, 2000; Galbraith et al, 2002). In agreement with this, evidence shows that in the absence of Vinculin or its ability to bind actin, cells are less stiff and are unable to remodel the cytoskeleton, suggesting that the Vinculin-actin interactions are crucial for force transmission (Alenghat et al., 2000; Mierke et al., 2008; le Duc et al., 2010; Huveneers et al., 2012; Grashoff et al., 2010).

At the same time, Vinculin is also involved in embryonic development, since Vinculin deficient embryos only develop until the 10^{th} day of gestation, exhibiting defects in the neural tube as well as heart malformation (Xu et al., 1998; Saunders et al, 2006). Additionally, when Vinculin is inactivated in embryonic stem ES cells, in fibroblasts of Vinculin null embryos and F9 embryonal carcinoma cells, it leads to reduced adhesion and increased cell motility in comparison with wild type cells (Coll et al., 1995; Volberg et al., 1995; Xu et al., 1998).

3.8 ILK

Integrin-linked kinase (ILK) is a 50 kD multidomain serine/threonine kinase that localizes at FAs. It encompasses three main domains, the N-terminus, which is comprised of four ankyrin repeats that interact with PINCH protein, a central pleckstrin homology-like domain (PHIP) that binds to phosphatidylinositol 3,4,5-triphosphate (PIP3), and the C-terminus domain which contains a protein kinase catalytic domain and a β1 integrin-binding site (Hannigan et al, 1996; Tu et al, 1999; Li et al, 1999; Delcommenne et al, 1998). ILK has a crucial role in several integrin-mediated processes, such as cell adhesion, differentiation, and assembly of the fibronectin matrix, as well as in the Wnt signaling pathway (Novak et al, 1998; Hannigan, 1996; Wu et al, 1998; Tu et al, 2001). Furthermore, ILK is implicated in the capture of the microtubules at the cell cortex and in the regulation of vesicular transport (Wickstrom et al., 2010).

The localization of ILK at FAs is mediated through three independent interactions. First, several studies suggest that ILK interacts with the LD1 motif of Paxillin, an event that targets ILK to FAs. In agreement with this, it has been shown that ILK contains a sequence within its C-terminus domain that is similar to the Paxillin Binding Subdomain (PBS) sequence, which several proteins that bind to Paxillin contain, including Vinculin and FAK (Brown et al, 1996; Nikolopoulos et al, 2000; Tachibana et al, 1995). Mutations in this region inhibit the targeting of ILK to FAs, due to the disruption of the Paxillin-ILK interaction (Nikolopoulos and Turner, 2001). Another protein that contributes to ILK targeting to FAs is the adapter protein PINCH, which contains a LIM domain that binds ILK (Tu et al, 1999). Eliminating the binding site in ILK, which interacts with PINCH, also inhibits localization of ILK at FAs (Li et al, 1999). Finally, the third interaction is that with the integrin cytoplasmic domains which provide docking sites for ILK at FAs. Importantly, the expression of an ILK mutant that contains the PINCH binding site but lacks the binding sites for Paxillin and Integrin, exhibits a failure in localization of ILK at FAs (Li et al, 1999).

3.9 Adherens Junctions

Adherens junctions (AJs) are multi-protein complexes essential for the development and survival of multicellular organisms (Townesand Holtfreter, 1955; Takeichi, 1991; Steinberg, 1996). The formation of AJs at the lateral membranes of cells results in the initiation, mediation, and stabilization of cell-cell contacts. Additionally, AJs are implicated in intracellular signaling, as well as in the regulation of transcriptional activity and the reorganization of the actin cytoskeleton. They are composed of calcium-dependent transmembrane glycoprotein Cadherins, such as E- and N- Cadherin, and catenin family members p120 catenin, α-catenin and β-catenin. Cadherins of neighboring cells form calcium-dependent homophilic interactions resulting in the recruitment of intracellular proteins and connection to the actin cytoskeleton (**Figure 1.7**, Takeichi, 1988; Gumbiner, 2000; Nollet et al., 2000). Interestingly, AJs are highly dynamic complexes that can alter their assembly or disassembly during epithelial to mesenchymal transition (EMT), a developmental and an oncogenic process, resulting in the loss of cell-cell adhesion and increased migration rate (Hay and Zuk, 1995; Cano et al., 2000; Berx and Van Roy, 2001, Conacci-Sorrell et al., 2002; Palacios et al., 2002).

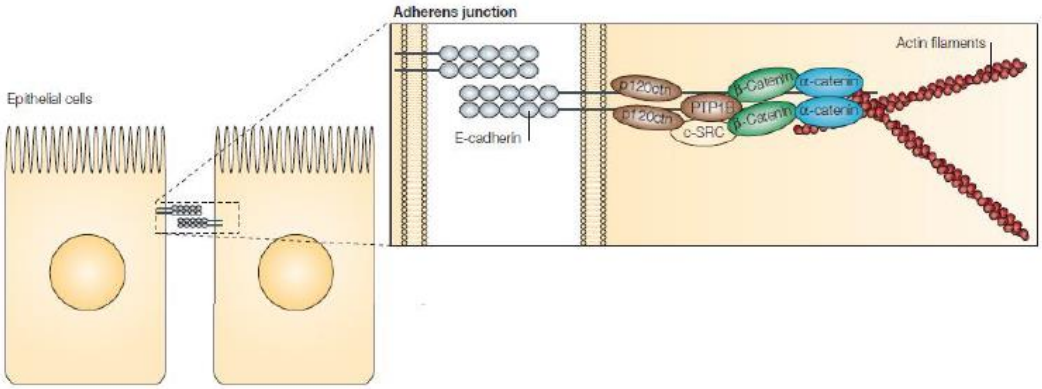

Figure 1.7: Adherens Junction structure. Adherens junctions are cadherin-based complexes formed at the lateral membrane of neighboring cells. They are comprised of transmembrane glycoprotein Cadherins and intracellular components such as p120 catenin, α-catenin, and β-catenin (Yeatman, 2004)

3.9.1 Cadherins

Cadherins are a large superfamily of transmembrane glycoproteins involved in the cell-cell adhesion, containing the type I cadherins (E-, N-, P-, and R cadherin), the type II cadherins (Cadherin-6 and VE-cadherin), the desmosomal cadherins (desmocollins and desmogleins) and a subfamily of cadherin-like molecules (Takeichi, 1988; Gumbiner,2000; Nollet et al., 2000). Several studies have implicated cadherins in many developmental processes as well as in the adult organism. For example, cadherins regulate the separation of embryonic layers and the formation of tissue boundaries, the formation of the nervous system (Osterhout et al., 2011; Takeichi, 1995; Kim et al., 2000; Tepass et al., 2002), while they are also involved in cell signaling (Watanabe et al., 2009) and the maintenance of homeostasis (Nishimura and Takeichi, 2009).

Cadherins are composed of three main domains, the extracellular domain, the transmembrane domain and the cytoplasmic domain. Classical cadherins, such as N-Cadherins, have an extracellular domain with five ectodomain modules (EC1-5) that contains Ca2+ binding motifs (Shapiro et al., 1995; Aberle et al.1996; Shapiro and Weis, 2009; Tepass et al., 2000). In order to trans-interact each cadherin must bind Ca2+ at these motifs that result in the acquisition of a rod-like conformation (Gumbiner, 1996; Patel et al.,2006; Pokutta et al., 1994). The heterodimerization of neighboring cadherins is achieved through interaction of the EC1 domains, while homodimerization between cadherins within the adherens junction is established through EC1-EC2 interactions between the cadherin molecules (Boggon et al., 2002). Also, they have a transmembrane domain that anchors cadherins on the cell membrane and a short cytoplasmic domain that can mediate direct or indirect intracellular interaction with proteins of the catenin family (Shapiro and Weis, 2009). Specifically, p120 catenin interacts with the juxtamembrane domain (JMD) of the cytoplasmic region of the cadherin (Yap et al., 1998), while β-catenin interacts with an extended region of the C-terminal domain (Aberle et al., 1994). These positions within the cytoplasmatic domain are known as catenin binding domains (CBD) and are crucial for the recruitment of catenins at the AJs. Cadherins interact with α-catenin indirectly, by its interaction with β-catenin (Tominaga et al., 2008).

3.9.1.1 N-Cadherins

N-Cadherin (Neural Cadherin) is a 130kDa protein involved in AJs formation. It is mainly expressed in the nervous system, where it regulates axonal growth and synapse formation (Doherty and Walsh, 1996). Interestingly, cells expressing N-Cadherin adopt motile characteristics, compared with cells expressing E-Cadherin where they suppress invasiveness and become epithelial (Islam et al., 1996).

3.9.2 Catenins

Catenins, including p120 catenin, α-catenin, and β-catenin, are cytoplasmatic proteins that localize at AJs, where they act as a connection between cadherins and the actin cytoskeleton. Many studies identified the role of catenins in the formation, clustering, and disassembly of the adhesions, as well as in signaling pathways (Capaldo and Macara, 2007; Daniel and Reynolds, 1995; Nishimura and Takeichi, 2009; Reynolds et al., 1992, 1994; Nishimura and Takeichi, 2009; Yamada and Nelson, 2007). Specifically, β-catenin interacts with the catenin binding domain (CBD) of cadherins (Aberle et al., 1994, Tominaga et al., 2008), while at the same time it also binds α-catenin through the tyrosine residue Y142, which can interact with actin bundles (Rimm et al., 1995). Conclusively, b-catenin serves as a link between cadherins and the actin cytoskeleton (Yamada et al., 2005). Moreover, the interaction of p120 catenin with the juxtamembrane domain (JMD) of cadherins results in the stabilization of cadherin-catenin complex at the cell surface (Xiao et al., 2003, Davis et al., 2003; Lampugnani et al., 1997; Thoreson et al., 2000; Ireton et al., 2002).

3.9.3 Turnover of Adherens Junctions

As mentioned before AJs are formed at the lateral membrane between cell to cell adhesions while FAs are formed at the basal membrane. Both adhesion systems are connected with the actin cytoskeleton and regulate actin dynamics through the control of the Rho family of GTPases. Also, they are involved in the sensing of forces exerted on cells, due to the recruitment of proteins which act as mechanosensors at the adhesions. At the same time, both share common proteins, such as Vinculin and Src (Yano et al., 2004; Yamamoto et al., 2015; Bays et al., 2014, Tsukita et al., 1991). Several published data support that these two systems can affect one another, both in a positive and negative manner, but their difference in the spatial distribution within each cell can be challenging to address the direct effect the one has on the other (Yano et al., 2004, Yamamoto et al., 2015; Bays et al., 2014, Tsukita et al., 1991).

Recent unpublished data from our laboratory have revealed that, when cells are seeded on N-Cadherin substrates, they form linear AJs on their basal membrane, which subsequently colocalize with active integrin β1, a major component of FAs. AJ formation precedes integrin activation, which is spatially guided by the AJs. Once integrin activation takes place at the AJs, it promotes the downstream recruitment of several focal adhesion proteins at the sites of AJs, including Paxillin, Talin, FAK, and ILK. At this state, this type of adhesions is named hybrid adhesions. Another observation is that, once integrin β1 is activated, major AJ components are gradually removed from the adhesion, indicating that integrin β1 activation promotes the

disassembly of AJs, a notion that it is also supported by the spatial segregation of the FA components in respect to AJ components within the same hybrid adhesion (**Figure 1.8)**. Integrin β1 activation and the recruitment of the several FA proteins may promote the disassembly of AJs through phosphorylation of their major components and promotion of their endocytosis. It is known that the Src kinase, a member of focal adhesions, can phosphorylate cadherins and promote their endocytosis (Fujita et al., 2002).

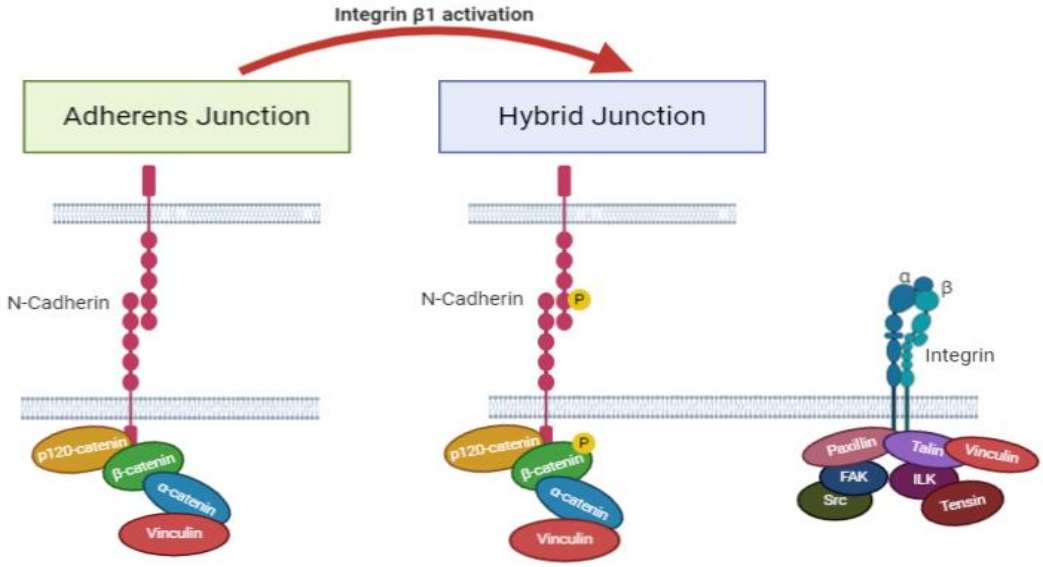

Figure 1.8: Schematic representation of the Hybrid Adhesion formation upon β1 integrin activation (Scheme made by online program Biorender)

3.10 Embryonic Development

Development of *Xenopus laevis* embryos up to the general body plan is composed of three stages: cleavage in which the blastula is formed, gastrulation which leads to the formation of the three embryonic germ layers and the anteroposterior and dorsoventral axes, and neurulation in which formation of the central nervous system results from the ectoderm on the dorsal side of the embryo (**Figure 1.9**, Slack, 2013).

Gastrulation involves coordinated cellular movements that result in the spreading of the marginal zone (tissue belt around the equator) towards the blastopore, the internalization of the marginal zone through the blastopore and the blastopore closure (Vogt, 1929; Holtfreter, 1943; Keller and Schoenwolf, 1977; Slack, 2013). These are essential for the establishment of the three embryonic germ layers, ectoderm on the outside, mesoderm in the middle, and endoderm

on the inside. In the blastula, a thin blastocoel roof on the animal hemisphere and a massive vegetal region form a wall that encloses the blastocoel. During gastrulation, the blastocoel roof, which most of it eventually will form the ectoderm, undergoes epiboly to expand and enclose the whole embryo surface. Specifically, deep cells of the blastocoel roof integrate into one layer through radial intercalation and expand by flattening and occupying more area (Keller and Danilchik, 1988; Keller 1980; Slack, 2013; Holtfreter, 1943). Parallel with the expansion of deep cells, the most superficial cell layer expands by cell division, spreading, and flattening. Additionally, the cells of the vegetal region will form the endoderm and in the marginal zone the mesoderm will become a separate middle layer between the ectoderm and endoderm (Vogt, 1929; Keller, 1986). The end of gastrulation is driven by the thinning and expansion of the animal cap, which also allows the closure of the blastopore.

Mesodermal cells migrate towards the blastopore through a surface, known as the fibrillar FN matrix, that is localized along the blastocoel roof. The assembly of this FN network in embryos is a result of a process named Fibronectin fibrillogenesis (Boucaut and Darribere, 1983a; Boucaut and Darribere, 1983b; Collazo et al., 1994; Lee et al., 1984; Nakatsuji and Johnson, 1983; Nakatsuji et al., 1985). During gastrulation, only surfaces upon which mesoderm will migrate are coated with fibronectin. In agreement with this, several studies have suggested that the specific distribution of FN is due to spatially localized receptors that bind fibronectin, such as integrins (Lee et al, 1984). Additionally, it has been shown that interaction with FN is essential for mesoderm migration on the blastocoel roof, because it controls the formation of protrusions in mesoderm cells and thus increases their motility. Indeed, mesodermal cells of embryos injected with the GRGDSP peptide that can't interact with FN, exhibit inhibition of mesoderm cell migration (Winkbauer, 1990; Winkbauer and Keller, 1996). Interestingly, when the assembly of the FN network is disrupted, a failure of radial intercalation movements occurs, as well as thickening of the blastocoel roof, proposing that the integrin-dependent interaction of the FN matrix and deep cells are required for the establishment of cell polarity in these cells of both dorsal marginal zone and blastocoel roof. Thus, it was suggested that in the marginal zone, FN is involved in the radial intercalation movements, while in the blastocoel roof it serves to maintain the existing thinning of the animal cap (Marsden and DeSimone, 2001).

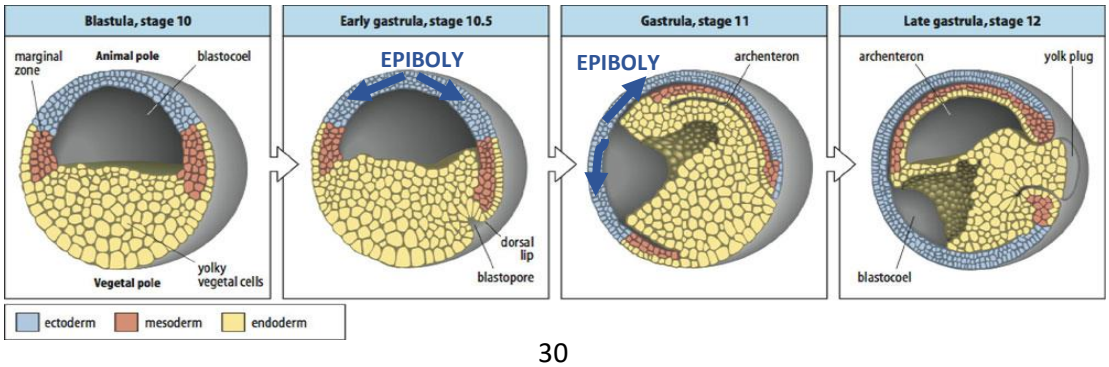

Figure 1.9: Schematic representation of gastrulation stages in *Xenopus* embryo (Adapted from: <http://www.mun.ca/biology/desmid/brian/BIOL3530/DB_03/DBNVert1.html> [Accessed 1 June 2020]).

3.10.1 Importance of Paxillin in Development

As mentioned before, Paxillin has also been studied from the perspective of embryonic development. The essential role of Paxillin in development was initially highlighted through knockout experiments in mice. Paxillin deficient embryos were detected only before E9.5. The expression of Paxillin is initially restricted to extraembryonic structures at E6.5 to E7.5, such as the parietal endoderm and amnion, but at later stages it broadens. Thus, Paxillin is involved in the development of both extraembryonic and embryonic structures, including mesodermally derived structures, such as the heart and somites. Interestingly, Paxillin null embryos phenotypically resemble the Fibronectin null embryos, suggesting that Paxillin is crucial for transducing signals generated by fibronectin receptors during development. Moreover, fibroblasts derived from these embryos display abnormal FAs, decreased turnover, reduced fibronectin-induced phosphorylation of FAK, Cas and MAPK, and reduced rates of cell migration and spreading. Conclusively, it was proposed that Paxillin is crucial for fibronectin signaling both *in vivo* and *ex vivo*, probably due to regulation of cell spreading, tyrosine phosphorylation and FA dynamics (Hagel et al, 2002). Additionally, studies in *Zebrafish* embryos, suggested that during the morphogenesis of the early zebrafish embryo, Paxillin and FAK are concentrated at sites of cell-cell adhesion in the epithelial enveloping layer and are implicated in the integration of cadherin-based and integrin-based cell adhesion (Crawford et al, 2003). Also, *Zebrafish* embryos, that lack Paxillin, exhibit defects in axial and skeletal muscle development, as well as in the cardiovascular system, including contractility and heart failure. These results are due to the destabilization of the interaction of Paxillin, FAK, and Vinculin (Hirth et al., 2016). Finally, it was shown that Paxillin plays a critical role in the oocyte maturation in *Xenopus*, due to its interaction with embryonic PolyAdenylation Binding Protein (ePABP), followed by the enhancement of Mos protein translation and resulting in oocyte maturation (Miedlich et al, 2017).

4. Materials and Methods

4.1 Cells, Cell Culture and Transfection

HeLa cell line (ATCC) was cultured at 37°C with 5% CO2 in Dulbecco's modified Eagle's Medium (DMEM) supplemented with 10% Fetal Bovine Serum (FBS) and 1% Antibiotics. Paxillin null cells were cultured in DMEM with 10% FBS, 1% Antibiotics, 1mM sodium pyruvate and 1mM L-Glutamine. p130Cas null cells were cultured in DMEM with 10% FBS, 1% Antibiotics, 1mM non-essential amino acids and 1mM L-Glutamine. Transient transfection of HeLa cells with GFP Paxillin C-terminus (pCS108), memCherry (pCS2+) and of Paxillin null cells with RFP Paxillin WT (pCS108), GFP Paxillin WT, memCherry (pCS2+) was performed using Lipofectamine 2000 (Invitrogen) according to the manufacturer's protocol.

4.2 Substrate coatings

Glass coverslips were initially sonicated for 15 minutes, washed in distilled water and incubated in isopropanol, before being air dried at 65°C. Then the coverslips were exposed to UV light of 185m and 254 nm via the UV ozone cleaner for 10 minutes for charging, while Ibidi slides were initially incubated in 70% ethanol and subsequently exposed to UV light of 185m and 254 nm via the UV ozone cleaner for charging. Both glass coverslips and ibidi slides were incubated with bovine plasma Fibronectin at a concentration of 10 μg/ml (Santa Cruz Biotechnology) in 1×PBS for 60 minutes at 37°C, followed by two washes with 1X PBS before seeding of cells.

4.3 Generation of Fibronectin micro-patterned substrates

For the generation of micro-patterns with the use of PLL-g-Peg, the already established protocol by Piel et al. was modified and used accordingly (Azioune et al., 2009). Glass coverslips were initially sonicated for 15 minutes, washed in distilled water and incubated in isopropanol, before being air dried at 65°C. Up next, they were exposed under UV light of 185m and 254 nm for 10 minutes for charging. Next, coverslips were incubated at 37°C with PLL-g-Peg (30 μg/ml, 30μl per coverslip) for 30 minutes, before being washed three times with 1X PBS and air dried. The coverslips were then placed on the custom-made photolithography quartz mask (JD Photo-Data) in the according positions depending on the pattern of choice, through 2μl of distilled water with the pegylated side facing the mask. The photolithography mask was then placed inverted under UV light exposure of 185m and 254 nm and 4000V for 10 minutes. Next, coverslips were removed carefully from the mask after addition of 1X PBS in order to float. Afterwards, incubation with FN (10 μg/ml, 30μl for each coverslip) for 1 hour at 37°C followed, before the cells were seated.

4.4 Generation of N-Cadherin substrates

Glass coverslips were initially cleaned and charged in Piranha solution (Sulfuric Acid and Hydrogen Peroxide, 3:1) for 1 hour. After several washes with distilled water, coverslips were dried at 50°C for 15 minutes and exposed to UV light of 185m and 254 nm via the UV ozone cleaner for charging for 10 minutes. Subsequently, coverslips were incubated in concentrate silane (3-Aminopropyl) triethoxy-silane (Alfa Aesar) for 10 minutes and then washed 5-10 times with distilled water. Then, coverslips were baked at 150°C for 10 minutes. Up next, coverslips were incubated with Goat Anti-Human IgG (10 μg/ml, SSA015 Sino Biological) for 1 hour at 37°C, followed by two 1X PBS washes. Afterwards, they were incubated in N-Cadherin Fc (Recombinant CDH2/Fc, Sino Biological) at a concentration of 10 μg/ml for 1 hour at 37°C and washed twice with 1X PBS, before seeding cells.

4.5 In vitro fertilization and microinjections of Xenopus laevis embryos

Ovulation of embryos was induced by administrating 750 units of human chorionic gonadotropin (hCG) via injections into the dorsal lymph sac of female frogs. After 14-16 hours, the eggs were collected in 0.33 X MMR (Marc's Modified Ringers) by gently massaging the belly of ovulating frogs. Male frogs were euthanized, by submersion into a 0.005% benzocaine solution for 20-30 minutes at room temperature (RT) and testes were isolated and kept in a 90% L-15 medium containing 10% fetal calf serum (FCS) and 50μg/mL Gentamycin, at 4ºC. Next, *Xenopus* embryos were fertilized *in vitro* by dissolving a small piece of testis and mixing it with the collected eggs. After fertilization, the thick jelly membranes surrounding the embryos were removed using a 2% L-cysteine solution in 0.33 X MMR (pH 7.8) and then washed with 0.33X Marc's Modified Ringer's (0.3X MMR).

Microinjections were performed in 4% Ficoll in 0.33X MMR solution. Injections of de-jellied embryos were performed by using glass capillary pulled needles, forceps, a Singer Instruments MK1 micromanipulator and a Harvard Apparatus pressure injector. Specifically, microinjections with capped mRNA, *in vitro* transcribed using the mMachine SP6 kit (Ambion), at the two-cell or 4-cell stage, at the animal pole of blastomeres of embryos were done as required for each experiment. The injections amount per embryo was GFP PaxC 500pg. After injections, embryos were cultured for 1 hour in 4% Ficoll in 0.33 X MMR and then washed and maintained in 0.1 X MMR. Subsequently, they were allowed to develop to the appropriate stage and then imaged live or fixed in 1 X MEMFA. Fixed embryos were sectioned (animal cap dissection and sagittal sectioning) prior to immunostaing. *Xenopus laevis* embryos were staged according to the study by Nieuwkoop and Faber (1967).

4.6 Immunostaing

4.6.1 Immunostaing on Xenopus laevis embryos

For immunofluorescence, sectioned embryos were first fixed in 1X MEMFA (10% 10XMEMFA, 10% 3.7% formaldehyde, 80% water) for 2 hours at room temperature, permeabilized in PBST (1 X PBS + 0.5% Triton-X100 + 1% DMSO) for 2 hours at room temperature and blocked in PBDT + 10% normal donkey serum for 30 minutes at room temperature. Next, primary antibodies were added in block solution and incubated for 4 hours at room temperature or overnight at 4°C. The following primary antibodies were used: β catenin rabbit antibody (1:500, Sino), β tubulin E7S mouse antibody (1:200 DSHB), E-cadherin mouse antibody (1:200, 5D3, Hybridoma), α tubulin rat antibody (1:300, Santa Cruz), anti GFP rabbit antibody (1:1000, Proteintech), *Xenopus* Fibronectin mouse antibody (1:300, DSHB), C-cadherin mouse antibody (1:50, DSHB). Afterwards, the embryos were washed 4x5 minutes in PBDT, before the addition of secondary antibodies (in block solution) for 2 hours at room temperature. The secondary antibodies used were: 488 donkey anti-Rabbit (1:500, Invitrogen), 555 donkey anti-Mouse (1:500, Invitrogen), Alexa 633 donkey anti-Mouse (1:250, Invitrogen), Cy3 donkey anti-Rat (1:500, Jackson Immunoresearch), Cy3 donkey anti-Mouse (1:500, Jackson Immunoresearch), Phalloidin 633 (1:250, Invitrogen). After 4x5 minutes washes in PBST, embryos were post-fixed in 1XMEMFA for 30 minutes at room temperature. Following that, embryos were washed 4x5 minutes in 1XPBS. Clearing of the embryos was performed after dehydration with methanol for 3x10minutes followed by immersing them in Murray's Clearing Medium (2:1 BB/BA).

4.6.2 Immunostaing on cells

HeLa and Paxillin null cells were washed three times with 1XPBS and fixed for 12 minutes in 4% paraformaldehyde (PFA) solution in 1XPBS or for 20 minutes in 1:1 Methanol/Acetone solution. PFA fixation was followed by incubation in a 50 mM glycine solution (pH=7.8) in 1X PBS for 10 minutes. Next, permeabilization of cells was done using 0,1% Triton-X solution in 1X PBS for 10 minutes. After several washes with 1XPBS, Permeabilized or Methanol/Acetone fixated cells were blocked using 10% donkey serum in 1X PBS for 30 minutes. Following that, cells were incubated with primary antibodies diluted in 10% donkey serum solution in 1X PBS for 1 hour at room temperature. The primary antibodies used were: Paxillin rabbit (1:1000, Sino), FAK mouse (1:1000, Sino), Vinculin rabbit (1:1000, Sino), active β1-Integrin 9EG7 rat (1:800,), PY20 mouse (1:500, Santa Cruz), Talin goat (1:500, Santa Cruz), Paxillin rabbit (1:800, Novus), FAK mouse (1:800, BD), Vinculin mouse (1:600, Santa Cruz), ILK mouse (1:600, Santa Cruz), β tubulin E7S mouse antibody (1:300, DSHB). The primary antibodies

were washed 3x5minutes in 1XPBS, before the addition of secondary antibodies (in block solution) for 1 hour at room temperature. The following secondary antibodies were used: 488 donkey anti-Rabbit (1:500, Invitrogen), 555 donkey anti-Mouse (1:500, Invitrogen), Phalloidin 633 (1:250, Invitrogen), 488 donkey anti-Mouse (1:500, Invitrogen), Cy3 donkey anti-Rat (1:500, Jackson Immunoresearch), Alexa 633 donkey anti-Rabbit (1:250, Invitrogen), Alexa 647 donkey anti-Goat (1:500, Jackson Immunoresearch), 555 donkey anti-Rabbit (1:500, Invitrogen), Alexa 633 donkey anti-Mouse (1:250, Invitrogen), Alexa 633 donkey anti-Goat (1:250, Invitrogen). The secondary antibodies were washed three times in 1XPBS. For mounting, prolong anti-fade agent (Invitrogen) was used on a microscope slide and the glass coverslip was placed inverted on top of it.

4.7 Fluorescence Recovery After Photobleaching (FRAP)

HeLa cells co-transfected with GFP PaxC and RFP Paxillin were seeded overnight at 37°C on cleaned, charged glass coverslips coated with FN. FRAP experiments were performed using an LD C-Apochromat 40x water immersive objective on a Zeiss LSM 710 scanning laser confocal microscope. For GFP excitation the 488 nm line of an Argon Krypton laser was used, and fluorescence emission was collected between 493 to 562 nm. For RFP excitation the 543nm line of an Argon Krypton laser was used, and fluorescence emission was collected between 599 to 758 nm. After the acquisition of a pre-bleach image, a region of interest (ROI) was photobleached. Recovery was observed over a period of 1 min.

4.9 Acceptor Photo-bleaching FRET

Hela cells co-expressing GFP Paxillin C-terminal and RFP Paxillin were seeded overnight at 37 on cleaned, charged glass coverslips coated with FN. A 543nm laser was used for acceptor (RFP Paxillin) photo-bleaching (100% power), within a region of interest (ROI). A 488nm laser was used for acquisition of GFP (donor) and emission was detected between 493-538nm. A 543nm laser was used for acquisition of RFP and emission was detected between 599-758 nm. One frame was acquired as a pre-bleaching control and a rectangular ROI was bleached, within one frame. Zeiss Zen 2010 software was used for FRET analysis.

4.10 Imaging

After immunofluorescence staining, cells and embryos were imaged either with a Zeiss Axio Imager Z1 microscope equipped with a Zeiss Axiocam MR3 and the AxioVision software 4.8 or with a Zeiss LSM 710 scanning laser confocal microscope, with the Zen 2010 software, or with a Zeiss LSM 910 airyscan laser confocal microscope with the Zen 2010 software. Live

imaging of cells and embryos was performed on a Zeiss Axiovert 200M with the AxionVision software 4.8.

4.11 Quantification and Statistical analysis

All quantification was performed with the Imaris 9.1.0, AxioVision LE software and Zen (Blue + Black edition) software. For the FA-localization of individual proteins, a manual selection of each FA was performed in individual cells, and for the quantification the mean cytosolic intensity was subtracted from the mean FA intensity for each protein. Statistical analysis was performed with the GraphPad Prism software (Version 7.01). While for the quantification of the AJs-localization of individual proteins, AJs in singles cells were manually selected and the mean cytosolic intensity for each protein was subtracted from that on individual AJs.

5. Results

The role of focal adhesion proteins, p130Cas and Paxillin, in the orientation of the mitotic spindle in vitro and in vivo

The aim of this study was to examine the role of the two proteins, p130Cas and Paxillin, members of the FAs and the CMC, in the determination of mitotic spindle orientation both *in vitro* and *in vivo* (Schaller, 2001; Sakai et al., 1994; Harte et al., 1996). It has been shown that cell lines lacking these proteins display defects in terms of spindle orientation with respect to the plane of adhesion (z axis) (Petridou and Skourides, 2016; Petridou and Skourides, 2014). However, SO cues lead to the orientation of the spindle with respect to the plane of adhesion, but also with respect to the geometry adhesion (xy axis), in which case the major determinant is the interphase geometry of the cell. Spindle orientation with respect to the geometry adhesion has not been analyzed in cells lacking p130Cas or Paxillin, and thus we wanted to examine it. In an effort to address this, we used null cell lines lacking these proteins, such as Paxillin null and p130Cas null cells, while also utilized a fragment of Paxillin as a dominant-negative in control HeLa cells.

Prior to addressing the role of these two proteins in SO with respect to the geometry adhesion, we initially used the HeLa cell line as a reference point, a cell line shown to be oriented with respect to the adhesion geometry (**Figure 1.10C**, unpublished data from our laboratory). Interestingly, these cells had an elongated shape with a well-defined long axis, which in most cases represented the major force vector during interphase, and the division plane was parallel to that. However, SO quantifications revealed a subset of cells failed to follow this axis. It became clear that during mitotic cell rounding these cells displayed shape anisotropy that did not match the long interphase adhesion geometry. Effectively these cells were switching to a new long axis which did not match the interphase long axis. This could be due to delayed detachment from a region of the substrate or more likely due to force anisotropy around the cortex deforming it. Irrespective of the basis of this observation the last axis of asymmetry (often temporally coinciding with prometaphase) is a far more accurate predictor that the long interphase axis. This observation made by a PhD student in the lab, lead to the creation of a second method of determining if cells can respond to spatial adhesive cues and quantifications were carried out using both methods (**Figure 1.10A and 1.10B**). Conclusively, it was suggested that this axis, named as long prometaphase axis, was a better determinant for SO than the long interphase axis, even when cells were surrounded by other cells, due to the possibility that the

anisotropy of the cell right before full rounding may be a better indicator of the force distribution around the cortex of the mitotic cell. In addition, it is also possible that cell-cell interaction in confluent cells can affect the distribution of force around the cortex of the mitotic cell and thus alter the orientation of the spindle to be different than it was during interphase, since cells cannot disassemble their AJs as easily as FAs, resulting in exerting forces on the cortex due to cell-cell adhesion. Thus, all quantifications that follow were done by using the long prometaphase axis as the reference point indicating the expected division axis (**Figure 1.10C**).

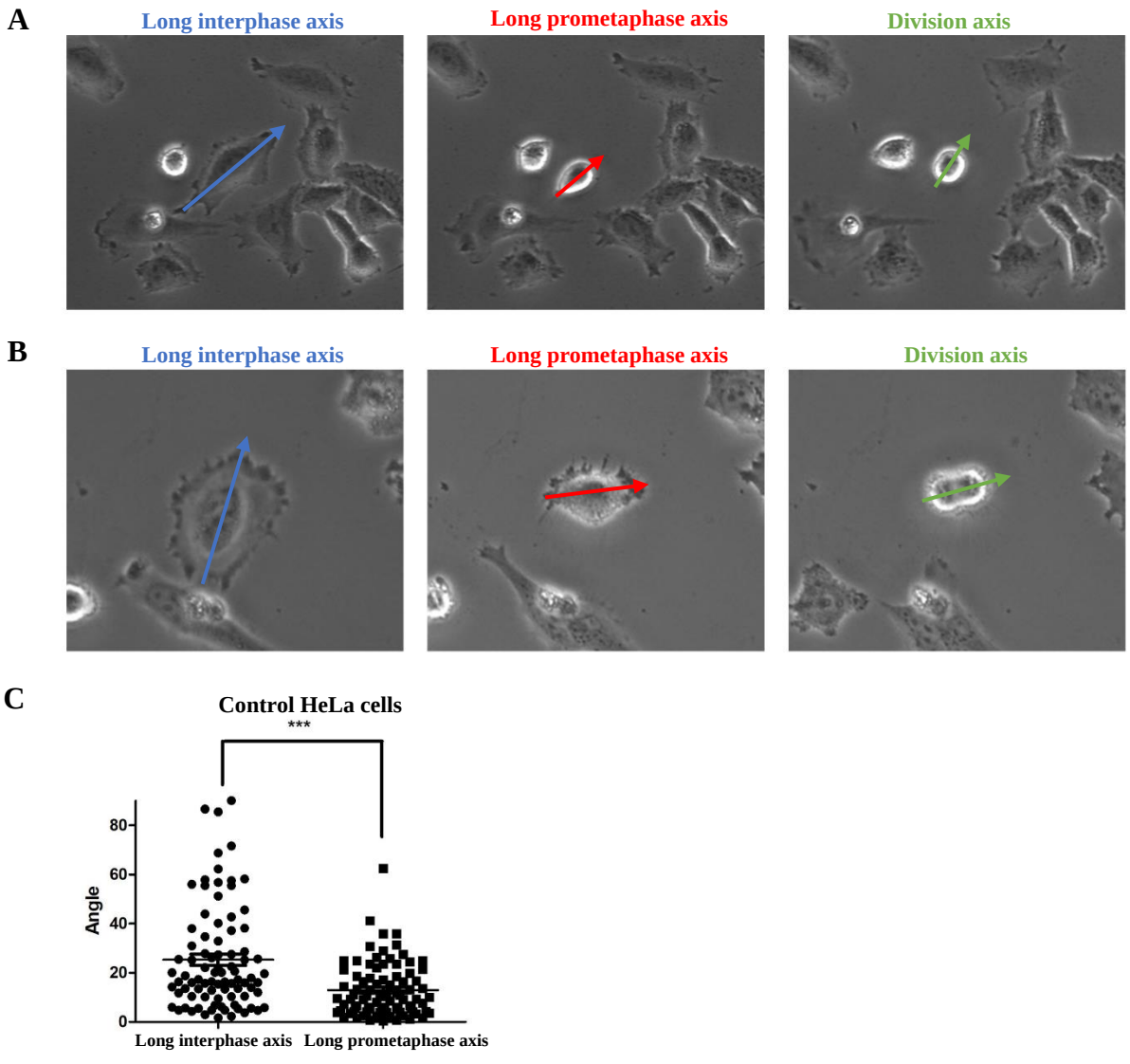

Figure 1.10: Use of HeLa cell line as a control, that follows the long prometaphase axis to orient mitotic spindle

(A) Live imaging of HeLa cells seeded on FN coated slide over 24 hours. Brightfield view of representative control cell that displays similar long interphase (blue line) and long prometaphase (red line) axes. Both axes are corresponding with the division axis (green line).

(B) Live imaging of HeLa cells seeded on FN coated slide over 24 hours. Brightfield view of representative control cell that shows a different long interphase axis (blue line) than long prometaphase axis (red line). The long prometaphase axis corresponds better with the division axis (green line).

(C) Quantification of the long interphase axis to the division axis and long prometaphase axis to division axis ratios measured at individual control HeLa cells. Statistical significance from paired t-test. Error bars represent Standard Error of the Mean (S.E.M). The mean division angle in mitotic cells parallel to the long interphase axis is 25,29 ± 2,271°, n=86 cells, while in mitotic cells parallel to long prometaphase axis is 12,95 ± 1,185°, n=86 cells. HeLa cells are oriented and prefer the long prometaphase axis than the long interphase axis to orient their spindle.

5.1 p130Cas null fibroblasts maintain shape anisotropy throughout mitosis and as a consequence display correct orientation with respect to adhesion geometry

As mentioned in the introduction, the p130Cas protein is a member of the CMC and has a crucial role in the orientation of the mitotic spindle with respect to the plane of adhesion (Petridou and Skourides, 2016). Hence, we wanted to examine its role in the orientation of mitotic spindle with respect to the geometry adhesion. For this purpose, the p130Cas null cell line in which the specific protein is absent was used, and live imaging was performed over 24 hours in order to acquire a sufficient number of mitotic cells. Quantifications revealed that the long prometaphase axis is a better predictor of SO in p130Cas null cells, with most of them being oriented when compared to HeLa cells. Specifically, mean division angle in mitotic cells parallel to the long interphase axis was 21,22 ± 1,869°, in mitotic cells parallel to long prometaphase axis was 15,61 ± 1,58°, and in control mitotic cells was 12,95 ± 1,185° (**Figure 1.11A**). Interestingly, unlike HeLa cells, which consistently become fully round during metaphase, most p130Cas nulls remained anisotropic during mitosis and never fully rounded up. However, the few cells that rounded up displayed random SO. Specifically, the mean division angle in rounded cells was 34,64 ± 7,733°, while in not rounded cells was 12,76 ±

1,539° (**Figure 1.11B)**. The fact that cells which retain shape anisotropy and a long axis throughout mitosis, orient along this axis is not surprising given the intrinsic cell shape sensing through astral microtubules. Unless a cell fully rounds up, force sensing around the cortex would only serve to further refine SO however would in principle be dispensable. In essence the failure of these cells to round up would mask any defects in force sensing and the CMC precluding any definitive conclusions to be made.

These observations suggest that either p130Cas is implicated in SO in the xy axis, causing misorientation in its absence in fully rounded cells, or that the specific cell line carries some sort of defect in the case of full rounding. To distinguish between the two hypothesis, it was necessary to rescue the cell line with the introduction of WT p130Cas and observe whether spindle will become oriented in round mitotic cells, but this would be extremely challenging since the percentage of mitotic cells that became fully round was very small and re-introduction of the WT protein (in a subset of those) would not be sufficient to provide the necessary numbers for quantification. In addition, studies have shown that mice embryos lacking p130Cas died in utero and exhibit growth retardation (Honda et al., 1998), explaining the fact that these cells had very few mitotic events taking place during the live movies and their growth rate was slow, making this experiment even more challenging. Thus, the p130Cas cell line was a poor choice to study the role of the protein in this context, since it was unclear if we would be able to get useful data from it. Hence, we moved on to the second protein of interest.

A (a)

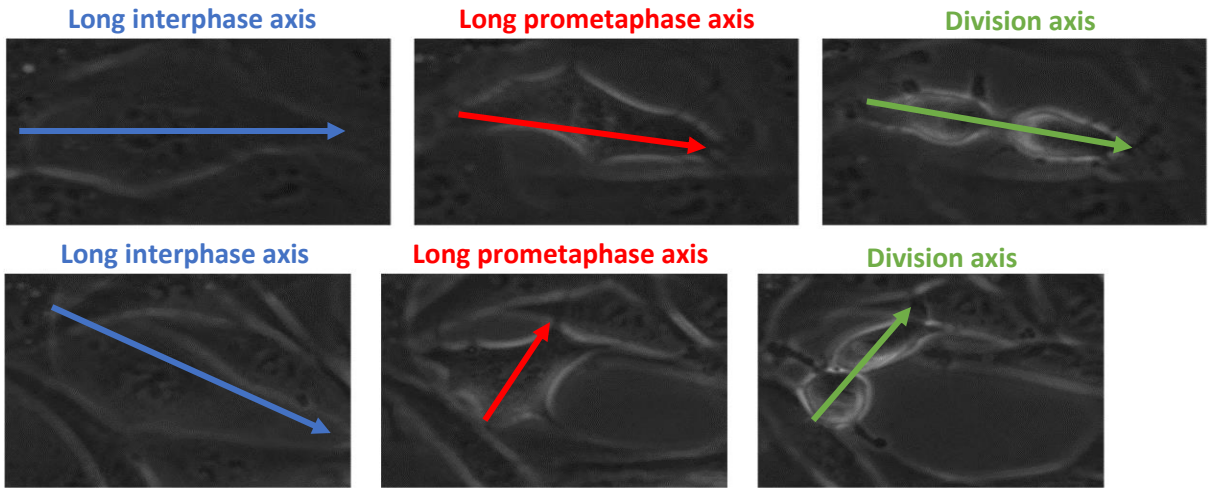

(b)

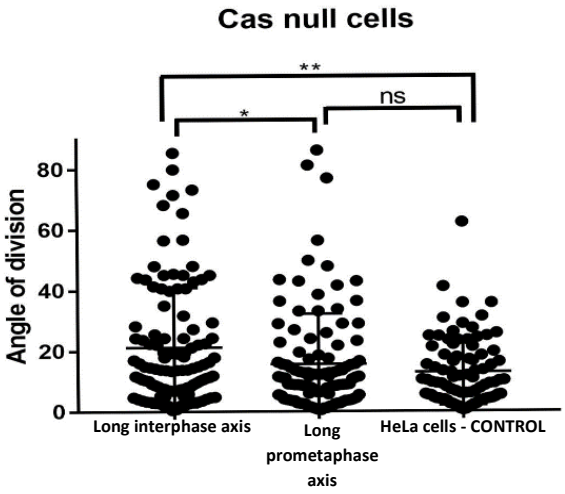
Cas null cells
**
*
ns
Angle of division
0
20
40
60
80
Long interphase axis
Long prometaphase axis
HeLa cells - CONTROL

B (a)

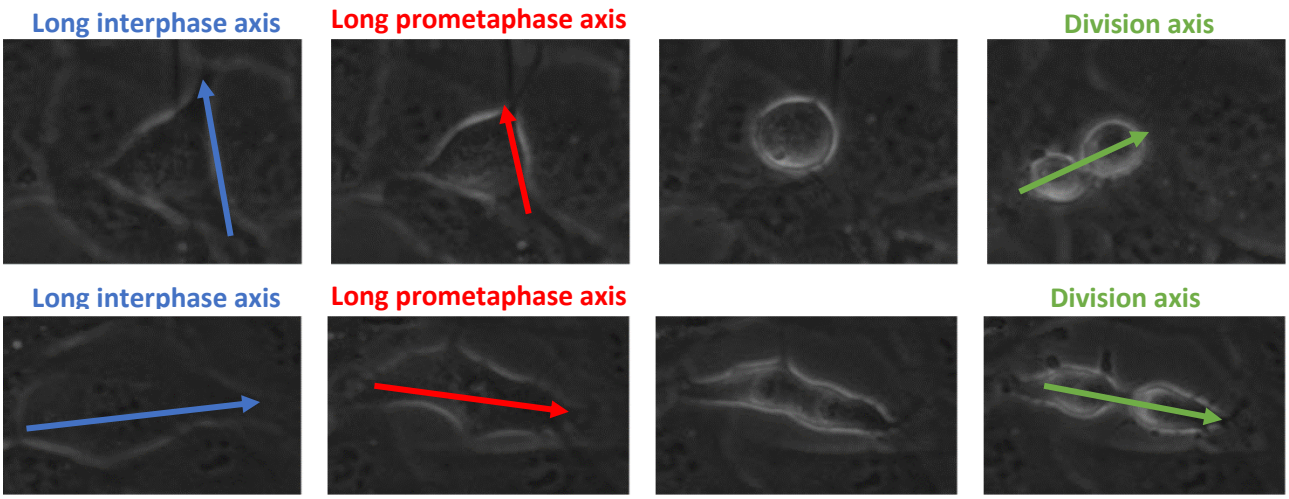
Long interphase axis
Long prometaphase axis
Division axis
Long interphase axis
Long prometaphase axis
Division axis

(b)

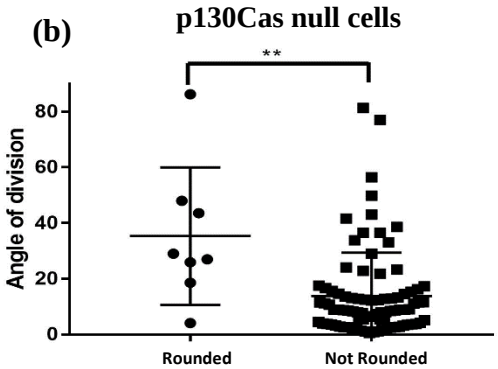
p130Cas null cells
**
Angle of division
0
20
40
60
80
Rounded
Not Rounded

Figure 1.11: Long prometaphase axis is a better predictor of spindle orientation in p130Cas null cells, which are oriented when anisotropic during metaphase, and misoriented when fully round

(A) (a) Live imaging of p130Cas null cells seeded on FN coated slide over 24 hours. Example of brightfield view of cells in which the division axis corresponds only with the long prometaphase axis or with both long interphase and long prometaphase axis, respectively.

(b) Quantification of the long interphase axis to the division axis and long prometaphase axis to division axis ratios measured in individuals p130Cas null cells. Statistical significance from paired t-test, n, number of p130Cas null cells, five independent experiments. Error bars represent S.E.M. The mean division angle in mitotic cells parallel to the long interphase axis is 21,22 ± 1,869°, n=111, in mitotic cells parallel to long prometaphase axis is 15,61 ± 1,58°, n=110 and in control mitotic cells is 12,95 ± 1,185°, n=86. p130Cas null cells are oriented when anisotropic and prefer better the long prometaphase axis than the long interphase axis to orient their spindle.

(B) (a) Live imaging of p130Cas null cells seeded on FN coated slide over 24 hours. Brightfield view of representative control cells that round up and become misoriented or remain anisotropic and become oriented, respectively with the images.

(b) Quantification of long prometaphase axis to division axis ratios measured in rounded and not rounded p130Cas null cells respectively. P values calculated by Mann-Whitney test; n, number of p130Cas null cells, 5 independent experiments. Error bars represent S.E.M. The mean division angle in rounded cells is 34,64 ± 7,733°, n=9, while in not rounded cells is 12,76 ± 1,539°, n=86. Once p130Cas null cells remain anisotropic during mitosis, they are oriented, while when they round up, they display misorientation.

5.2 Paxillin null fibroblasts maintain shape anisotropy throughout mitosis and consequently display correct orientation with respect to adhesion geometry

The second protein of interest was Paxillin, an adaptor protein of FAs (Schaller, 2001). Paxillin is known to be involved in SO with respect to the substrate based on previous published data, since cells lacking Paxillin displayed defects in SO with respect to the substrate (Petridou and Skourides, 2014). In order to address its implication in SO with respect to the geometry adhesion, we initially performed live imaging for 24 hours of the Paxillin null cell line, a mouse fibroblast derived cell line which lacks this protein. As shown in **Figure 1.12A**, there was not a clear preference of these cells for the long interphase axis or the prometaphase axis to orient their spindle. Specifically, the mean division angle in mitotic cells parallel to the long interphase axis was 25,88 ± 2,369°, while in mitotic cells parallel to long prometaphase axis was 21,01 ± 2,14°. As in the p130Cas null cell line, most of these cells remained anisotropic during mitosis and did not fully round up, with a lower percentage of them becoming round during metaphase. We, therefore, compared them with control HeLa cells and observed a slight misorientation that increased to total randomization of the spindle in fully rounded cells, something that was also observed in the p130Cas null cells, suggesting that rounded cells have a SO defect. Specifically, the mean division angle in rounded cells was 34,69 ± 5,287°, in not rounded cells was 19,47 ± 1,724° and in control cells was 12,95 ± 1,185° (**Figure 1.12A and 1.12B**).

A possibility as to why fully round cells during mitosis get misoriented, is that these cells do not have the ability to form proper retraction fibers during mitosis. RFs are known to keep the cell attached to its substrate while in mitosis, and at the same time they can exert force on the mitotic cortex guiding SO to be parallel to the major force vector. Lack of RFs would lead to spindle misorientation, since exertion of force on the cortex would be absent. Subsequently, to exclude the possibility that these cells, lacking Paxillin, have a defect in forming RFs, that are necessary for force exertion on the cortex, we transfected them with memRFP in order to observe the membrane and any other membrane based structures (such as RFs that are actin filled membrane tubes) and imaged them live. As shown in **Figure 1.12C**, Paxillin null cells form normal RFs, indicating that the cell line has no defect in RF formation and possibly no issues in exertion of force on the cortex.

A (a)

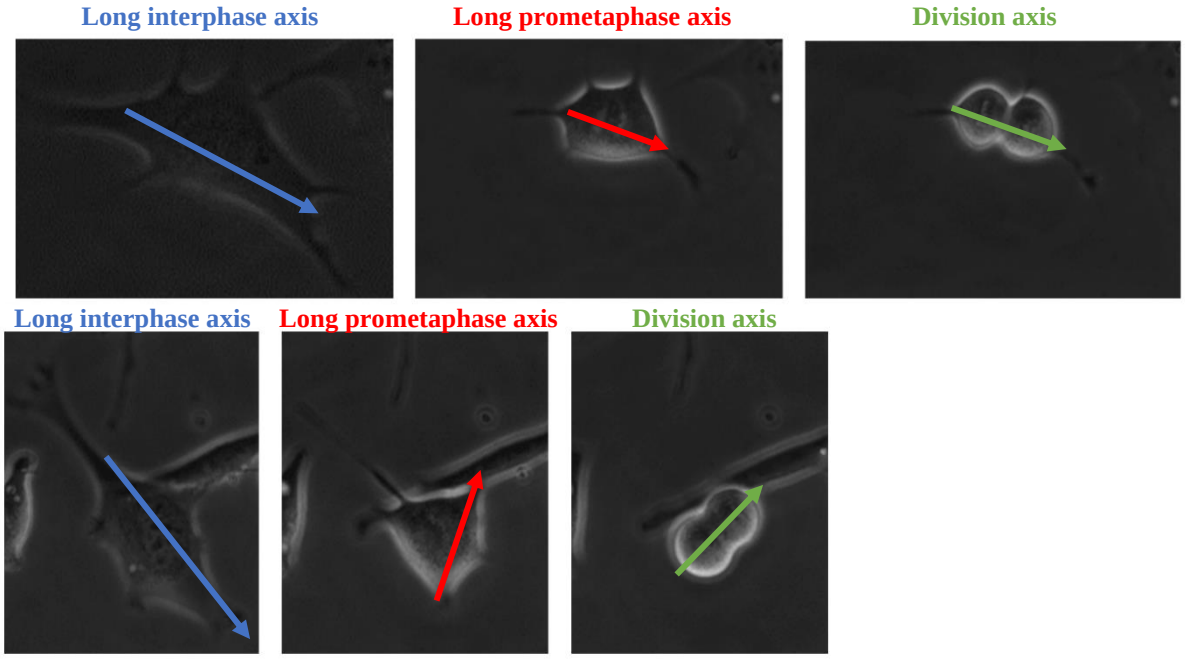
Long interphase axis
Long prometaphase axis
Division axis
Long interphase axis
Long prometaphase axis
Division axis

(b)

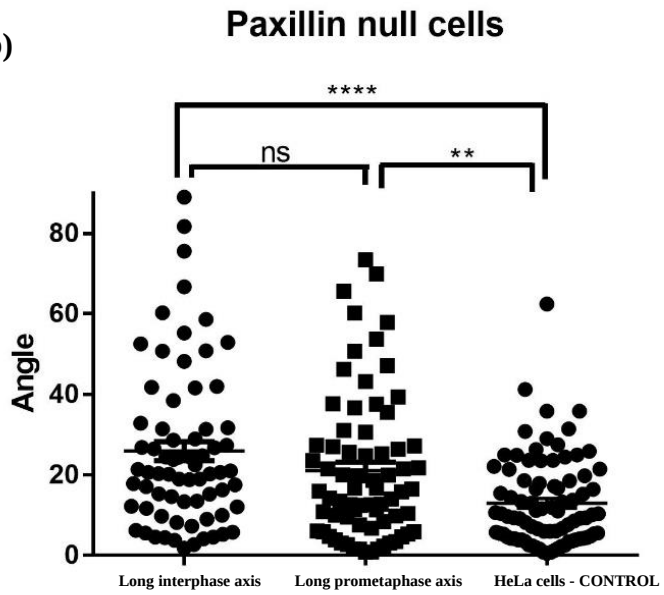
Paxillin null cells
****
ns
**
Angle
0
20
40
60
80
Long interphase axis
Long prometaphase axis
HeLa cells - CONTROL

B (a)

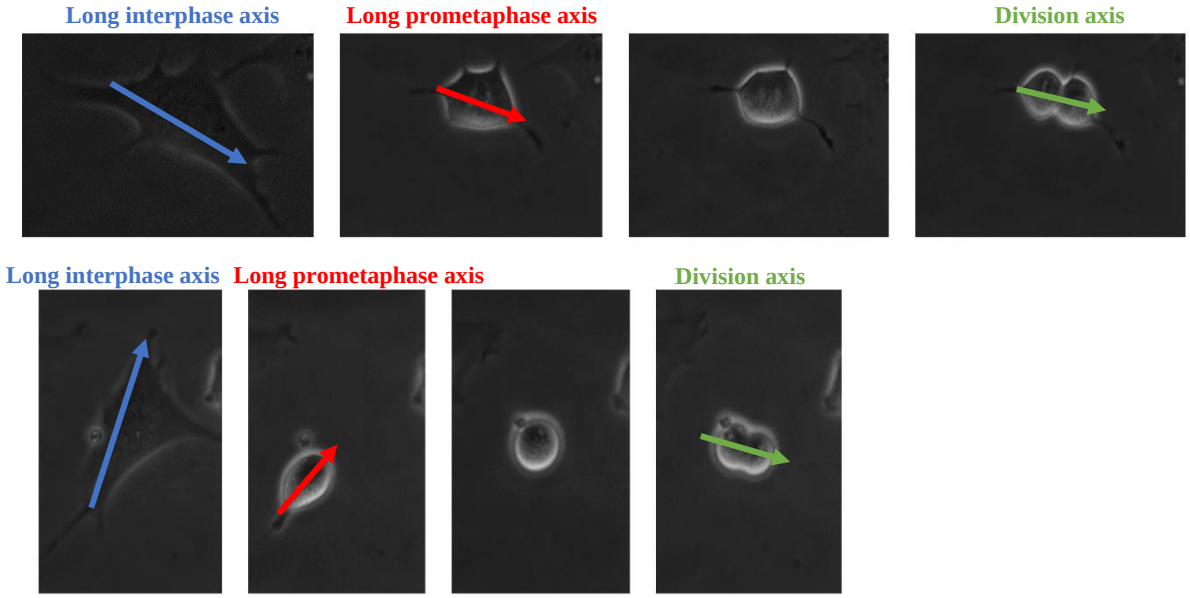
Long interphase axis
Long prometaphase axis
Division axis
Long interphase axis
Long prometaphase axis
Division axis

(b)

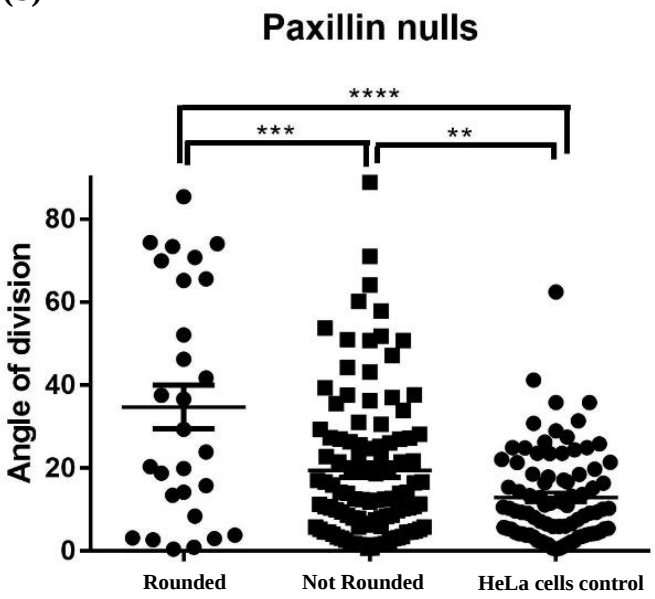
Paxillin nulls
****
***
**
Angle of division
0
20
40
60
80
Rounded
Not Rounded
HeLa cells control

C

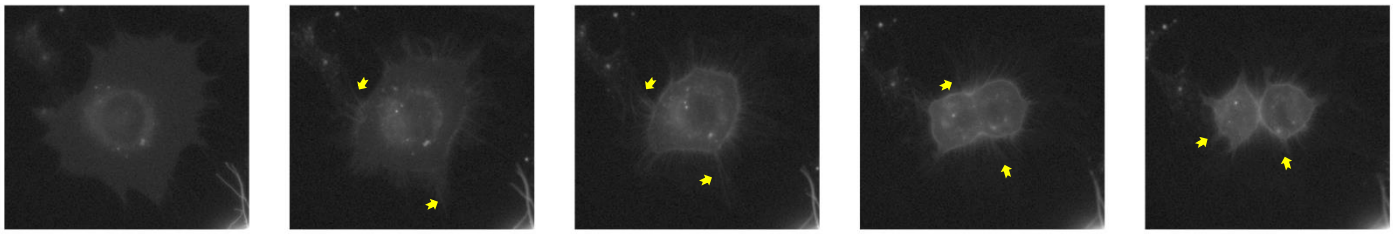

Figure 1.12: Paxillin null cells which remain anisotropic during mitosis display moderate spindle misorientation, that becomes fully randomized in rounded cells, without having defects in RF formation

(A) (a) Live imaging of Paxillin null cells seeded on FN coated slide over 24 hours. Example of brightfield view of cells in which the division axis corresponds only with the long prometaphase axis or with both long interphase and long prometaphase axis, respectively.

(b) Quantification of the long interphase axis to the division axis and long prometaphase axis to division axis ratios measured in individuals Paxillin null cells. Statistical significance from paired t-test, n, number of Paxillin null cells, seven independent experiments. Error bars represent S.E.M. The mean division angle in mitotic cells parallel to the long interphase axis is 25,88 ± 2,369°, n=70, while in mitotic cells parallel to long prometaphase axis is 21,01 ± 2,14°, n=71. Paxillin null cells are slightly misoriented compared with control cells.

(B) (a) Live imaging of Paxillin null cells seeded on FN coated slide over 24 hours. Brightfield view of representative control cells that round up and become misoriented or remain anisotropic and become oriented, respectively with the images.

(b) Quantification of long prometaphase axis to division axis ratios measured in rounded and not rounded Paxillin null cells and in HeLa cells. P values calculated by Mann-Whitney test; n, number of cells, seven independent experiments. Error bars represent S.E.M. The mean division angle in rounded cells is 34,69 ± 5,287°, n=28, in not rounded cells is 19,47 ± 1,724°, n=105 and in control cells is 12,95 ± 1,185°, n=86. Once Paxillin null cells remain anisotropic during mitosis, they are oriented, while when they round up, they display misorientation.

(C) Still images from live movie of a Paxillin null cell expressing memRFP during mitosis. Yellow arrowheads indicate the retraction fibers.

5.2.1 Use of micropatterned substrates for the investigation of spindle orientation in Paxillin null cells

Since we observed that the average cells that maintain their anisotropy during mitosis were oriented, while fully rounded cells displayed misorientation, we wanted to examine if seeding Paxillin null cells on linear micropatterns would push their shape anisotropy to the extreme and result in oriented spindles in most of the cells. For this purpose, we used micropatterning, a widely used approach that provides the opportunity to guide cell shape and eventually spindle orientation, due to the specific adhesion geometry that is provided to cells cultured on micropatterns. When cells are seeded on shapes that have a clear long axis, such as a long line, they acquire that shape and when they enter mitosis, they are shown to orient their spindle parallel to the long axis of the interphase shape. This is explained by the fact that the longest RFs (and the ones exerting the most force) will be formed along the long interphase axis creating a footprint as to where the cell was attached before, and thus the major force vector on the cortex of the mitotic cell will align with that. Controlling the shape of the interphase cell makes prediction of the orientation of the division easier and more specific.

We then went on to seed Paxillin null cells on linear patterns to force them in a very elongated shape, where their spindle should be oriented parallel to the longest axis and compared them with cells that were cultured on a non-pattern substrate. Immunofluorescence (IF) experiments were also carried out using the antibody against β-tubulin, in order to visualize the spindles of cells cultured in linear micropatterns. As shown in **Figure 1.13A and 1.13B**, cells seeded on these micropatterned substrates displayed a clear anisotropic shape during metaphase, resulting in a decreased number of rounded cells, and that shape guided the spindle to be parallel to the long axis even better due to the increased anisotropy. Consistent with the above result, quantifications revealed that cells on micropatterns were oriented and had an average angle below 5 degrees in respect to the long axis, in comparison with cells on a non-patterned substrate that display an average angle above 20 degrees, suggesting that null cells with a heavily anisotropic cortex that remains anisotropic during mitosis do not have any defects in spindle orientation (**Figure 1.13C**).

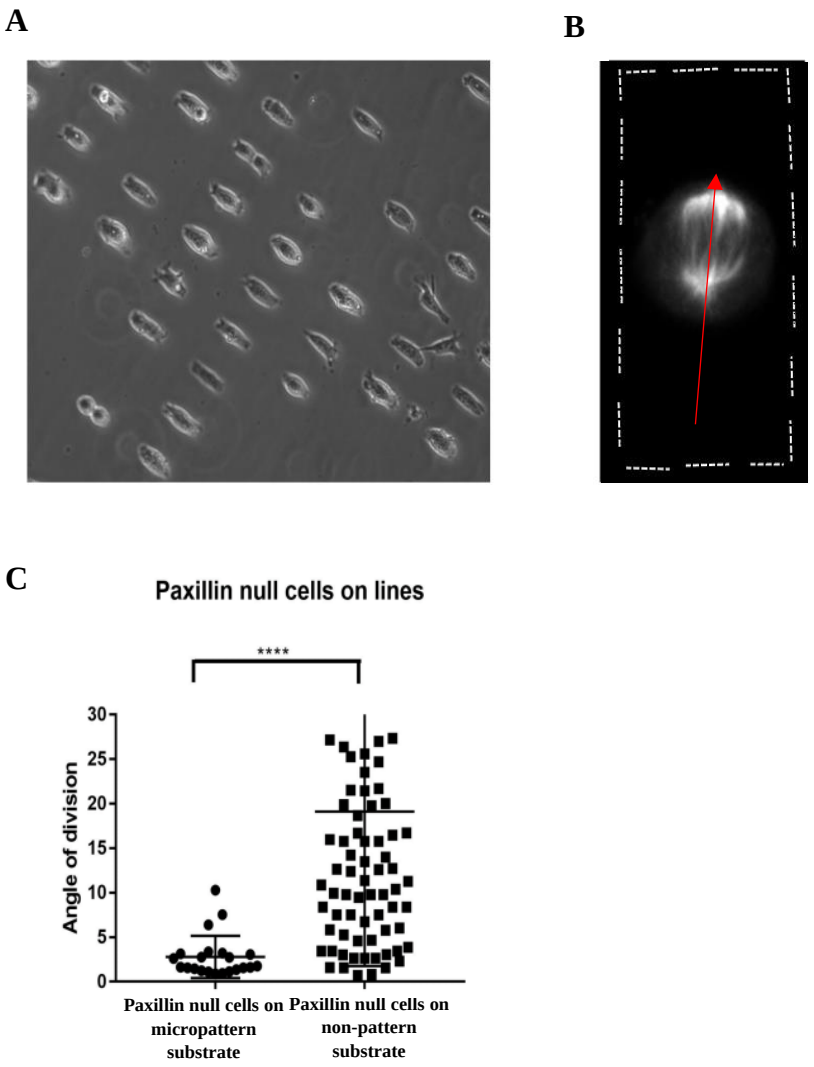

Figure 1.13: Paxillin null cells seeded on Fibronectin micro-patterned substrates verify that when they remain anisotropic, they do not show defects in spindle orientation

Paxillin null cells were seeded sparsely on Fibronectin patterns on PLL-Peg coated glass and live imaged over 24 hours. Spindles are visualized through staining for β-tubulin.

(A) Brightfield view of cells spread on linear pattern adopting an elongated shape

(B) A mitotic cell on a linear pattern that is shown by white dotted lines. The spindle is oriented parallel to the long axis.

(C) Quantification of long prometaphase axis to division axis ratios measured in Paxillin null cells seeded on micropatterns and cells seeded on non-micropatterns substrate respectively. P values calculated by Mann-Whitney test; n, number of Paxillin null cells, three independent experiments. Error bars represent S.E.M. The mean division angle in cells on micropatterns is 2,789 ± 0,5055°, n=22 while in cells on the non-micropattern substrate is 19,12 ± 1907°, n=83. When Paxillin null cells were pushed to extreme anisotropy, most of them were oriented, suggesting that probably cells remaining anisotropic don't have defects in spindle orientation.

5.2.2 p130Cas and Paxillin null round mitotic cells display spindle misorientation

Both null cell lines that were used in the previous experiments are mouse embryonic fibroblasts. Unpublished data from our laboratory has shown that other fibroblasts, including FAK null cells or NIH3T3, also remain anisotropic during mitosis, suggesting the possibility that fibroblasts never fully round up in their normal environment and remaining anisotropic is an inherent property. Additionally, due to their low contractile actin (Shakiba et al., 2020), they are unable to round efficiently, reinforcing the possibility that anisotropy during mitosis is indeed an inherent property of fibroblasts. It is also known that, every cell that divides symmetrically has inherited the mechanism of sensing the astral microtubule length that results in the positioning of the mitotic spindle at the center of the cell, and also the alignment of the spindle where the astral microtubules will be the longest, and thus strongest, when captured on the cortex (Tame et al., 2014). Indeed, this mechanism is built-in in fibroblasts, but it is uncertain if this is the mechanism that leads to the lack of misorientation in these cells when they remain anisotropic during mitosis. Unpublished data from our laboratory suggested that when anisotropy remains there is a default mechanism through astral microtubules, but when cells round up, they need force sensing through RFs to orient their spindle with respect to their initial adhesion. Conclusively, if memory remains due to anisotropy, cells do not need the RFs to exert forces on the cortex anymore in order to orient their spindles (**Figure 1.14**). Since we showed that null cells can form retraction fibers and thus eliminated the possibility of no force exertion on the cortex, the most likely explanation is that these cells are failing to sense these forces and properly orient their spindles when they round-up, supporting the involvement of Paxillin in the mechanosensing in these cells.

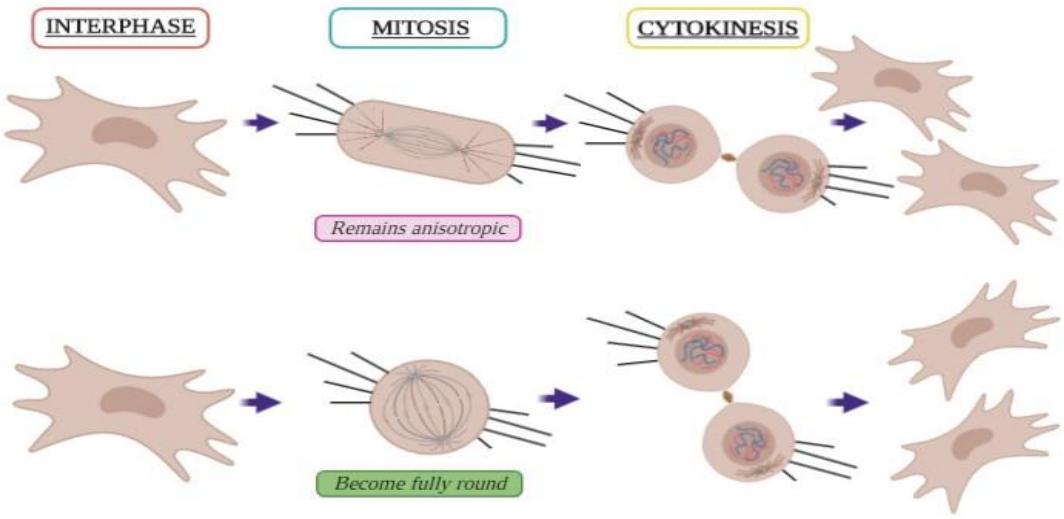

Figure 1.14: Schematic representation of mitotic cells and outcome of division both in the case when cells remain anisotropic or become fully round (Scheme made by online program Biorender)

5.2.3 Expression of Paxillin W.T in Paxillin null round mitotic cells fails to rescue spindle orientation defects

We moved on to examine if the misorientation that rounded cells display can be rescued by the re-introduction of Wild Type Paxillin in these cells. Paxillin null cells were transfected with Paxillin and then imaged live. Quantifications revealed that, in a similar fashion as the nulls, cells expressing Paxillin WT did not have a preference for long interphase axis or prometaphase axis to orient their spindle. Specifically, the mean division angle in mitotic cells parallel to the long interphase axis was 26,06 ± 1,799°, while in mitotic cells parallel to long prometaphase axis was 21,41 ± 1,544° (**Figure 1.15A**). Subsequently, we compared Paxillin null cells with cells expressing Paxillin W.T and with control HeLa cells. Remarkably, only a moderate rescue was observed overall, while rounded cells appeared to be non-rescuable at all, remaining misoriented even after the re-introduction of Paxillin. Specifically, the mean division angle in rounded cells was 36,3 ± 5,307°, in not rounded cells was 17,32 ± 1,964° and in control HeLa cells was 12,95 ± 1,185° (**Figure 1.15B**).

Conclusively, since the only cells exhibiting a defect in SO were the ones that became fully round, which were a very small number in comparison with the majority of the rest remaining anisotropic and oriented, and since this defect was not rescued with the re-introduction of Paxillin WT, we were not able to arrive to a safe conclusion with the use of this null cell line. For that reason, we went on to use a different approach to characterize the involvement of Paxillin in SO, with the use of a Paxillin dominant negative and its introduction in HeLa cells.

A (a)

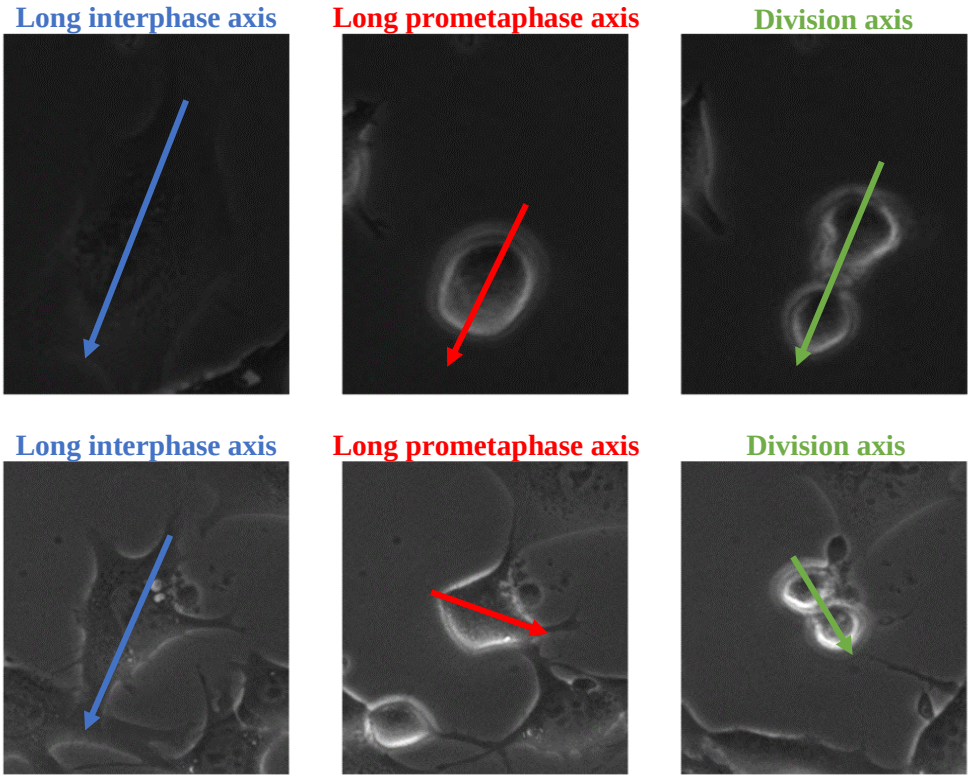
Long interphase axis
Long prometaphase axis
Division axis
Long interphase axis
Long prometaphase axis
Division axis

(b)

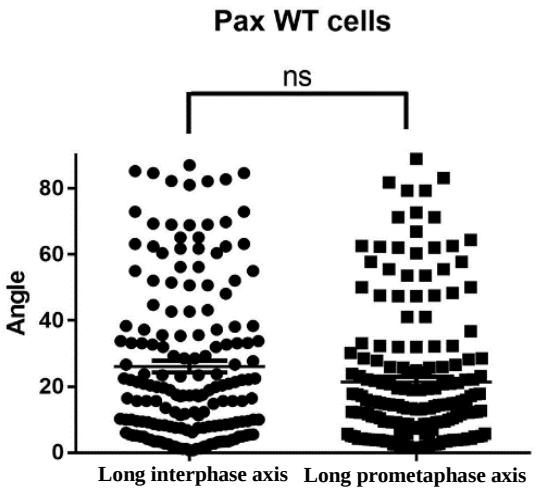
Pax WT cells
ns
Angle
0
20
40
60
80
Long interphase axis
Long prometaphase axis

B (a)

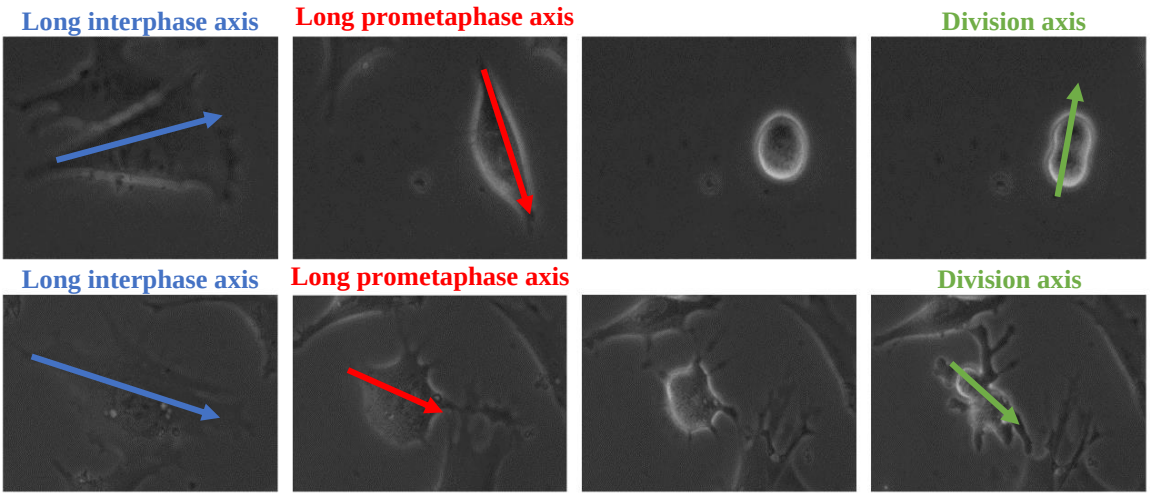
Long interphase axis
Long prometaphase axis
Division axis
Long interphase axis
Long prometaphase axis
Division axis

(b)

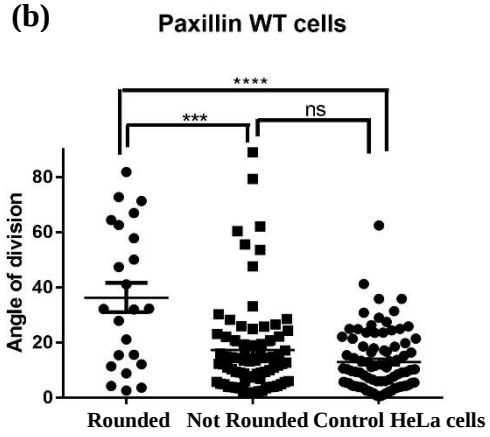
Paxillin WT cells
****
***
ns
Angle of division
0
20
40
60
80
Rounded
Not Rounded
Control HeLa cells

(c)

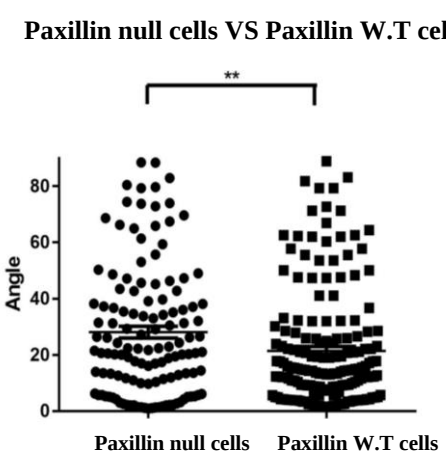
Paxillin null cells VS Paxillin W.T cells
**
Angle
0
20
40
60
80
Paxillin null cells
Paxillin W.T cells

(d)

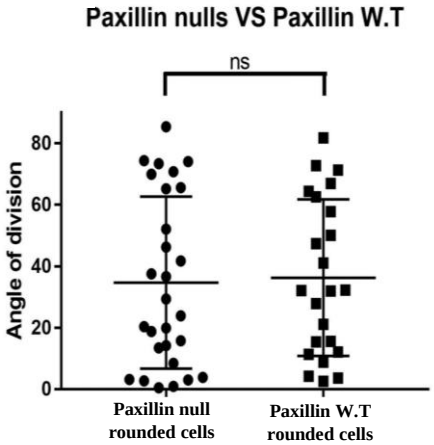
Paxillin nulls VS Paxillin W.T
ns
Angle of division
0
20
40
60
80
Paxillin null rounded cells
Paxillin W.T rounded cells

Figure 1.15: Paxillin null cells cannot be efficiently rescued after re-introduction of WT Paxillin

(A) (a) Live imaging of Paxillin null cells expressing Paxillin WT, seeded on FN coated slide over 24 hours. Example of brightfield view of these cells in which the division axis corresponds with both long interphase and long prometaphase axis or only with the long prometaphase axis, respectively.

(b) Quantification of the long interphase axis to the division axis and long prometaphase axis to division axis ratios measured in individual cells expressing Paxillin W.T. Statistical significance from paired t-test, n, number of Paxillin W.T expressors, five independent experiments. Error bars represent S.E.M. The mean division angle in mitotic cells parallel to the long interphase axis is 26,06 ± 1,799°, n=171, while in mitotic cells parallel to long prometaphase axis is 21,41 ± 1,544°, n=177. Cells expressing Paxillin W.T don't show a preference for long interphase axis or long prometaphase axis.

(B) (a) Live imaging of Paxillin null cells expressing Paxillin W.T seeded on FN coated slide over 24 hours. Brightfield view of representative expressor cells that round up and become misoriented or remain anisotropic and become oriented, respectively with the images.

(b) Quantification of long prometaphase axis to division axis ratios measured in rounded and not rounded expressor cells respectively and in control HeLa cells. P values calculated by Mann-Whitney test; n, number of expressor cells, five independent experiments. Error bars represent S.E.M. The mean division angle in rounded cells is 36,3 ± 5,307°, n=23, in not rounded cells is 17,32 ± 1,964°, n=77 and in control cells is 12,95 ± 1,185°, n=86. Cells expressing Paxillin W.T displayed SO defects when become fully rounded up.

(c) Quantification of long prometaphase axis to division axis ratios measured in Paxillin null cells and Paxillin null cells expressing Paxillin W.T, respectively. P values calculated by Mann-Whitney test; n, number of expressor cells, five independent experiments. Error bars represent S.E.M. The mean division angle in rounded cells is 28,08 ± 2,069°, n=127 while in not rounded cells is 21,41 ± 1,544°, n=177. Re-introduction of Paxillin in Paxillin null cells show a slight rescue overall probably due to the big number of cells.

(d) Quantification of long prometaphase axis to division axis ratios measured in round Paxillin null cells and round Paxillin null cells expressing Paxillin W.T, respectively. P values calculated by Mann-Whitney test; n, number of expressor cells, five independent experiments. Error bars represent S.E.M. The mean division angle in Paxillin null rounded cells is 47,50 ± 6,000°, n=20 while in not rounded cells is 37,89 ± 5,671°, n=21. Re-introduction of Paxillin in round Paxillin null cells cannot rescue at all the defects in SO.

5.3 Characterization of the effects of Paxillin C-terminus expression in HeLa cell line

We then moved on to design and test a new dominant negative that would block the scaffolding functions of Paxillin in HeLa cells, in order to examine its role in SO. This approach was considered safer than downregulation of Paxillin given that Paxillin homologues, including Hic5 and Leupaxin, could potentially create redundancy (Fujita et al., 1998, Hagel et al., 2002, Thomas et al., 1999b). Previous work revealed that the LIM domains, and more specifically LIM 3 and LIM 4 of Paxillin (López-Colomé et al., 2017., Theodosiou et al., 2015, Zhu et al., 2019), are necessary for its targeting at FA sites, while its LD motifs are responsible for its interaction with many proteins, including FAK and ILK (**Figure 1.16**, Brown et al., 1998, Brown and Turner, 2004). Importantly, some of these proteins, such as FAK, are relying on Paxillin to be targeted at FAs and possibly to be recruited at the CMC at the lateral cortex of the mitotic cell, participating in proper SO with respect to the plane of the substrate (z axis) (Petridou and Skourides, 2016).

We therefore needed to generate a construct which can act as a DN, preserving the ability to get targeted at FAs, while inhibiting any downstream signaling Paxillin would promote. Thus, we generated a fragment of the protein that contains the LIM domains, but lacks the LD motifs, making this construct able to target FAs through the LIM domains, while the lack of the LD motifs would prevent any interaction with other proteins, inhibiting Paxillin's scaffolding activity. The construct was fused with GFP for visualization and was used in order to address Paxillin role in SO *in vitro* and *in vivo*. This DN will be hereafter referred to as PaxC.

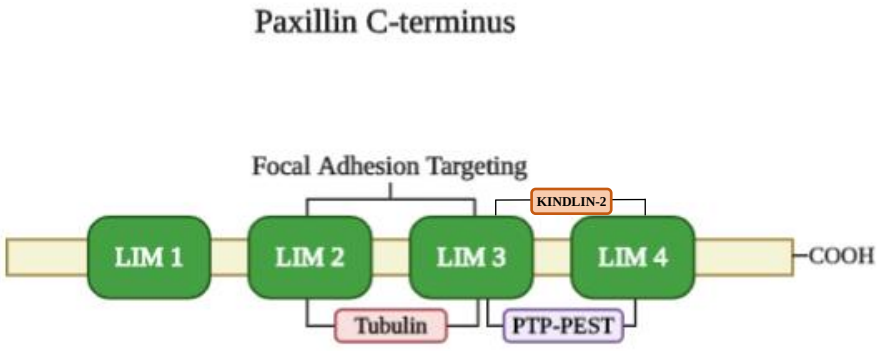

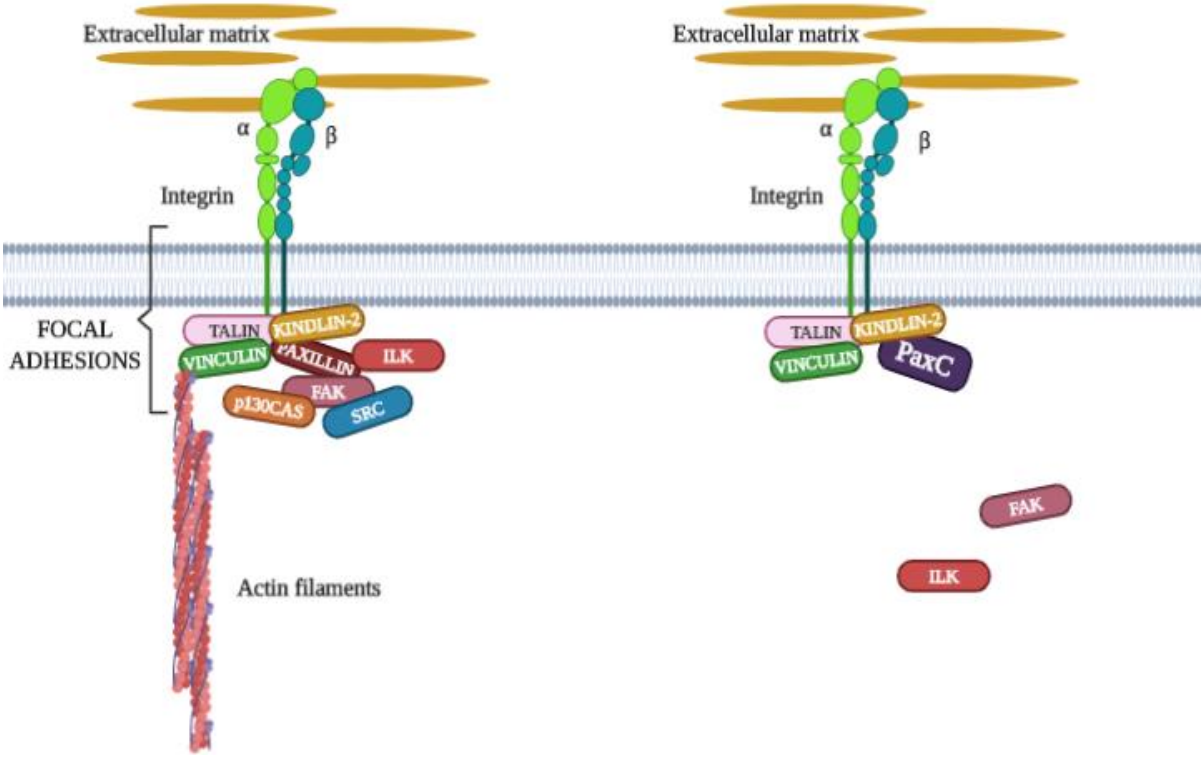

Figure 1.16: Schematic representation of the Paxillin C-terminus structure and its function as a Dominant Negative (Schemes made by online program Biorender)

(A) Structure of the C-terminus of Paxillin, which contains four LIM domains.

(B) The localization of Paxillin at FAs through its LIM domains, where it recruits other proteins, including FAK and ILK, through its LD motifs.

(C) The localization of PaxC at FAs through its LIM domains, where it acts as a DN by abolishing the interactions with several proteins due to the lack of the LD motifs.

5.3.1 Paxillin C-terminus expression does not affect cell spreading, migration or mitotic duration in HeLa cells

Since it has been shown that fibroblasts from Paxillin knockout mice displayed reduced rates of cell migration and defects on cell spreading (Hagel et al., 2002), we initially went on to characterize the effects of PaxC expression in these processes as well as in the duration of mitosis in HeLa cells. For this purpose, we transfected these cells with GFP PaxC, seeded them on a FN coated slide and imaged them for a period of 24 hours. In order to quantify the spreading efficiency of cells we measured the cell diameter before and after mitosis, taking into consideration that the diameter of control HeLa cells is between 15-20 μm. Quantification of the ratio of spreading before mitosis and after mitosis of individual cells showed that the expression of PaxC didn't affect cell spreading (**Figure 1.17A**). In addition, as shown in **Figure 1.17B**, further analysis of the time-lapse movie showed that the DN expression did not affect duration of mitosis of individual cells. Additionally, quantification of the mean track length of individual cells showed that migration of these cells was not affected by the expression of PaxC (**Figure 1.17C**). For this purpose, we used the iMaris Software and manually tracked individual cells over a period of 24 hours, while the software was automatically calculating the track length of each cell. Collectively, these data suggest that PaxC is a poor DN with respect to FA dependent functions of the protein.

A

Spreading of HeLa cells expressing Paxillin C-terminus

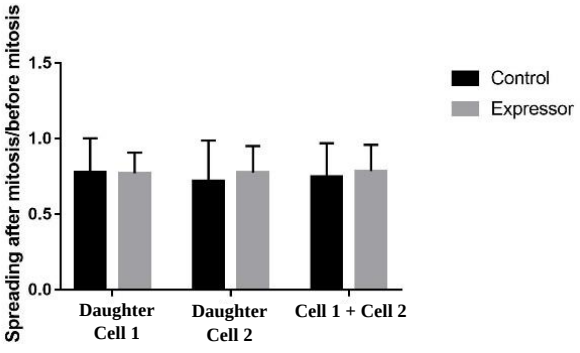

B

Duration of Mitosis of HeLa cells expressing Paxillin C-terminus

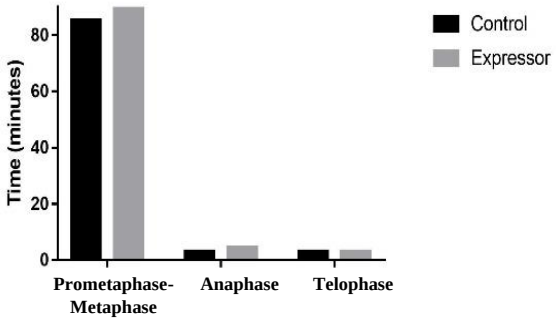

C

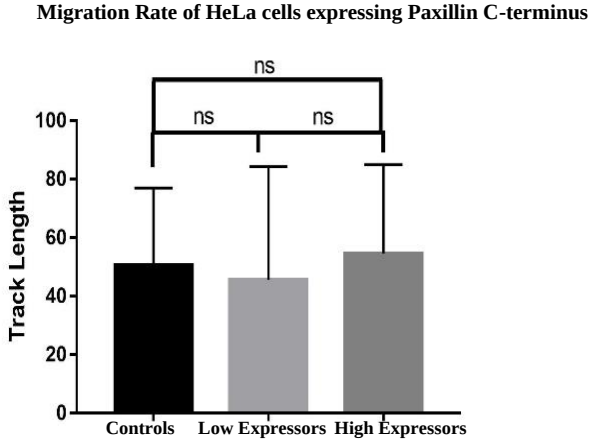

Figure 1.17: Expression of Paxillin C-terminus does not affect cell spreading, cell migration and duration of mitosis in HeLa cells.

(A) Quantification of before mitosis to after mitosis spreading ratios measured in HeLa cells expressing PaxC. P-values calculated by 2way ANOVA test. Expression of PaxC does not affect cell spreading. Error bars represent standard S.E.M.

(B) Expression of PaxC does not affect duration of mitosis in HeLa cells. The time of each individual mitotic cell was measured and compared with control HeLa cell.

(C) Expression of PaxC does not affect cell migration. The track length is 50,51 ± 3,984, n=44 cells for controls, 45,62 ± 7,892, n=24 cells for low expressors and 54,59 ± 6,08, n=25 cells for high expressors. Error bars represent standard S.E.M.

5.3.2 Expression of Paxillin C-terminus leads to dose-dependent displacement of Paxillin from FAs in HeLa cells

Since expression of PaxC did not affect cell spreading, migration or duration of mitosis, we moved on to examine its ability to act as a DN and displace its primary target, the protein Paxillin, from FAs. Initially, HeLa cells were transfected with GFP PaxC, seeded on fibronectin-coated coverslips for two hours, fixed and stained for Paxillin, in order to determine if the endogenous protein is displaced from the FAs, and Vinculin, that was used as an FA marker (**Figure 1.17A)**. In order to detect only endogenous Paxillin, the antibody that was used recognizes an epitope outside of the C-terminus. Vinculin staining was used as the reference of a protein that would remain constant, since it is known to be recruited at the FAs prior to Paxillin and it was not expected to be affected by the expression of the PaxC. As expected PaxC displayed strong FA localization and as shown in **Figure 1.17B** and **1.17C**, its expression led to the partial displacement of Paxillin from FAs, while Vinculin localization was unaffected.

In order to quantify the efficiency of displacement of endogenous Paxillin we calculated the ratio of Paxillin to Vinculin signal intensity at FAs in control and transfected cells. The results revealed that PaxC expression led to a 1.5-fold reduction of the Paxillin to Vinculin ratio in expressor cells, indicating the ability of PaxC to partially displace Paxillin from FAs. We then examined how the levels of PaxC expression affected displacement efficiency. Interestingly, we discovered that PaxC displaced Paxillin in a dose-dependent manner. Specifically, in cells expressing relatively high levels of PaxC, we noticed a significant loss of Paxillin from FAs, while in low expressors, the displacement levels were very low, compared to control cells (**Figure 1.17B and 1.17C**). Expressors were classified as high or low by using the median GFP intensity of the cytosol from all the cells in the experiment. The above result suggest that PaxC can be used as a DN since it prevents the recruitment of Paxillin at FAs, however the low efficiency by which it does so also suggests that for a strong DN effect at FAs, very high levels of this construct would need to be expressed.

A

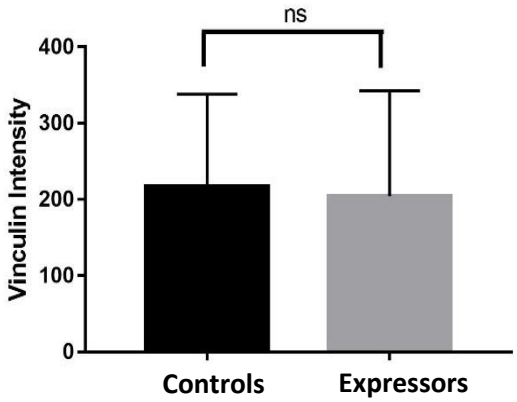
ns
400
300
200
100
0
Vinculin Intensity
Controls
Expressors

B

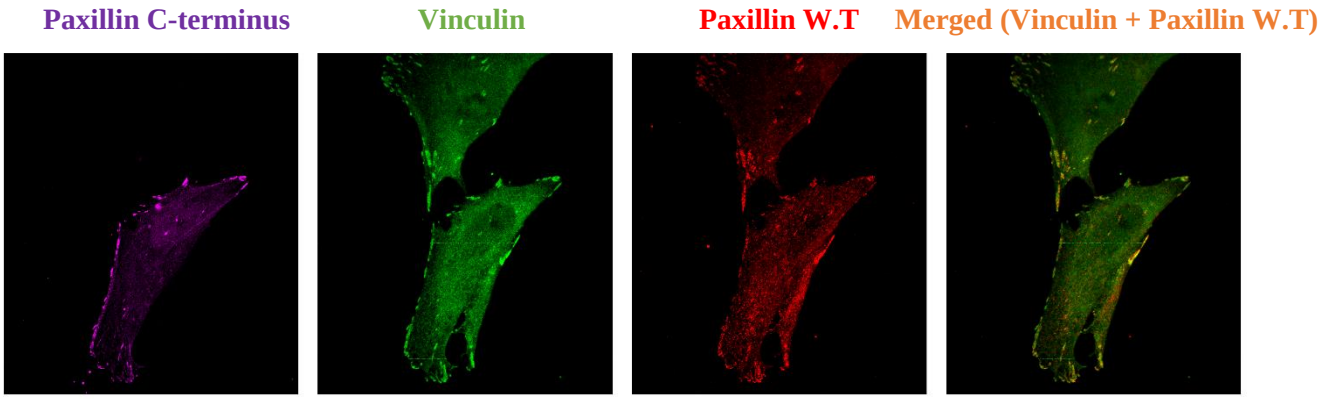
Paxillin C-terminus
Vinculin
Paxillin W.T
Merged (Vinculin + Paxillin W.T)

C

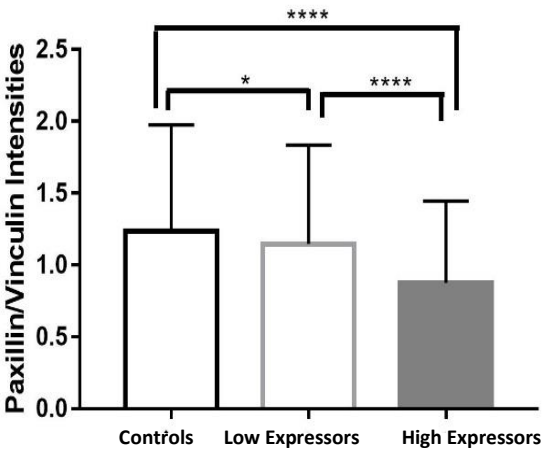
****
*
****
2.5
2.0
1.5
1.0
0.5
0.0
Paxillin/Vinculin Intensities
Controls
Low Expressors
High Expressors

Figure 1.17: Expression of Paxillin C-terminus leads to a dose-dependent displacement of endogenous Paxillin from FAs.

(A) Quantification of Vinculin mean intensity from FAs of control cells and cells expressing GFP PaxC, from a two-tailed unpaired t-test. Error bars represent S.E.M. The mean intensity in control cells is 217,3 ± 4,856, n=618 focal adhesions, and in expressor cells is 204,3 ± 4,74, n= 848 focal adhesions. Since Vinculin localization at FAs is unaffected, it is used as an FA marker.

(B) Confocal images of PFA fixed HeLa cells, transiently transfected with GFP PaxC and stained for Paxillin and Vinculin. In control cells Paxillin is present at FAs, which are labeled with Vinculin. In expressor cells there is a dose-dependent and partial displacement of Paxillin from FAs. In contrast, Vinculin localization at FAs is unaffected.

(C) Quantification of the Paxillin/Vinculin mean intensity ratio from the FAs of control and expressor cells, from a two-tailed unpaired t-test. Error bars represent S.E.M. The mean ratio in control cells is 1,239 ± 0,0299, n=608 focal adhesions, in low expressors is 1,146 ± 0,03276, n=442 focal adhesions, and in high expressors is 0,8764 ± 0,02894, n=386 focal adhesions. Expression of PaxC result in a dose-dependent displacement of Paxillin from FAs.

5.3.3 Expression of Paxillin C-terminus leads to dose-dependent displacement of FAK and ILK from FAs in HeLa cells

Given the displacement of Paxillin from the FAs in expressors cells, we went on to examine how the localization of other FA proteins that interact with Paxillin, such as FAK and ILK, would be affected. For this purpose, we carried out immunofluorescence (IF) experiments on HeLa cells transfected with PaxC and stained with antibodies against FAK or ILK, along with Vinculin as a marker for FAs. As shown in **Figure 1.18**, there was a visible displacement of both FAK and ILK from the FAs of the expressor cells respectively, while Vinculin levels remained unaltered in both experiments. Quantification of FAK to Vinculin mean intensities revealed a 2.5-fold reduction of the FAK to Vinculin ratio in expressor cells, while ILK to Vinculin mean intensities revealed a 2-fold reduction of ILK to Vinculin ratio in expressors. Additionally, similarly with Paxillin displacement, both FAK and ILK displacement exhibited a dose-dependence as expected. Overall, these data confirm that PaxC acts as a DN, by perturbing the scaffolding functions of the protein. In line with the moderate ability of the PaxC to displace endogenous Paxillin effective displacement of FAK and ILK requires high levels of

PaxC expression which is in agreement with the small effect PaxC expression has on cell spreading and migration.

A

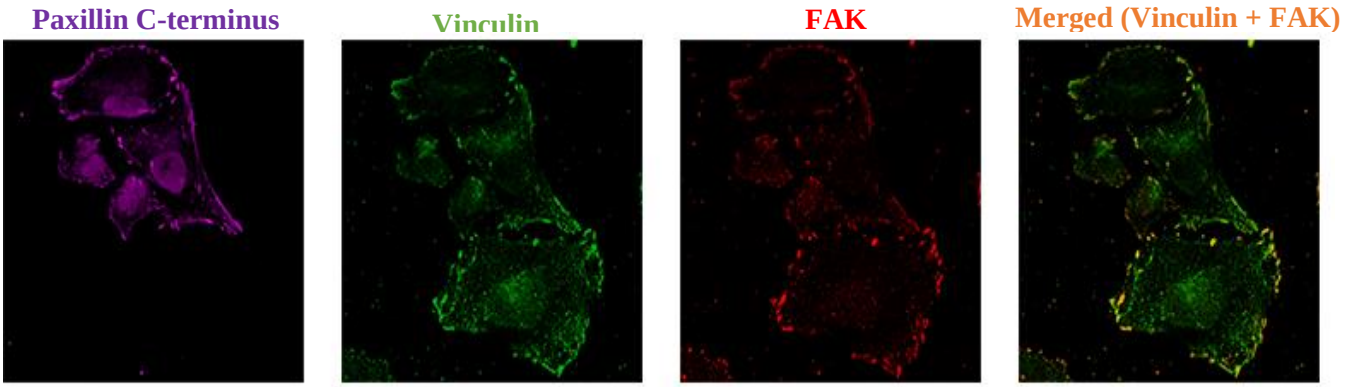

B

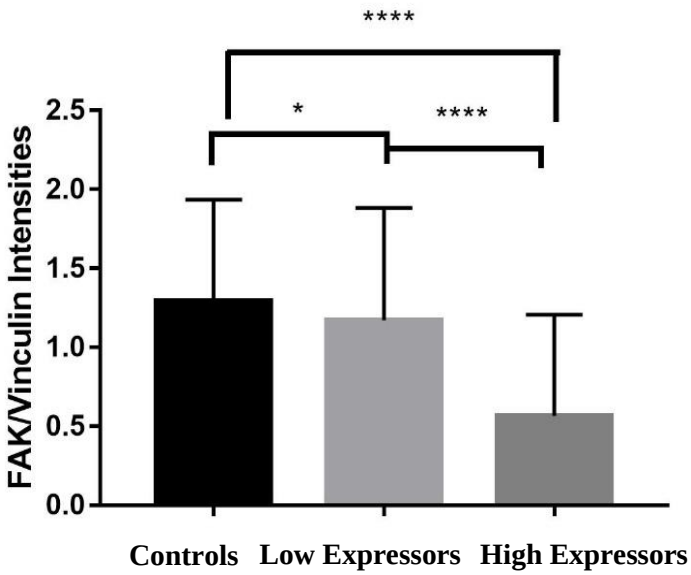

C

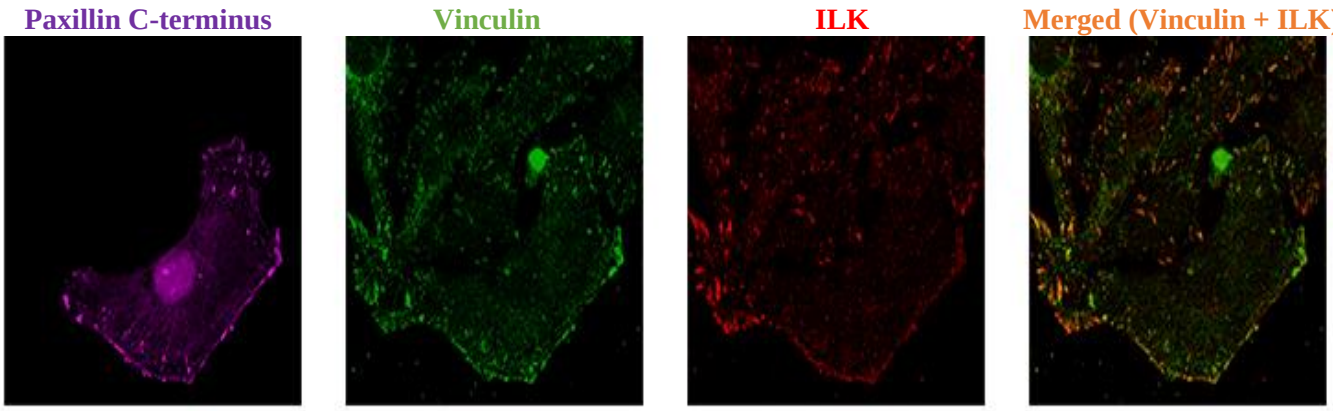
Paxillin C-terminus
Vinculin
ILK
Merged (Vinculin + ILK)

D

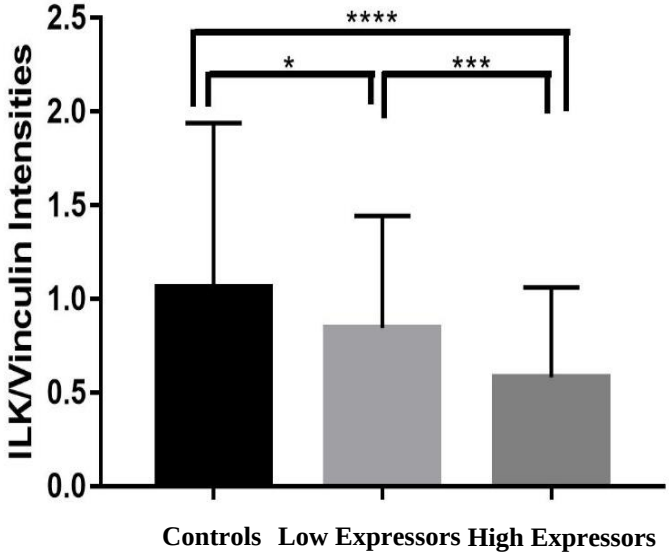
ILK/Vinculin Intensities
2.5
2.0
1.5
1.0
0.5
0.0
****
*
***
Controls
Low Expressors
High Expressors

Figure 1.18: Expression of Paxillin C-terminus leads to partial and dose-dependent displacement of FAK and ILK from FAs, respectively.

(A) Confocal images of PFA fixed HeLa cells, transiently transfected with GFP PaxC and stained for FAK and Vinculin. In control cells FAK is present at FAs, labeled with Vinculin. In expressor cells there is a dose-dependent and partial displacement of FAK from FAs. In contrast, Vinculin localization at FAs is unaffected.

(B) Quantification of the FAK/Vinculin mean intensity ratio from the FAs of control and expressor cells, from a two-tailed unpaired t-test. Error bars represent S.E.M. The mean ratio in control cells is 1,29 ± 0,03351, n=370 focal adhesions, in low expressors is 1,173 ± 0,06803, n=109 focal adhesions, and in high expressors is 0,566 ± 0,05544, n=134 focal adhesions. Expression of PaxC result in dose-dependent displacement of FAK from FAs.

(C) Confocal images of PFA fixed HeLa cells, transiently transfected with GFP Paxillin C-terminus and stained for ILK and Vinculin. In control cells ILK is present at FAs, labeled with Vinculin. In expressor cells there is a dose-dependent and partial displacement of ILK from FAs. In contrast, Vinculin localization at FAs is unaffected.

(D) Quantification of the ILK/Vinculin mean intensity ratio from the FAs of control and expressor cells, from a two-tailed unpaired t-test. Error bars represent S.E.M. The mean ratio in control cells is 1,062 ± 0,04883, n=324 focal adhesions, in low expressors is 0,8465 ± 0,06455, n=86 focal adhesions, and in high expressors is 0,5815 ± 0,0475, n=103 focal adhesions. Expression of PaxC result in dose-dependent displacement of ILK from FAs.

5.3.4 Paxillin C-terminus has a lower affinity for FAs than full length Paxillin

Since we showed that expression of PaxC leads to the displacement of Paxillin from FAs, but in a less efficient way than we hoped for, we went on to examine why the expression of relatively high levels of PaxC were still not able to displace all the endogenous protein. If the affinity of PaxC for FAs is lower than endogenous Paxillin, these observations can be explained. For this purpose, we went on to explore the above possibility by using Fluorescence Recovery After Photobleaching (FRAP) in live cells co-transfected with GFP PaxC and RFP Paxillin. By using this technique, the kinetic parameters of a protein of interest can be examined. Specifically, after photobleaching a group of a fluorescently tagged protein within a specific area of the cell, the recovery time of the remaining fluorescent molecules into the bleached area can be measured (Alberts et al., 2015).

As shown in **Figure 1.19A and 1.19B**, after photobleaching individual FAs, we observed that the Immobile Fraction (FI%) of RFP Paxillin was higher than that of GFP PaxC, suggesting that full-length Paxillin has a slower off-rate and thus, a higher affinity for FAs. The above results suggest that multiple interactions of Paxillin through its LD domains with other FA proteins, like FAK and more importantly with FA proteins which either do not depend on Paxillin for their FA localization like Vinculin or only partially do so like ILK, allow the full length protein to create a network of interactions that increase its residence time in the complex by reducing its off rate. This makes competition and displacement by PaxC less efficient within these large stable macromolecular complexes.

A

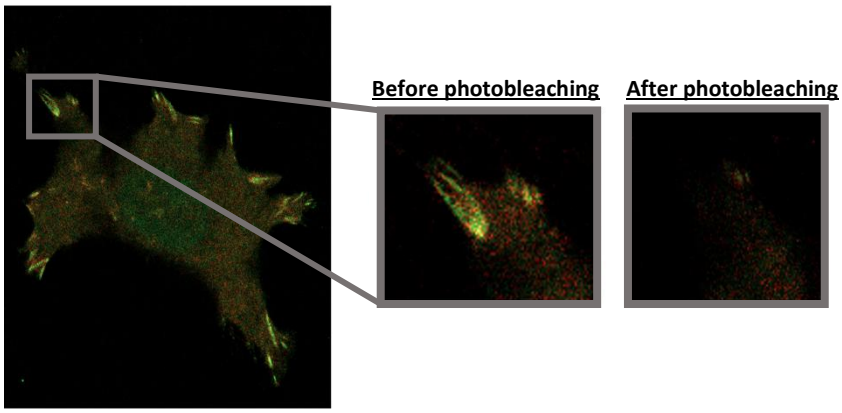

B

FI% of GFP Paxillin C-terminus	FI% of RFP Paxillin WT
17,252	27,917
18,550	26,591
6,850	25,151
15,139	21,244
9,027	28,100
17,268	25,588
19,705	27,683

Figure 1.19: Endogenous Paxillin has higher affinity for FAs than the PaxC

(A) Images showing HeLa cells co-transfected with GFP PaxC and RFP Paxillin and subjected to photobleaching of their FAs, before and after the bleaching event.

(B) Table showing all values of FI% for GFP PaxC and RFP Paxillin at each FA that was photobleached. RFP Paxillin has higher FI%, proposing that its off rate is slower and its affinity for FAs higher than that of the GFP PaxC.

5.3.5 Super-resolution confocal imaging and Acceptor Photo-bleaching FRET experiments reveal the spatial segregation between Paxillin C-terminus and endogenous Paxillin within individual FAs

We subsequently wanted to examine the spatial distribution of the PaxC and endogenous Paxillin in FAs, since endogenous Paxillin cannot be fully displaced from FAs. In order to address this, immunofluorescence experiments were carried out in PaxC expressing and control cells followed by imaging of the FAs using super-resolution microscopy. Additionally, in order to get a better picture of the distribution of the two within individual FAs, intensity profiles were generated perpendicular to the adhesion with PaxC represented by the green line and endogenous Paxillin with the red line. As shown in **Figure 1.20A**, these two molecules are mutually exclusive within individual FAs and each FA had retention of little foci that are positive for endogenous Paxillin and almost completely devoid of PaxC. This suggests that small PaxC resistant foci exist within FAs where due to the network of interactions generated

through the LD motifs. This fraction of endogenous Paxillin would correspond to the immobile fraction of the WT protein observed in FRAP experiments.

To further confirm that PaxC and endogenous Paxillin are spatially discrete, we performed intermolecular Förster resonance energy transfer (FRET) experiments between them, due to the overlap of the emission spectrum of GFP (donor) and absorption spectrum of RFP (acceptor). Specifically, in this technique if two molecules are in a close proximity the donor when excited, it can transfer the absorved energy to the acceptor. This energy transfer, known as FRET, is determined by exciting the donor and measuring emission from the acceptor (Alberts et al., 2015). In case the GFP PaxC and RFP Paxillin were in very close proximity, we expected to see an increase in GFP PaxC intensity when photobleaching RFP Paxillin. In order to address this, we then co-transfected HeLa cells with GFP PaxC (which would serve as the donor) and RFP Paxillin W.T (which would serve as the acceptor) and carried out acceptor photobleaching experiments. As shown in **Figure 20B**, after photobleaching of RFP Paxillin, GFP PaxC intensity decreased. This suggests that FRET is not taking place between the two molecules, indicating that they are not interacting and thus verified that they are clustered independently.

After verifying the spatial segregation of PaxC and Paxillin W.T within each FA, we moved on to examine if this segregation is indeed due to the network of interactions generated through the LD motifs of the endogenous protein. For this purpose and based on the fact that FAK is one of the well-known partners of Paxillin, we went on to examine the spatial correlation of FAK with Paxillin and PaxC. To do so, we performed immunofluorescence experiments on cells expressing GFP PaxC, using antibodies that recognize Paxillin WT and FAK, and generated intensity profiles with PaxC represented by a green line, endogenous Paxillin with a red line and FAK with a blue line. Indeed, we observed a clear spatial correlation between endogenous Paxillin and FAK, and no correlation between PaxC and FAK (**Figure 1.20C**). This confirms that the Paxillin clusters retain interactions with additional FA proteins and thus would present a much more difficult target for displacement for PaxC. Overall, these data suggest stochastic segregation of PaxC and endogenous Paxillin within each FA which relies on the additional binding partners that interact with the full-length protein.

A (a) **(b)**

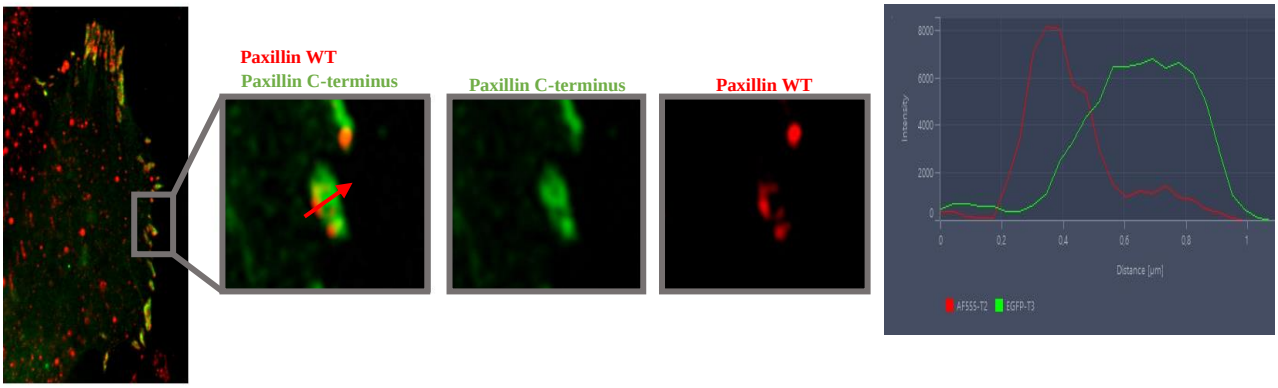
Paxillin WT
Paxillin C-terminus
Paxillin C-terminus
Paxillin WT
Intensity
Distance [µm]
AF555-T2
EGFP-T3

B (a)

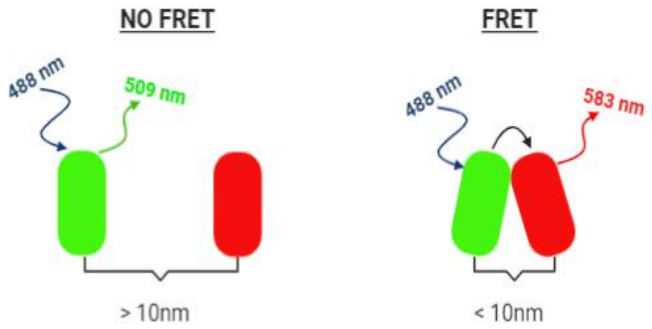
NO FRET
FRET
488 nm
509 nm
488 nm
583 nm
> 10nm
< 10nm

(b)

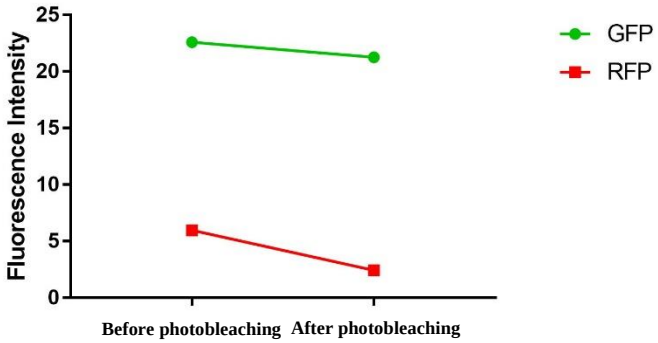
Fluorescence Intensity
25
20
15
10
5
0
GFP
RFP
Before photobleaching
After photobleaching

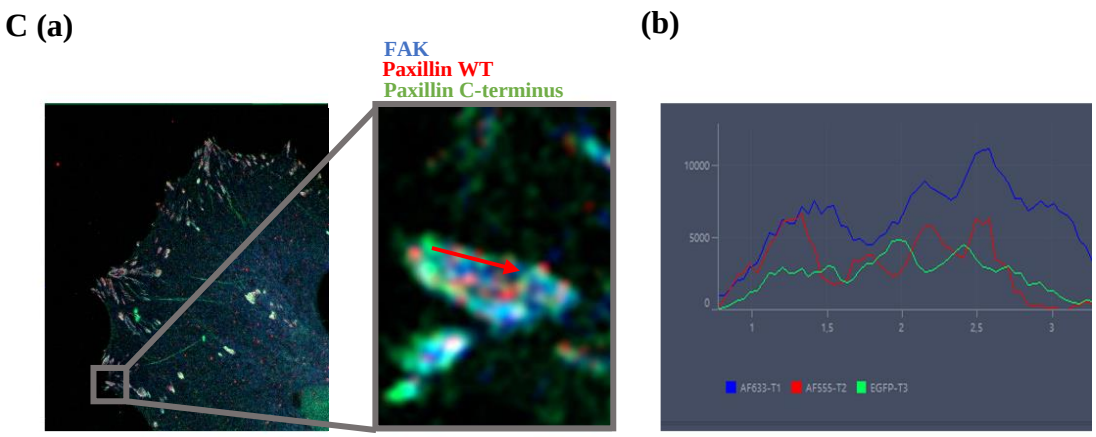

Figure 1.20: Stochastic segregation of endogenous Paxillin and Paxillin C-terminus within each FA.

(A)(a) Super-resolution images of a cell transfected with GFP PaxC seeded on FN coated slide for 1 hour, fixed and then stained for GFP and Paxillin. Profile generated perpendicular to FAs revealed that PaxC and Paxillin W.T are mutually exclusive within individual FA.

(b) Diagram showing the intensity distribution of GFP PaxC and Paxillin along a 1μm straight line. The distribution of GFP PaxC intensity is different than that of Paxillin, showing that these two molecules are spatially segregated.

(B)(a) Schematic representation of FRET. When the donor (GFP) and the acceptor (RFP) are in close proximity, after donor's excitation, it can transfer the absorved energy to the acceptor, while when they are above 10nm apart the energy cannot be transferred. This energy transfer can be determined by exciting the donor and measuring emission from the acceptor (Scheme made by online program Biorender).

(b) Mean fluorescence intensity of GFP and RFP before and after photobleaching, in live HeLa cells expressing GFP PaxC and RFP Paxillin W.T. Both mean intensities of RFP (acceptor) and GFP (donor) drop after photobleaching, indicating that no FRET is taking place between them (n= 8 regions from a total of 2 cells). The error bars represent S.E.M.

(C)(a) Super-resolution images of a cell transfected with GFP PaxC seeded on FN coated slide for 1 hour, fixed and then stained for GFP, Paxillin, and FAK. Profile generated parallel to focal adhesions showed a correlation between Paxillin and FAK, while no correlation between PaxC and FAK.

(b) Diagram showing the intensity distribution of GFP PaxC, Paxillin and FAK along a 3 μm straight line. The distribution of GFP PaxC intensity is different than that of Paxillin and FAK,

while the distribution of Paxillin intensity is correlated with that of FAK, showing that PaxC is spatially segregated from Paxillin and FAK.

5.3.6 Expression of Paxillin C-terminus leads to suppression of integrin β1-mediated AJ turnover in HeLa cells

As mentioned in the introduction, previous work from our laboratory has revealed that ligand independent β1 integrin activation at the vicinity of the adherens junctions leads to their gradual disassembly and turnover. This has been ascribed to the fact that integrin β1 promotes the recruitment of several proteins, such as Src kinase and FAK, at AJs in a similar way as it does at FAs, which have the ability to promote phosphorylation and removal of components from the adhesion. Src has been shown that it can phosphorylate members of the AJs, such β-catenin (Behrens et al., 1993). For Src localization at FAs FAK is necessary, while Paxillin is crucial for FAK recruitment. Thus, a hypothesis is that Paxillin is recruited at AJs downstream of integrin β1 activation, and subsequently recruits FAK to either phosphorylate downstream targets or interact with other kinases, such as Src. If the turnover of AJs through integrin activation takes place due to the recruitment of downstream FA proteins, including Paxillin then it is expected that if Paxillin promotes this process then in its absence the AJs will be stabilized. AJ driven integrin activation and subsequent FA protein recruitment most closely resembles the CMC. The complex is far more dynamic and integrins at AJs relies entirely on actomyosin contractility for both activation and clustering. This would make competition by PaxC more potent than at FAs since no stable protein networks are formed which favor the full-length protein. In an effort to examine the possible role of Paxillin in this process, while at the same time evaluating the potency of PaxC as a DN in a context that resembles the CMC, we expressed the PaxC in HeLa cells, seeded them on N-Cadherin substrate until AJ formation and stained for active β1 integrin and β catenin. As shown in **Figure 1.21**, β-catenin intensity was found to be significantly higher in respect to the controls and adherens junctions appeared more defined. The overall phenotype is suggestive of suppressed adherens junction turnover due to the expression of PaxC, in a way consistent with what has been described for cells with inhibited β1 integrin activation (Unpublished data from our laboratory). In conclusion, Paxillin has a role in recruiting downstream targets that will promote AJ turnover.

A

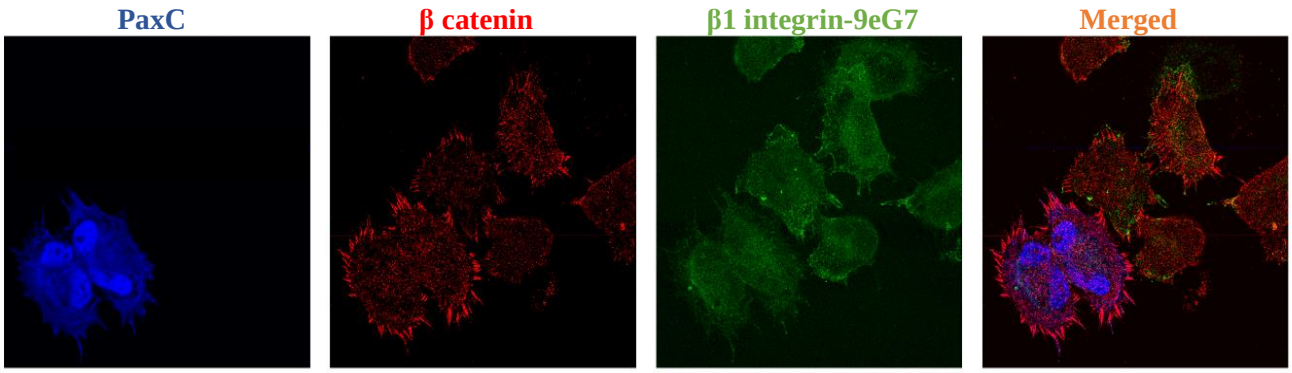

B

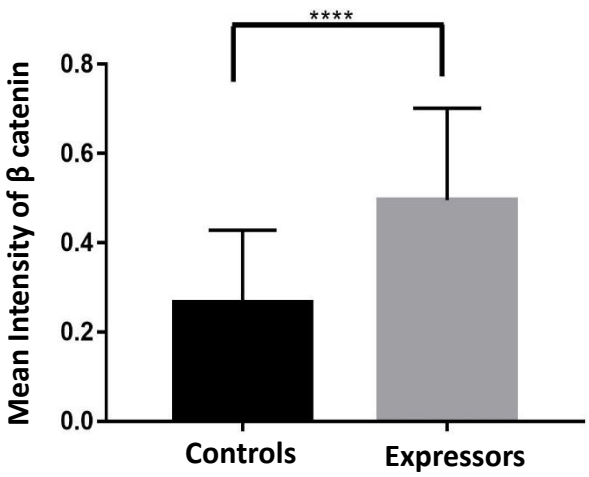

Figure 1.21: Expression of Paxillin C-terminus results in inhibition of integrin β1-mediated AJ turnover.

(A) Super resolution image of control and expressor cells on N-Cadherin substrate, stained for active integrin β1 and β-catenin. Integrin is inhibited at adherens junctions in expressors and β-catenin signal intensity increases, proposing that PaxC inhibits the AJ turnover.

(B) β-catenin intensity quantification at the AJs of control and expressor cells. The intensity increases significantly in expressors, suggesting that PaxC at AJs inhibit their disassembly.

5.4 Expression of the Paxillin C-terminus in HeLa cells elicits severe spindle orientation defects

Subsequent to the characterization of the PaxC construct, our results so far support that this construct can block endogenous Paxillin functions, since it displaces it from FAs as well as known signaling molecules that are dependent on Paxillin, including FAK and ILK. Although PaxC was not as potent in displacing Paxillin from FAs, its ability to influence AJ turnover was quite potent suggesting that in the context of the CMC which is even more dynamic and no long term interactions among its members are established, it should be quite effective in competing with endogenous Paxillin and prevent transient interactions with proteins like FAK and ILK. Thus, allowing us to use it as a tool to directly address a possible role of Paxillin in SO responses to topological cues. In order to address this, HeLa cells were transfected with PaxC, seeded on FN coated slides, and imaged for 24 hours. After quantification, we observed that cells expressing the PaxC display drastic SO defects with an average deviation from the predicted axis of around 45 degrees, compared to the control cells that had an average angle of 16 degrees (**Figure 1.22A**). This is essentially randomization of SO and can only be seen in cells treated with nocodazole or through elimination of the LGN/NuMa/Gαi tripartite complex and clear evidence that Paxillin is necessary for force sensing and spindle responses to mechanical stimuli (Fink et al., 2011, Lazaro-Diequez et al., 2015). Both expressor and control cells showed proper rounding up during mitosis. Therefore, to exclude the possibility that expressor cells display defects in SO due to failure in the formation of retraction fibers, we imaged these cells live and show that they exhibit a normal formation of RFs (**Figure 1.22B**). Collectively, the above data show that cells expressing PaxC no longer follow cues derived from adhesion geometry, and thus fail to orient their spindle along the long interphase and prometaphase axes. We thus conclude that Paxillin is a member of the CMC and necessary for SO responses to external forces.

A (a)

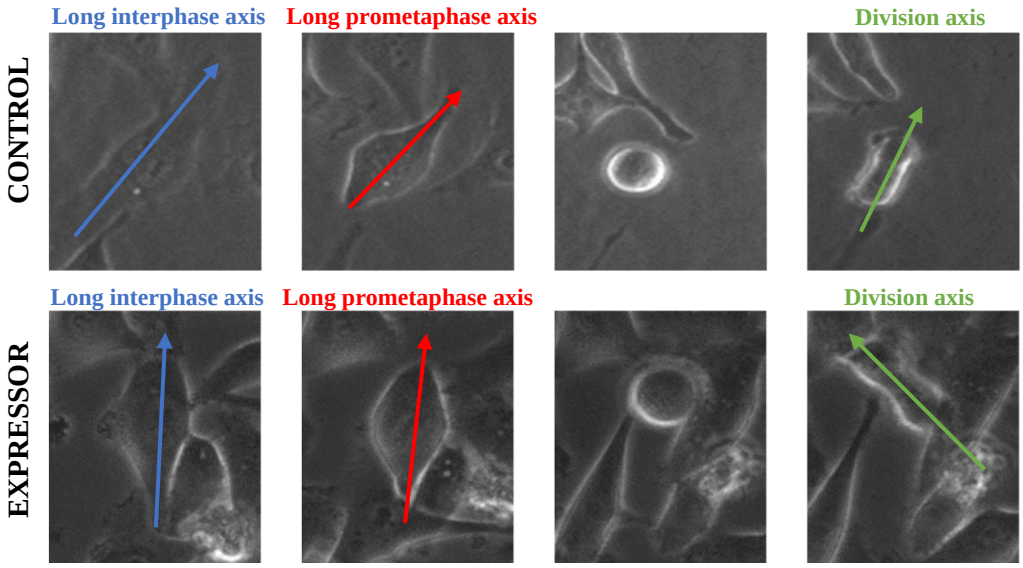
Long interphase axis
Long prometaphase axis
Division axis
CONTROL
Long interphase axis
Long prometaphase axis
Division axis
EXPRESSOR

(b)

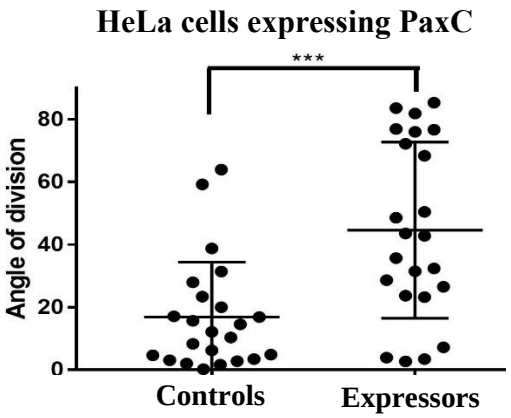
HeLa cells expressing PaxC
***
Angle of division
80
60
40
20
0
Controls
Expressors

B

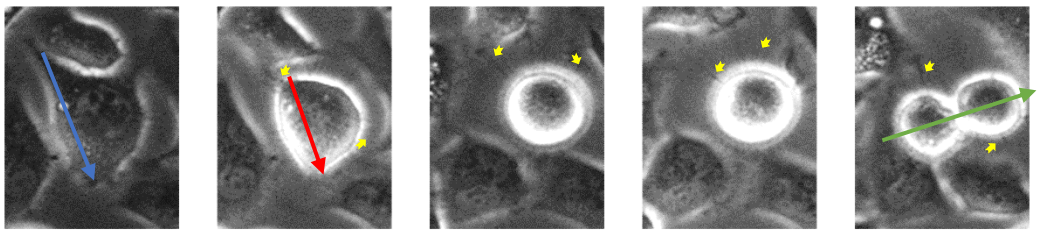

Figure 1.22: Expression of Paxillin C-terminus in HeLa cells results in spindle misorientation with respect to the geometry adhesion

(A) (a) Live imaging of control and expressor HeLa cells, respectively, seeded on FN coated slide over 24 hours. Brightfield view of the above cells, in which the expressor is misoriented and the control cell is oriented with respect the geometry adhesion.

(b) Quantification of the long prometaphase axis to the division axis ratios measured in individual control cells and cells expressing PaxC. P values calculated by Mann-Whitney test; n, number of cells, ten independent experiments. Error bars represent S.E.M. The mean division angle in control cells is 16,87 ± 3,647°, n=23 while in expressor cells is 44,55 ± 5,864°, n=23. Expression of PaxC in HeLa cells lead to their misorientation with respect to geometry adhesion.

(B) Stills images from live movie of HeLa cells expressing PaxC during mitosis. Yellow arrowheads indicate where the RFs.

5.5 Expression of Paxillin C-terminus in Xenopus embryos

With the above experiments, we showed that Paxillin is required for spindle responses to external force, and hence for proper SO with respect to geometry adhesion *in vitro*. Subsequently, given the observed misorientation *in vitro* due to PaxC expression, we wanted to explore a possible role of Paxillin in SO *in vivo*. Therefore, we decided to examine this process in a tissue in which it is well known and documented that proper SO is crucial for morphogenesis, in *Xenopus* embryos. As described in the introduction, during gastrulation the animal cap, which is the perspective neuroectoderm, needs to expand drastically through a process named epiboly, to allow the mesodermal and endodermal tissues to become internalized. This expansion is achieved via cell flattening and increased cell divisions of the superficial cells, combined with a simultaneous integration of deep cell layers into one through radial intercalation. By stage 9, the two-layer stratified arrangement is achieved and maintained by the oriented cell divisions of both deep and superficial layers within the plane of the epithelium (**Figure 1.23**, Keller and Danilchik, 1988). In case that these divisions are misoriented then the expansion of this tissue cannot be accomplished, leading to failure of blastopore closure.

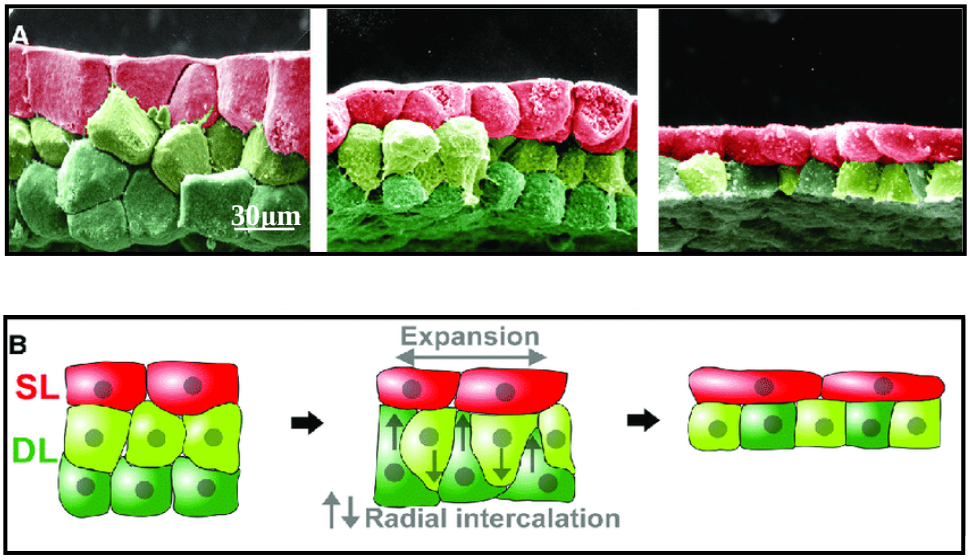

Figure 1.23: A) SEM images from *Xenopus* animal cap during epiboly. Red color represents superficial cells, while green represents deep cells **B)** Schematic representation of epiboly in *Xenopus* where expansion and flattening of superficial cells and radial intercalation of deep cells occurs (Szabo et al., 2016)

5.5.1 Expression of Paxillin C-terminus in Xenopus embryos leads to gastrulation defects

To examine a possible role of Paxillin in the early morphogenesis of the prospective neuroectoderm, embryos were injected with 500pg of GFP PaxC, at both blastomeres of two-cell stage embryos. Injected embryos were then imaged alongside control embryos on an inverted microscope for 5 hours, starting approximately at the beginning of gastrulation (stage 10), in order to visualize blastopore formation and closure (which is completed at stage 12). As shown in **Figure 1.24**, blastopore formation was not affected by the expression of PaxC, but blastopore closure failed or was extremely delayed in comparison with control embryos, hence indicating that expressor embryos display defects in epiboly, indicating the involvement of Paxillin in this process.

A

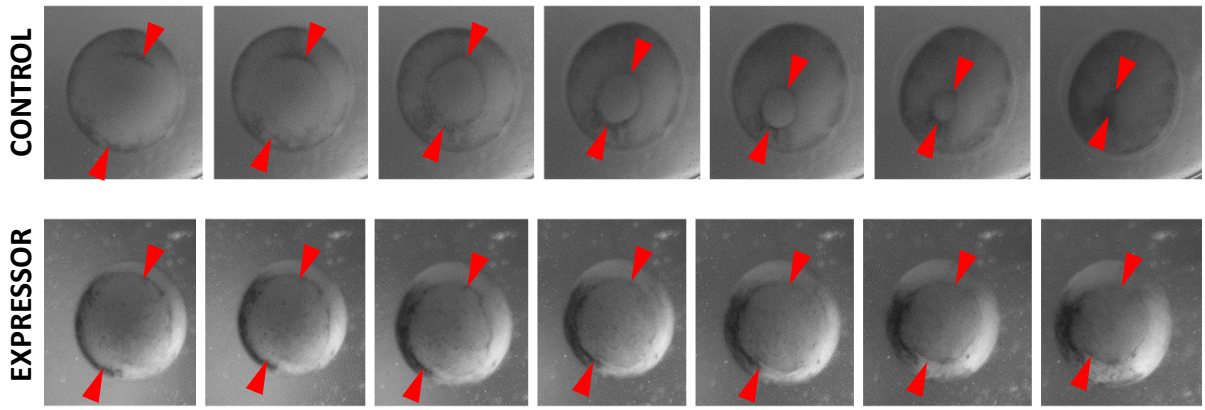

B

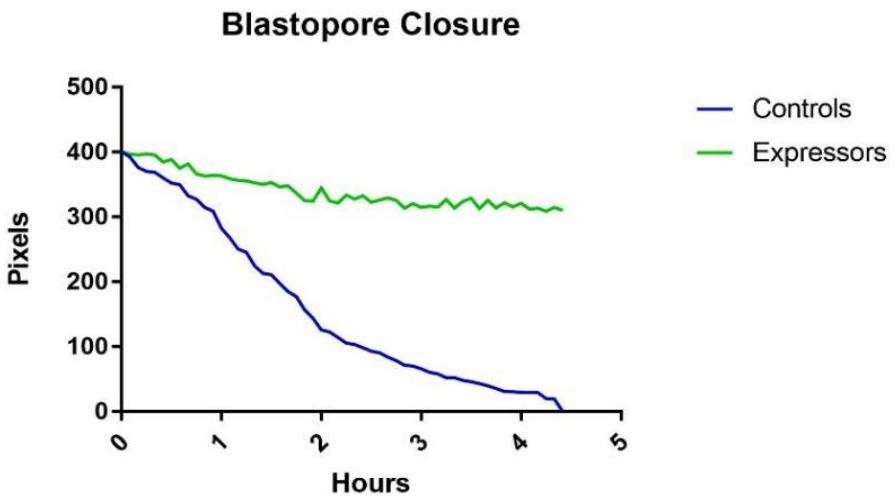

Figure 1.24: Expression of Paxillin C-terminus in the animal cap results in defective blastopore closure

(A) Images from time-lapse imaging of over 5 hours from stage 10 (start of gastrulation) till stage 12 (end of gastrulation), showing blastopore closure in control and in embryos injected with 500pg of GFP PaxC. Red arrowheads indicate the diameter of the blastopore.

(B) Graph showing the change in blastopore diameter in pixels, that was determined by measuring the distance between the red arrowheads from the **(A)**, over a period of five hours in control and expressor embryos.

5.5.2 Expression of Paxillin C-terminus leads to thickening of the animal cap during gastrulation

In order to understand why PaxC expression elicits defects in blastopore closure during gastrulation, we sagittaly sectioned both control and expressor embryos in order to examine their animal cap tissue for abnormalities. Initially, embryos were injected with GFP PaxC at both blastomeres of two-cell stage embryos with the total amount of 500pg mRNA. Control and expressor embryos were dissected at st.10.5 (gastrula stage) parallel to their dorsoventral axis. As shown, we observed a big difference between the animal caps of control and expressor embryos. Specifically, expressors display visible thickening of the animal cap with multiple cell layers, while controls showed a normal two-cell layer epithelium (**Figure 1.25A**). In order to exclude the differences that may be present from one embryo to another and to examine the direct effects of our construct in this process in each individual embryo, we injected them with PaxC at the dorsal and its opposing ventral blastomere at the four-cell stage with 500pg total amount of mRNA, so that half of the embryos would express while the other half would serve as an internal control. Subsequently, sagittal sections were generated at st.10, perpendicular to the dorsoventral axis, resulting in the simultaneous imaging of an injected and a non-injected side within the same embryo. These sections revealed again the thickening of the animal cap in the injected area, while the non-injected area exhibits a normal two-cell layered animal cap (**Figure 1.25B**). The above data has shown that the severe gastrulation defects resulted were due to the expression of PaxC.

A

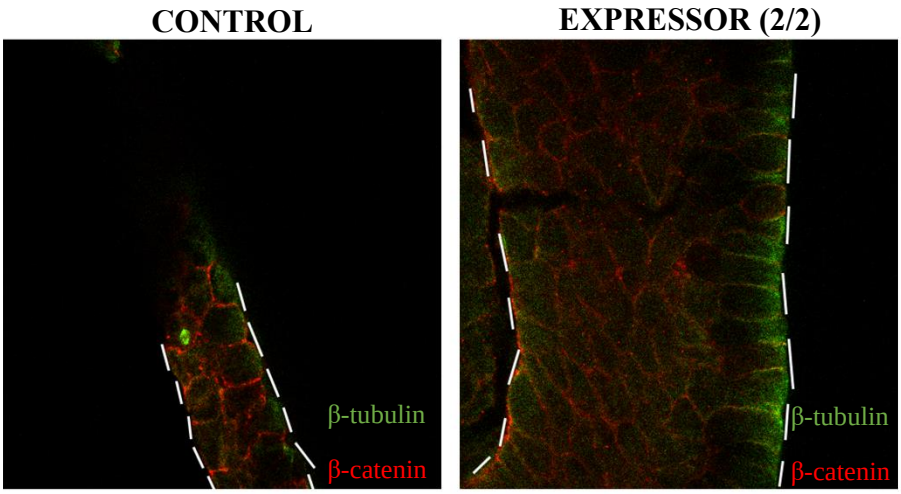

B

(2/4)

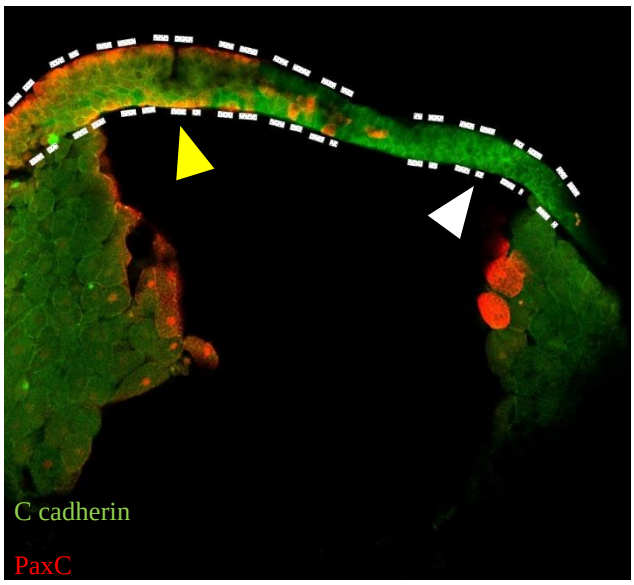

Figure 1.25: Expression of Paxillin C-terminus leads to epiboly defects and thickening of the animal cap

(A) Sagittal sections of st.10,5 control embryos and embryos injected with PaxC at the two-cell stage embryos. Embryos expressing PaxC display thickening of the animal cap, while controls cells have a normal two cell layered structure.

(B) Sagittal sections of st.10 embryos injected with PaxC at the four-cell stage, targeting only one side of the embryo. Expression of the PaxC leads to thickening of the epithelium, while in the non-injected side of the same embryo remains the two-cell layer epithelium of the animal cap. Yellow arrowhead indicates the injected side, while white arrowhead indicates the non-injected side of the embryo.

5.5.3 Epiboly defects elicited by Paxillin C-terminus expression in Xenopus embryos is a consequence of spindle misorientation in the deep cells of the animal cap

As described in the introduction, one of the processes which are necessary for blastopore closure and signals the end of gastrulation is epiboly. During epiboly, numerous deep cell layers of the animal cap integrate into one layer through radial intercalation, while superficial cells of the animal cap expand by cell division and flattening resulting in the expansion of the animal cap allowing it to encompass the whole embryo. (Keller, 1980, Keller and Danilchik, 1988). Our data revealed that expression of PaxC leads to failure of blastopore closure and to the thickening of the animal cap. Tightly regulated cell divisions control the expansion and maintenance of the two-cell layer arrangement of the animal cap. Normally, spindle orientation is retained within the plane of the epithelium, with the division axis parallel to this plane, to ensure that both deep and superficial cells orient their spindles parallel to the animal cap surface plane (Marsden and DeSimone, 2001). This ensures that daughter cells of both deep and outer cell layers are retained within their respective planes after each division allowing the expansion of the tissue to take place while maintaining the two cell layers. Interestingly, embryos that lack the FN matrix, show a delay in blastopore closure and a thickened animal cap due to an increased number of deep cells that display misorientation (Marsden and DeSimone, 2001). Therefore, the thickening of the animal cap could be a result of defective radial intercalation of the deep cell layers, or the formation of misoriented mitotic spindles.

In order to explore if the observed thickening of the epithelium when expressing the PaxC was due to spindle misorientation, as it was observed in embryos lacking FN matrix, we fixed and stained dissected embryos, both controls and expressors, with an antibody against β-tubulin to visualize their spindles. As shown in **Figure 1.26A and 1.26B**, deep cells of the animal cap were clearly misoriented, while cells of the outermost layer were not affected, thus the randomization of cell polarity was limited only to deep cells, similar as in embryos lacking FN matrix. Overall, these results suggest that the defects in epiboly elicited by PaxC expression are stemming from misorientation of mitotic divisions in the deep cell layer of the animal cap.

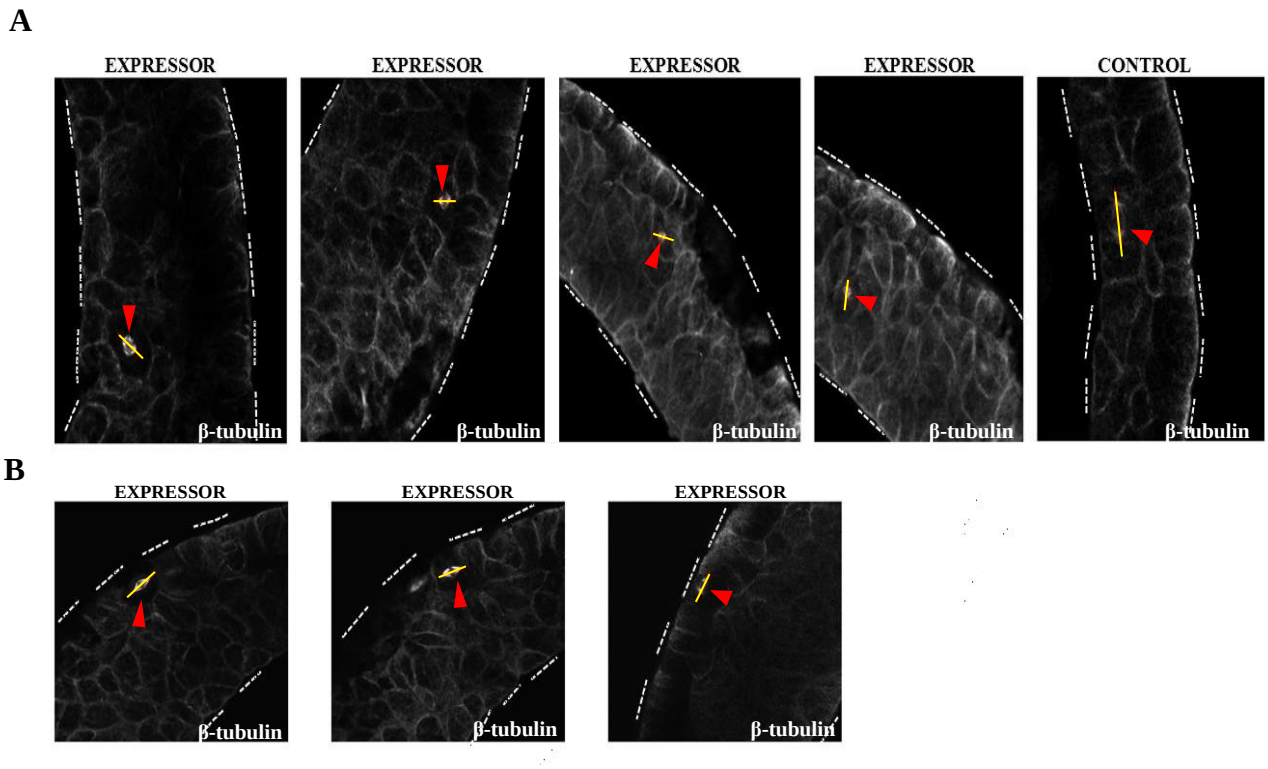

Figure 1.26: Expression of Paxillin C-terminus leads to epiboly defects due to misorientation of the deep-layer cells of the animal cap

(A) Expression of PaxC results in the loss of polarity in deep cells of the animal cap leading to the multilayer animal cap. Embryos were stained with β-tubulin for the visualization of the mitotic spindle. Red arrowheads indicate mitotic spindles, while a red line shows the division axis of the cell.

(B) Outer cells of embryos expressing PaxC display proper orientation along the plane of the epithelium. For mitotic spindles to be visualized staining with β-tubulin was done. Red arrowheads indicate mitotic spindles, while a yellow line represents the division axis of the cell.

5.5.4 Expression of Paxillin C-terminus in Xenopus embryos leads to defects in FN matrix formation

As mentioned in the introduction, Fibronectin fibrillogenesis takes place at the blastocoel roof of the animal cap at early stages of *Xenopus* development. During gastrulation, along the blastocoel roof is detected an elaborate network of FN (Boucaut and Darribere, 1983a; Boucaut and Darribere, 1983b; Collazo, 1994). It has been shown that embryos injected with antibodies that block FN matrix assembly, display thickening of the animal cap due to deep cells misorientation (Marsden and DeSimone, 2001). This phenotype is similar with what we observed when PaxC was expressed in embryos. Importantly, Paxillin was implicated indirectly in early fibronectin matrix assembly in fibroblasts, through its ability to recruit ILK and FAK at FAs. Specifically, it has been shown that ILK forms a complex with the adaptor proteins, PINCH1 and Parvin, resulting in the reinforcement of α5β1-actin linkage and serve as a platform to recruit Tensin (Vouret-Craviar et al., 2004). In turn, Tensin is crucial for a process where translocation of a5b1 integrins induce initial FN matrix assembly via cytoskeleton-generated tension to FN molecules (Pankov et al., 2000). Additionally, it was shown that FAK is implicated in the proper FN network formation and patterning, since FAK knockout fibroblasts displayed defects in this process (Ilic et al., 2004). Based on these and on our previous data showing the displacement of both ILK and FAK from FA when expressing PaxC, we wanted to examine if expression of PaxC affects FN fibrillogenesis during gastrulation, and hence leading to misorientation of deep cell layers of the animal cap. For this purpose, we injected embryos with 500pg of GFP PaxC at both blastomeres of two-cell stage embryos and then fixed them at st.10.5-11. Next, animal caps were dissected from control and expressor embryos and stained for FN with an antibody against *Xenopus* Fibronectin. As shown in **Figure 1.27**, FN fibril formation was inhibited in embryos expressing our construct compared to control embryos. These results suggest that expression of PaxC leads to defects in epiboly indirectly by inhibiting FN fibrillogenesis and implicate Paxillin in this process.

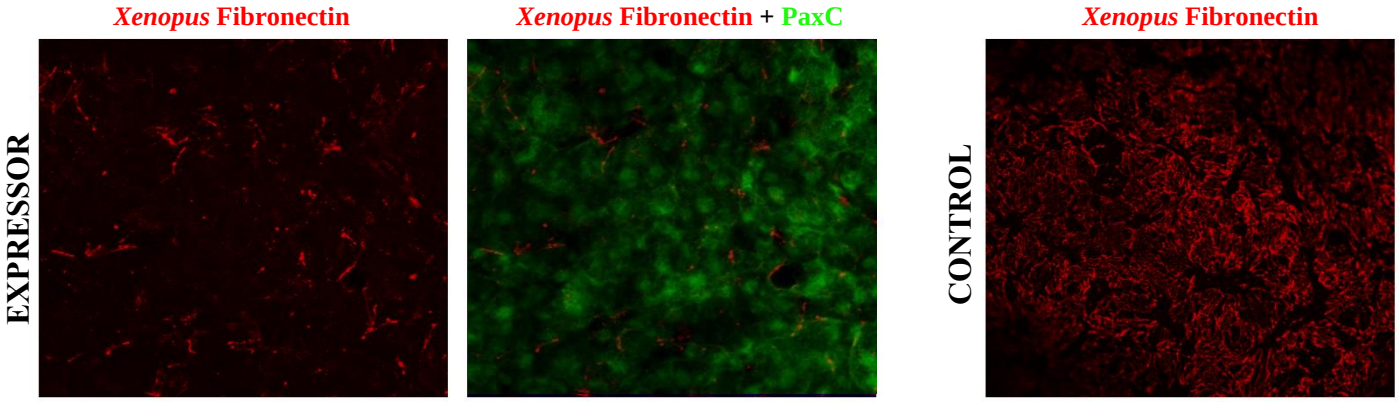

Figure 1.27: Expression of Paxillin C-terminus inhibits Fibronectin fibril formation

Images of dissected animal caps of st.10,5-st.11 control embryos and embryos injected with PaxC and stained for Fibronectin with an antibody against *Xenopus* Fibronectin. Fibril formation under the deep cells of the blastocoel roof is blocked in expressor embryos, while in controls is unaffected.

6. Discussion

During mitosis the mitotic spindle is formed, which then segregates the genetic material into the daughter cells (Walczak and Heald, 2008). In addition to spindle formation, it is crucial that the orientation of the mitotic spindle is proper with respect to the geometry adhesion as well as with respect to the plane of adhesion. As mentioned in the introduction, SO is implicated in many developmental processes in the embryo as well as in the maintenance of the adult tissues. Cell fate, maintenance of the epithelial structure, organogenesis are some of the processes that spindle orientation controls (Fish et al, 2006; Quyn et al, 2010; Pease and Tirnauer; 2011; Baena-Lopez et al, 2005; Quesada-Hernández et al, 2010; Lu and Johnston; 2013; Gonzalez, 2007; Knoblich, 2010).

Due to the importance of SO, it has been studied extensively in order to understand further the mechanisms responsible for the process *in vitro* and *in vivo*. So far it has been shown that the control of SO is mainly based on the activity of different cues. These cues can be either internal due to cell polarity, geometric or external due to cell contacts with the environment or other cells, signaling and mechanical (Hertwig, 1884; Kotak et al., 2012; Pietro et al., 2016; Nestor-Bergmann et al., 2014). It is not clear yet if these cues control spindle orientation independently or if they coordinate.

Previous work from our laboratory led to the discovery of the CMC at the lateral cortex of mitotic cells, where integrin β1 was activated. This activation leads to the recruitment of several FA proteins, such as FAK, p130Cas, and Src. It was suggested that the CMC can control SO responses to external forces (Petridou and Skourides, 2016). Since FAK targeting at FAs is exclusively reliant on its interaction with another protein of FAs, Paxillin (Hildebrand et al., 1993), it was suggested that probably Paxillin is also a member of the CMC despite no direct evidence that FAK is recruited to the CMC through the same mechanism. Possibly, Paxillin is targeted first at the cortex and then recruits the other members, similarly to what happens at FAs, in which recruitment of Paxillin precedes the recruitment of FAK, p130Cas, and Src (Schaller, 2001). Interestingly, spindle misorientation with respect to the plane of adhesion was observed in cells lacking p130Cas and Paxillin (Petridou and Skourides, 2014; Petridou and Skourides, 2016). However, SO responses to adhesion geometry within the plane of attachment has never been studied in these cells and the question of whether these two SO responses are in fact relying on the same mechanism has not been convulsively demonstrated. Additionally, Z axis misorientaion of the p130Cas and Paxillin null fibroblasts could be due to defective adhesion something which has not been examined.

In this thesis, we wanted to explore a possible role of p130Cas and Paxillin in the orientation of the mitotic spindle with respect to geometry of adhesion *in vitro*. Initially, we used cell lines, lacking p130Cas and Paxillin respectively, and examine their orientation. Nevertheless, the usage of these null cell lines raised several problems, and therefore we moved on to an alternative approach, where we used the C-terminus of Paxillin as a dominant-negative. Furthermore, we characterized the effects of PaxC expression in the control HeLa cell line and examined its effects on mitotic spindle orientation. Additionally, to address the role of Paxillin in SO during embryonic development, we expressed our construct in *Xenopus* embryos.

As already mentioned, Paxillin contains the LD motifs, through which it interacts with other binging partners, and the LIM domains, which are responsible for Paxillin targeting to FAs (Brown et al., 1998, Turner and Brown, 2004). This well-characterized structure of Paxillin was used as the basis for utilizing the C-terminus of Paxillin as a dominant-negative, that can be recruited at FAs but not interact with its partners. Additionally, by using a DN and not by removing Paxillin itself, we eliminate the possibility that expression of the paxillin homologues, such as Hic-5 and Leupaxin, will compensate for the loss of Paxillin in these cells and mask any phenotype (Hagel et al., 2002, Fujita et al., 1998, Thomas et al., 1999b).

By using time-lapse imaging, we initially showed that the expression of PaxC in HeLa cells does not affect spreading, cell migration or the duration of mitosis of these cells. Since this construct did not affect cell behavior of HeLa cells suggesting that it was not effectively blocking Paxillin function at FAs, we went on to directly explore its effects on Paxillin and downstream target localization at FAs.

When introduced into HeLa cells, the PaxC is enriched at FAs, competing the endogenous protein and thus leading to its displacement. However, we observed that the displacement of endogenous Paxillin in high expressors was partial, while in low expressors the displacement levels were significantly low. These experiments revealed that PaxC can partially displace endogenous Paxillin from FAs in a dose-dependent manner. Due to the fact that Paxillin is necessary for the targeting of several proteins at FAs, including FAK and ILK, through its LD motifs (Brown et al., 1998), we went on to examine the effects of Paxillin displacement on FA composition. Importantly, localization of both FAK and ILK at FAs was affected, indicating that PaxC indeed acts as a DN, since it cannot interact with other binding proteins and displaces them from FAs. Additionally, we showed that both the displacement of FAK and ILK were also dose dependent.

The fact that relatively high levels of PaxC did not eliminate all the endogenous protein from FAs raised several questions. One explanation for this observation would be if the affinity of

the endogenous protein for FAs was higher than that of PaxC. To test this possibility, we used FRAP experiments and showed that indeed the affinity of endogenous Paxillin for FAs is higher, while the off rate is slower, due to the network of interactions full length Paxillin creates with other FA proteins, such as Vinculin and FAK. These multiple interactions are increasing the residence time of Paxillin at these large macromolecular complexes resulting in the less efficient displacement of the protein by the expression of the PaxC. Thus, very high levels of PaxC expression are necessary to displace the full-length protein from FAs. The next question that needed to be answered was how these two molecules are distributed within each individual FA since they both remain there. To address this, we went on to take a closer look at the spatial topology of these molecules at FAs. With the use of super-resolution microscopy, we showed that clusters of endogenous Paxillin exist, that appeared to be devoid of the PaxC construct. Interestingly, these clusters were positive for FAK, unlike the rest of adhesions where the signal of FAK was absent and the PaxC was present. These data suggested that the spatial segregation of PaxC and endogenous Paxillin within each FA results due to the ability of the endogenous protein to interact with other partners, such as FAK.

Considering the effects of PaxC expression on FAs, we further investigated possible consequences of its expression in AJs, a complex responsible for cell-cell adhesion (Takeichi, 1991; Steinberg, 1996). Unpublished work from our laboratory, has shown that plasma membrane tension driven activation of β1 integrin at the vicinity of the AJs results in their disassembly. Importantly, it was shown that activation of integrin β1 leads to the recruitment of FAK and Src at AJs, where they promote AJ disassembly possibly through phosphorylation of their components (Fujita et al., 2002, Behrens et al., 1993). Expression of PaxC in cells inhibits the turnover of AJs, which are more defined in comparison with that of control cells. Interestingly, this phenotype is similar to previous data from our laboratory, in which cells were inhibited for the enzymatic activity of FAK and Src (Unpublished data from our laboratory). Thus, it is possible that Paxillin is required for the recruitment of FAK at AJs upon β1 integrin activation, as it similarly does in FAs. FAK subsequently recruits Src, and they promote the disassembly and turnover of AJs. It is interesting to note however how drastic the effects of PaxC were in this context of hybrid adhesions compared to FAs. Hybrid adhesions were shown to reply entirely on actin contractility given the absence of ligand to retain integrin β1 in an activated state. The complex is thus far more dynamic than FAs and complex network interactions are not established. As such, endogenous paxillin possibly has a smaller advantage in terms of affinity compared to FAs which makes PaxC competition more efficient and effective. Future experiments could be carried out to determine a) if endogenous paxillin is in fact completely displaced from AJs in the presence of PaxC and b) if FAK and ILK are completely displaced from hybrid adhesions in the presence of PaxC.

Given the misorientation of cells lacking Paxillin with respect to the plane of adhesion (Petridou and Skourides, 2014), we went further to investigate the role of Paxillin in SO with respect to the geometry adhesion. Our work showed that cells expressing PaxC were misoriented, probably due to a failure in following cues from external forces. In addition to the previous work from our laboratory (Petridou and Skourides, 2014), these data indicated the role of Paxillin in the process of SO both with respect to the plane of adhesion and with respect to the geometry adhesion. It is possible that Paxillin indeed is a member of the CMC, as suggested before, and hence since PaxC can't recruit FAK, and eventually p130Cas and Src at the cortex of the mitotic cell, it leads to a deficient SO due to a failure to respond to external forces.

Based on the above effects of PaxC as a DN *in vitro*, we move on to test it as a DN of Paxillin *in vivo*. For this purpose, we expressed the PaxC at the animal cap in the *Xenopus* embryo in order to examine possible effects during gastrulation. As described in the introduction, gastrulation is a well-characterized process during which the three-layered structure gastrula occurs, and the major embryonic axes are form. The epiboly of the animal cap along with the blastopore lip formation at the dorsal vegetal side of the embryo lead to the initiation of gastrulation in *Xenopus* embryos. Epiboly results in the expansion of the animal cap in order to cover the whole embryo, and eventually in the internalization of the mesodermal and endodermal tissues (Keller,1980; Keller and Danilchik, 1988). Additionally, the epibolic movement was shown to be permissive for blastopore closure. This process is driven by both an increase in cell number due to mitotic divisions and cell flattening of superficial cells combined with radial intercalation of deep cell layers, resulting in the two-cell layered epithelium of the animal cap. During gastrulation, embryos expressing PaxC displayed severe defects in epiboly, such as delayed blastopore closure. Dissected embryos revealed a visible thickening of the normally two-cell layered epithelium of the animal cap, which stem from either defective radial intercalation of the deep cell layers or the misorientation of mitotic spindles of both deep cell layers and superficial layer.

We went on to visualize the mitotic spindles of mitotic cells in embryos expressing PaxC, in order to explain if the appearance of the defective phenotype was because of defects in SO. We observed randomized SO and cell polarity of the inner cell layers, while the orientation of the outer cell layer wasn't affected. This phenotype is similar to what has been shown in embryos lacking the FN matrix, in which the normally parallel to the plane of the epithelium alignment of mitotic spindles in dividing deep cells was randomized (Marsden and DeSimone, 2001). Overall, these data showed that defects in epiboly due to PaxC expression stem from spindle misorientation of deep cells of the animal cap.

During gastrulation, under the deep cells on the blastocoel roof a rich FN fibrillar network is formed, on which migration of the head mesendoderm takes place (Boucaut and Darribere, 1983a; Boucaut and Darribere, 1983b; Collazo, 1994). Dissected animal caps were stained with an antibody against *Xenopus* Fibronectin and showed that expression of PaxC inhibits FN fibrillogenesis, suggesting that the previously observed defects in SO could be secondary to defects in FN fibril formation. Given the fact that loss of this network has been shown to elicit spindle misorientaion of the deep cells it is not possible to conclude if Paxillin has a role in SO of the deep cells. Interestingly outer cells do not rely on FN for SO and are correctly oriented in embryos that lack FN. Outer cells were also orientated when PaxC was expressed suggesting that all defects stem from loss of FN. However, outer cells are fully polarized and LGN is excluded from their apical surface making them very difficult to lose orientation parallel to the epithelium plane. We only examined if these cells maintain SO within the plane of the epithelium however we have not examined if they can respond to force or geometrical cues, and thus cannot conclude if Paxillin is involved in this process *in vivo* despite the *in vitro* data suggesting that it is.

In conclusion, our results suggested that GFP PaxC acts as a potent DN of Paxillin protein both *in vitro* and *in vivo*. Importantly, we showed that Paxillin is implicated in SO with respect to the geometry adhesion, possibly due to its participation in the CMC. Considering the secondary role of Paxillin in FN fibrillogenesis *in vitro*, and based on our results on Xenopus embryos, we suggested that Paxillin is probably involved in FN fibrillogenesis during embryonic development.

Future work will focus on further examining the mechanisms by which Paxillin is involved in spindle orientation within the xy and z axis as well as its role in the CMC. By using the double mutant of Paxillin D146A/D268A, that abolishes interaction of FAK with both LD2 and LD4 (Scheswohl et al., 2008), we can investigate if the interaction of Paxillin and FAK is necessary for FAK recruitment at the CMC and also check whether abolishing the interaction can promote orientation defects. Additionally, we plan to express the PaxC in cells seeded on Cadherin FC substrates, on which cells lack basal integrin activation, to show that all observed defects in SO is due to failure in mechanosensing, and not on defects in adhesion integrin-dependent signaling. Furthermore, by expressing PaxC we can test whether Paxillin is involved in processes that are known to take place during mitosis but are yet not that well-characterized, such as actin cloud formation in mitotic cells. Actin clouds are waves of polymerized actin that move in a circular way below the cell cortex and around the spindle. The polymerized actin is more stable and remains at the site of the spindle poles for a longer amount of time in respect to the rest of the cell, thus suggesting that it probably has a role in guiding the capture of astral

microtubules at the proper sites of the cortex (Fink et al., 2011; Kwon et al., 2015). It would be interesting to examine whether the expression of PaxC, thus the concurrent inhibition of its interactions, would interfere with actin cloud formation or behavior.

Additional *in vivo* experiments will be required to better understand the role of Paxillin in SO of the outer epithelial cells. Importantly, superficial and deep cells are exposed to a different environment that leads to different cues by which in response these cells orient their spindle Specifically, deep cells display AJs and have contacts with the dense extracellular matrix, such as the FN matrix, while superficial cells have both adherens and tight junctions and are dividing in the absence of ECM-derived signals (Chalmers et al., 2003). Based on that, future experiments will be needed to examine if outer cells expressing PaxC can respond to geometry and mechanical cues. Expression of PaxC with the combination of laser ablation can be carried out on cell adjacent to mitotic as previously described by Petridou and Skourides, or wounds can be generated on the epithelium using hair knifes or gastromaster and in conjunction with live imaging track spindle responses in response to changes of the mechanical landscape around the cell as well as changes in geometry (Petridou and Skourides et al, 2014). Although before performing this experiment, we could first increase the injected dose of PaxC in embryos, to see if it will affect the outer cells, since *in vitro* the displacement of endogenous Paxillin was in a dose-dependent manner, and only high expressors could displace it from FAs. Subsequently, to investigate the role of Paxillin in FN matrix formation *in vivo* and if it's the same as *in vitro*, we can abolish ILK, by using antisense inhibition of protein expression, and examine its effects on FN fibrillogenesis during embryonic development.

7. Conclusions

In this study we examined the involvement of p130Cas and Paxillin, proteins of FAs, in spindle orientation *in vitro* and *in vivo*. Previous work from our laboratory showed that cells lacking these proteins displayed spindle misorientation with respect to the substrate, however it is not yet clear if the mechanisms that control spindle orientation with respect to the substrate and to the geometry adhesion are the same. In addition, the role of these proteins in spindle orientation was not previously addressed *in vivo*. The first aim was to investigate the role of these two proteins in spindle orientation with respect to the geometry adhesion *in vitro*. We initially used fibroblast null cell lines, lacking p130Cas and Paxillin, that eventually raised several problems and then we went on to use a different approach using the Paxillin C-terminus as a dominant negative in control HeLa cells. We showed that expression of PaxC in HeLa cells results in the partial displacement of Paxillin from FAs, which leads to the disruption of its scaffolding functions, such as the recruitment of FAK and ILK at FAs. However, DN effects required high levels of expression, and investigation using FRAP revealed that this is due to a lower affinity of the PaxC compared to the full-length protein for FAs. Additionally, by using super resolution confocal imaging we showed a clear spatial segregation of PaxC and endogenous Paxillin within individual FAs. Importantly, cells expressing PaxC displayed defects in SO with respect to the geometry adhesion, suggesting that Paxillin is involved in this process. Our final aim was to investigate the role of Paxillin in SO *in vivo*, by using *Xenopus* embryos and focusing on the morphogenesis of the prospective neuroectoderm. We showed that of PaxC leads to severe gastrulation defects due to defective epiboly. The defects in epiboly stem from spindle misorientation of the deep cells that results from the defects in Fibronectin matrix formation.

8. References

ABERCROMBIE, M. & DUNN, G. A. 1975. Adhesions of fibroblasts to substratum during contact inhibition observed by interference reflection microscopy. *Exp Cell Res,* 92**,** 57-62.

ABERLE, H., BUTZ, S., STAPPERT, J., WEISSIG, H., KEMLER, R. & HOSCHUETZKY, H. 1994. Assembly of the cadherin-catenin complex in vitro with recombinant proteins. *J Cell Sci,* 107 (Pt 12)**,** 3655-63.

ABERLE, H., SCHWARTZ, H. & KEMLER, R. 1996. Cadherin-catenin complex: protein interactions and their implications for cadherin function. *J Cell Biochem,* 61**,** 514-23.

ALBERTS, B., JOHNSON, A., LEWIS, J., MORGAN, D., RAFF, M., ROBERTS, K., WALTER, P., WILSON, J. AND HUNT, T., 2015. *Molecular Biology Of The Cell*. 6th ed. New York: Garland Science, Taylor & Francis Group, LLC, 896-906, 925-944, 980-1002.

ALENGHAT, F. J., FABRY, B., TSAI, K. Y., GOLDMANN, W. H. & INGBER, D. E. 2000. Analysis of cell mechanics in single vinculin-deficient cells using a magnetic tweezer. *Biochem Biophys Res Commun,* 277**,** 93-9.

Anastasiou, O., Hadjisavva, R. and Skourides, P., 2020. Mitotic cell responses to substrate topological cues are independent of the molecular nature of adhesion. *Science Signaling*, 13(620), eaax9940.

ARNAOUT, M. A., MAHALINGAM, B. & XIONG, J. P. 2005. Integrin structure, allostery, and bidirectional signaling. *Annu Rev Cell Dev Biol,* 21**,** 381-410.

AZIOUNE, A., STORCH, M., BORNENS, M., THERY, M. & PIEL, M. 2009. Simple and rapid process for single cell micro-patterning. *Lab Chip,* 9**,** 1640-2.

BAENA-LOPEZ, L. A., BAONZA, A. & GARCIA-BELLIDO, A. 2005. The orientation of cell divisions determines the shape of Drosophila organs. *Curr Biol,* 15**,** 1640-4.

BAKOLITSA, C., COHEN, D. M., BANKSTON, L. A., BOBKOV, A. A., CADWELL, G. W., JENNINGS, L., CRITCHLEY, D. R., CRAIG, S. W. & LIDDINGTON, R. C. 2004. Structural basis for vinculin activation at sites of cell adhesion. *Nature,* 430**,** 583-6.

BAYS, J. L., PENG, X., TOLBERT, C. E., GUILLUY, C., ANGELL, A. E., PAN, Y., SUPERFINE, R., BURRIDGE, K. & DEMALI, K. A. 2014. Vinculin phosphorylation differentially regulates mechanotransduction at cell-cell and cell-matrix adhesions. *J Cell Biol,* 205**,** 251-63.

BEHRENS, J., VAKAET, L., FRIIS, R., WINTERHAGER, E., VAN ROY, F., MAREEL, M. AND BIRCHMEIER, W., 1993. Loss of epithelial differentiation and gain of invasiveness correlates with tyrosine phosphorylation of the E-cadherin/beta-catenin complex in cells transformed with a temperature-sensitive v-SRC gene. *The Journal of Cell Biology,* 120(3), 757-766.

BELLIS, S. L., MILLER, J. T. & TURNER, C. E. 1995. Characterization of tyrosine phosphorylation of paxillin in vitro by focal adhesion kinase. *J Biol Chem,* 270**,** 17437-41.

BERGSTRALH, D. T., DAWNEY, N. S. & ST JOHNSTON, D. 2017. Spindle orientation: a question of complex positioning. *Development,* 144**,** 1137-1145.

BERRIER, A. L. & YAMADA, K. M. 2007. Cell-matrix adhesion. *J Cell Physiol,* 213**,** 565-73.

BERX, G. & VAN ROY, F. 2001. The E-cadherin/catenin complex: an important gatekeeper in breast cancer tumorigenesis and malignant progression. *Breast Cancer Res,* 3**,** 289-93.

BJERKE, M. A., DZAMBA, B. J., WANG, C. & DESIMONE, D. W. 2014. FAK is required for tension-dependent organization of collective cell movements in Xenopus mesendoderm. *Dev Biol,* 394**,** 340-56.

BOGGON, T. J., MURRAY, J., CHAPPUIS-FLAMENT, S., WONG, E., GUMBINER, B. M. & SHAPIRO, L. 2002. C-cadherin ectodomain structure and implications for cell adhesion mechanisms. *Science,* 296**,** 1308-13.

BOUCAUT, J. C. & DARRIBERE, T. 1983a. Fibronectin in early amphibian embryos. Migrating mesodermal cells contact fibronectin established prior to gastrulation. *Cell Tissue Res,* 234**,** 135-45.

BOUCAUT, J. C. & DARRIBERE, T. 1983b. Presence of fibronectin during early embryogenesis in amphibian Pleurodeles waltlii. *Cell Differ,* 12**,** 77-83.

BRAMI-CHERRIER, K., GERVASI, N., ARSENIEVA, D., WALKIEWICZ, K., BOUTTERIN, M. C., ORTEGA, A., LEONARD, P. G., SEANTIER, B., GASMI, L., BOUCEBA, T., KADARE, G., GIRAULT, J. A. & AROLD, S. T. 2014. FAK dimerization controls its kinase-dependent functions at focal adhesions. *EMBO J,* 33**,** 356-70.

BROWN, M. C., CURTIS, M. S. & TURNER, C. E. 1998a. Paxillin LD motifs may define a new family of protein recognition domains. *Nat Struct Biol,* 5**,** 677-8.

BROWN, M. C., PERROTTA, J. A. & TURNER, C. E. 1998b. Serine and threonine phosphorylation of the paxillin LIM domains regulates paxillin focal adhesion localization and cell adhesion to fibronectin. *Mol Biol Cell,* 9**,** 1803-16.

BROWN, M. C. & TURNER, C. E. 2004. Paxillin: adapting to change. *Physiol Rev,* 84**,** 1315-39.

CALALB, M. B., POLTE, T. R. & HANKS, S. K. 1995. Tyrosine phosphorylation of focal adhesion kinase at sites in the catalytic domain regulates kinase activity: a role for Src family kinases. *Mol Cell Biol,* 15**,** 954-63.

CAMPINHO, P., BEHRNDT, M., RANFT, J., RISLER, T., MINC, N. & HEISENBERG, C. P. 2013. Tension-oriented cell divisions limit anisotropic tissue tension in epithelial spreading during zebrafish epiboly. *Nat Cell Biol,* 15**,** 1405-14.

CANO, A., PEREZ-MORENO, M. A., RODRIGO, I., LOCASCIO, A., BLANCO, M. J., DEL BARRIO, M. G., PORTILLO, F. & NIETO, M. A. 2000. The transcription factor snail controls epithelial-mesenchymal transitions by repressing E-cadherin expression. *Nat Cell Biol,* 2**,** 76-83.

CAPALDO, C. T. & MACARA, I. G. 2007. Depletion of E-cadherin disrupts establishment but not maintenance of cell junctions in Madin-Darby canine kidney epithelial cells. *Mol Biol Cell,* 18**,** 189-200.

CARISEY, A., TSANG, R., GREINER, A. M., NIJENHUIS, N., HEATH, N., NAZGIEWICZ, A., KEMKEMER, R., DERBY, B., SPATZ, J. & BALLESTREM, C. 2013. Vinculin regulates the recruitment and release of core focal adhesion proteins in a force-dependent manner. *Curr Biol,* 23**,** 271-81.

CARMINATI, M., GALLINI, S., PIROVANO, L., ALFIERI, A., BISI, S. & MAPELLI, M. 2016. Concomitant binding of Afadin to LGN and F-actin directs planar spindle orientation. *Nat Struct Mol Biol,* 23**,** 155-63.

CHALMERS, A. D., STRAUSS, B. & PAPALOPULU, N. 2003. Oriented cell divisions asymmetrically segregate aPKC and generate cell fate diversity in the early Xenopus embryo. *Development,* 130**,** 2657-68.

CHEESEMAN, I. M. & DESAI, A. 2008. Molecular architecture of the kinetochore-microtubule interface. *Nat Rev Mol Cell Biol,* 9**,** 33-46.

CHEN, H., CHOUDHURY, D. M. & CRAIG, S. W. 2006. Coincidence of actin filaments and talin is required to activate vinculin. *J Biol Chem,* 281**,** 40389-98.

CHEN, H., COHEN, D. M., CHOUDHURY, D. M., KIOKA, N. & CRAIG, S. W. 2005. Spatial distribution and functional significance of activated vinculin in living cells. *J Cell Biol,* 169**,** 459-70.

COLL, J. L., BEN-ZE'EV, A., EZZELL, R. M., RODRIGUEZ FERNANDEZ, J. L., BARIBAULT, H., OSHIMA, R. G. & ADAMSON, E. D. 1995. Targeted disruption

of vinculin genes in F9 and embryonic stem cells changes cell morphology, adhesion, and locomotion. *Proc Natl Acad Sci U S A,* 92**,** 9161-5.

COLLAZO, A. 1994. Molecular Heterochrony in the Pattern of Fibronectin Expression during Gastrulation in Amphibians. *Evolution,* 48**,** 2037-2045.

CONACCI-SORRELL, M. E., BEN-YEDIDIA, T., SHTUTMAN, M., FEINSTEIN, E., EINAT, P. & BEN-ZE'EV, A. 2002. Nr-CAM is a target gene of the beta-catenin/LEF-1 pathway in melanoma and colon cancer and its expression enhances motility and confers tumorigenesis. *Genes Dev,* 16**,** 2058-72.

CORSI, J. M., ROUER, E., GIRAULT, J. A. & ENSLEN, H. 2006. Organization and post-transcriptional processing of focal adhesion kinase gene. *BMC Genomics,* 7**,** 198.

CRAWFORD, B. D., HENRY, C. A., CLASON, T. A., BECKER, A. L. & HILLE, M. B. 2003. Activity and distribution of paxillin, focal adhesion kinase, and cadherin indicate cooperative roles during zebrafish morphogenesis. *Mol Biol Cell,* 14**,** 3065-81.

CRITCHLEY, D. R. 2000. Focal adhesions - the cytoskeletal connection. *Curr Opin Cell Biol,* 12**,** 133-9.

DANIEL, J. M. & REYNOLDS, A. B. 1995. The tyrosine kinase substrate p120cas binds directly to E-cadherin but not to the adenomatous polyposis coli protein or alpha-catenin. *Mol Cell Biol,* 15**,** 4819-24.

DAVIS, M. A., IRETON, R. C. & REYNOLDS, A. B. 2003. A core function for p120-catenin in cadherin turnover. *J Cell Biol,* 163**,** 525-34.

DELCOMMENNE, M., TAN, C., GRAY, V., RUE, L., WOODGETT, J. & DEDHAR, S. 1998. Phosphoinositide-3-OH kinase-dependent regulation of glycogen synthase kinase 3 and protein kinase B/AKT by the integrin-linked kinase. *Proc Natl Acad Sci U S A,* 95**,** 11211-6.

DERAMAUDT, T. B., DUJARDIN, D., HAMADI, A., NOULET, F., KOLLI, K., DE MEY, J., TAKEDA, K. & RONDE, P. 2011. FAK phosphorylation at Tyr-925 regulates cross-talk between focal adhesion turnover and cell protrusion. *Mol Biol Cell,* 22**,** 964-75.

DESAI, A. & MITCHISON, T. J. 1997. Microtubule polymerization dynamics. *Annu Rev Cell Dev Biol,* 13**,** 83-117.

DI PIETRO, F., ECHARD, A. & MORIN, X. 2016. Regulation of mitotic spindle orientation: an integrated view. *EMBO Rep,* 17**,** 1106-30.

DOHERTY, P. & WALSH, F. S. 1996. CAM-FGF Receptor Interactions: A Model for Axonal Growth. *Mol Cell Neurosci,* 8**,** 99-111.

DUMONT, S. & MITCHISON, T. J. 2009. Force and length in the mitotic spindle. *Curr Biol,* 19**,** R749-61.

FERNANDEZ-MINAN, A., MARTIN-BERMUDO, M. D. & GONZALEZ-REYES, A. 2007. Integrin signaling regulates spindle orientation in Drosophila to preserve the follicular-epithelium monolayer. *Curr Biol,* 17**,** 683-8.

FINK, J., CARPI, N., BETZ, T., BETARD, A., CHEBAH, M., AZIOUNE, A., BORNENS, M., SYKES, C., FETLER, L., CUVELIER, D. & PIEL, M. 2011. External forces control mitotic spindle positioning. *Nat Cell Biol,* 13**,** 771-8.

FISH, J. L., KOSODO, Y., ENARD, W., PAABO, S. & HUTTNER, W. B. 2006. Aspm specifically maintains symmetric proliferative divisions of neuroepithelial cells. *Proc Natl Acad Sci U S A,* 103**,** 10438-10443.

FONAR, Y., GUTKOVICH, Y. E., ROOT, H., MALYAROVA, A., AAMAR, E., GOLUBOVSKAYA, V. M., ELIAS, S., ELKOUBY, Y. M. & FRANK, D. 2011. Focal adhesion kinase protein regulates Wnt3a gene expression to control cell fate specification in the developing neural plate. *Mol Biol Cell,* 22**,** 2409-21.

FUJITA, H., KAMIGUCHI, K., CHO, D., SHIBANUMA, M., MORIMOTO, C. & TACHIBANA, K. 1998. Interaction of Hic-5, A senescence-related protein, with focal adhesion kinase. *J Biol Chem,* 273**,** 26516-21.

FUJITA, Y., KRAUSE, G., SCHEFFNER, M., ZECHNER, D., LEDDY, H. E., BEHRENS, J., SOMMER, T. & BIRCHMEIER, W. 2002. Hakai, a c-Cbl-like protein, ubiquitinates and induces endocytosis of the E-cadherin complex. *Nat Cell Biol,* 4**,** 222-31.

GALBRAITH, C. G., YAMADA, K. M. & SHEETZ, M. P. 2002. The relationship between force and focal complex development. *J Cell Biol,* 159**,** 695-705.

GEIGER, B. 1979. A 130K protein from chicken gizzard: its localization at the termini of microfilament bundles in cultured chicken cells. *Cell,* 18**,** 193-205.

GEIGER, B., BERSHADSKY, A., PANKOV, R. & YAMADA, K. M. 2001. Transmembrane crosstalk between the extracellular matrix--cytoskeleton crosstalk. *Nat Rev Mol Cell Biol,* 2**,** 793-805.

GONZALEZ, C. 2007. Spindle orientation, asymmetric division and tumour suppression in Drosophila stem cells. *Nat Rev Genet,* 8**,** 462-72.

GRASHOFF, C., HOFFMAN, B. D., BRENNER, M. D., ZHOU, R., PARSONS, M., YANG, M. T., MCLEAN, M. A., SLIGAR, S. G., CHEN, C. S., HA, T. & SCHWARTZ, M. A. 2010. Measuring mechanical tension across vinculin reveals regulation of focal adhesion dynamics. *Nature,* 466**,** 263-6.

GRILL, S. W. & HYMAN, A. A. 2005. Spindle positioning by cortical pulling forces. *Dev Cell,* 8**,** 461-5.

GUMBINER, B. M. 1996. Cell adhesion: the molecular basis of tissue architecture and morphogenesis. *Cell,* 84**,** 345-57.

GUMBINER, B. M. 2000. Regulation of cadherin adhesive activity. *J Cell Biol,* 148**,** 399-404.

HAGEL, M., GEORGE, E. L., KIM, A., TAMIMI, R., OPITZ, S. L., TURNER, C. E., IMAMOTO, A. & THOMAS, S. M. 2002. The adaptor protein paxillin is essential for normal development in the mouse and is a critical transducer of fibronectin signaling. *Mol Cell Biol,* 22**,** 901-15.

HAGSTROM, K. A. & MEYER, B. J. 2003. Condensin and cohesin: more than chromosome compactor and glue. *Nat Rev Genet,* 4**,** 520-34.

HANKS, S. K., RYZHOVA, L., SHIN, N. Y. & BRABEK, J. 2003. Focal adhesion kinase signaling activities and their implications in the control of cell survival and motility. *Front Biosci,* 8**,** d982-96.

HANNIGAN, G. E., LEUNG-HAGESTEIJN, C., FITZ-GIBBON, L., COPPOLINO, M. G., RADEVA, G., FILMUS, J., BELL, J. C. & DEDHAR, S. 1996. Regulation of cell adhesion and anchorage-dependent growth by a new beta 1-integrin-linked protein kinase. *Nature,* 379**,** 91-6.

HART, K., TAN, J., SIEMERS, K., SIM, J., PRUITT, B., NELSON, W. AND GLOERICH, M., 2017. E-cadherin and LGN align epithelial cell divisions with tissue tension independently of cell shape. *Proceedings of the National Academy of Sciences*, 114(29), pp.E5845-E5853.

HARTE, M. T., HILDEBRAND, J. D., BURNHAM, M. R., BOUTON, A. H. & PARSONS, J. T. 1996. p130Cas, a substrate associated with v-Src and v-Crk, localizes to focal adhesions and binds to focal adhesion kinase. *J Biol Chem,* 271**,** 13649-55.

HAY, E. D. & ZUK, A. 1995. Transformations between epithelium and mesenchyme: normal, pathological, and experimentally induced. *Am J Kidney Dis,* 26**,** 678-90.

HENS, M. D. & DESIMONE, D. W. 1995. Molecular analysis and developmental expression of the focal adhesion kinase pp125FAK in Xenopus laevis. *Dev Biol,* 170**,** 274-88.

HERTWIG, O. AND HERTWIG, R., 1884. *Untersuchungen Zur Morphologie Und Physiologie Der Zelle*. Jena, 274.

HILDEBRAND, J. D., SCHALLER, M. D. & PARSONS, J. T. 1993. Identification of sequences required for the efficient localization of the focal adhesion kinase, pp125FAK, to cellular focal adhesions. *J Cell Biol,* 123**,** 993-1005.

HIRTH, S., BUHLER, A., BUHRDEL, J. B., RUDECK, S., DAHME, T., ROTTBAUER, W. & JUST, S. 2016. Paxillin and Focal Adhesion Kinase (FAK) Regulate Cardiac Contractility in the Zebrafish Heart. *PLoS One,* 11**,** e0150323.

HOLTFRETER, J., 1943. A study of the mechanics of gastrulation. Part I. *Journal of Experimental Zoology*, 94(3), 261-318.

HONDA, A., NOGAMI, M., YOKOZEKI, T., YAMAZAKI, M., NAKAMURA, H., WATANABE, H., KAWAMOTO, K., NAKAYAMA, K., MORRIS, A. J., FROHMAN, M. A. & KANAHO, Y. 1999. Phosphatidylinositol 4-phosphate 5-kinase alpha is a downstream effector of the small G protein ARF6 in membrane ruffle formation. *Cell,* 99**,** 521-32.

HONDA, H., ODA, H., NAKAMOTO, T., HONDA, Z., SAKAI, R., SUZUKI, T., SAITO, T., NAKAMURA, K., NAKAO, K., ISHIKAWA, T., KATSUKI, M., YAZAKI, Y. & HIRAI, H. 1998. Cardiovascular anomaly, impaired actin bundling and resistance to Src-induced transformation in mice lacking p130Cas. *Nat Genet,* 19**,** 361-5.

HOTCHIN, N. A. & HALL, A. 1995. The assembly of integrin adhesion complexes requires both extracellular matrix and intracellular rho/rac GTPases. *J Cell Biol,* 131**,** 1857-65.

HUMPHRIES, M. J. & NEWHAM, P. 1998. The structure of cell-adhesion molecules. *Trends Cell Biol,* 8**,** 78-83.

HUVENEERS, S., OLDENBURG, J., SPANJAARD, E., VAN DER KROGT, G., GRIGORIEV, I., AKHMANOVA, A., REHMANN, H. & DE ROOIJ, J. 2012. Vinculin associates with endothelial VE-cadherin junctions to control force-dependent remodeling. *J Cell Biol,* 196**,** 641-52.

HYNES, R. O. 1992. Integrins: versatility, modulation, and signaling in cell adhesion. *Cell,* 69**,** 11-25.

HYNES, R. O. 2002. Integrins: bidirectional, allosteric signaling machines. *Cell,* 110**,** 673-87.

ILIC, D., FURUTA, Y., KANAZAWA, S., TAKEDA, N., SOBUE, K., NAKATSUJI, N., NOMURA, S., FUJIMOTO, J., OKADA, M. & YAMAMOTO, T. 1995. Reduced cell motility and enhanced focal adhesion contact formation in cells from FAK-deficient mice. *Nature,* 377**,** 539-44.

ILIC, D., KOVACIC, B., JOHKURA, K., SCHLAEPFER, D. D., TOMASEVIC, N., HAN, Q., KIM, J. B., HOWERTON, K., BAUMBUSCH, C., OGIWARA, N., STREBLOW, D. N., NELSON, J. A., DAZIN, P., SHINO, Y., SASAKI, K. & DAMSKY, C. H. 2004. FAK promotes organization of fibronectin matrix and fibrillar adhesions. *J Cell Sci,* 117**,** 177-87.

IRETON, R. C., DAVIS, M. A., VAN HENGEL, J., MARINER, D. J., BARNES, K., THORESON, M. A., ANASTASIADIS, P. Z., MATRISIAN, L., BUNDY, L. M., SEALY, L., GILBERT, B., VAN ROY, F. & REYNOLDS, A. B. 2002. A novel role for p120 catenin in E-cadherin function. *J Cell Biol,* 159**,** 465-76.

ISLAM, S., CAREY, T. E., WOLF, G. T., WHEELOCK, M. J. & JOHNSON, K. R. 1996. Expression of N-cadherin by human squamous carcinoma cells induces a scattered fibroblastic phenotype with disrupted cell-cell adhesion. *J Cell Biol,* 135**,** 1643-54.

JANOSTIAK, R., PATAKI, A. C., BRABEK, J. & ROSEL, D. 2014. Mechanosensors in integrin signaling: the emerging role of p130Cas. *Eur J Cell Biol,* 93**,** 445-54.

JOHNSON, R. P. & CRAIG, S. W. 1994. An intramolecular association between the head and tail domains of vinculin modulates talin binding. *J Biol Chem,* 269**,** 12611-9.

JOHNSON, R. P. & CRAIG, S. W. 1995. F-actin binding site masked by the intramolecular association of vinculin head and tail domains. *Nature,* 373**,** 261-4.

JOHNSTON, C. A., HIRONO, K., PREHODA, K. E. & DOE, C. Q. 2009. Identification of an Aurora-A/PinsLINKER/Dlg spindle orientation pathway using induced cell polarity in S2 cells. *Cell,* 138**,** 1150-63.

KELLER, R. & DANILCHIK, M. 1988. Regional expression, pattern and timing of convergence and extension during gastrulation of Xenopus laevis. *Development,* 103**,** 193-209.

KELLER, R. E. 1980. The cellular basis of epiboly: an SEM study of deep-cell rearrangement during gastrulation in Xenopus laevis. *J Embryol Exp Morphol,* 60**,** 201-34.

KELLER, R. E. & SCHOENWOLF, G. C. 1977. An SEM study of cellular morphology, contact, and arrangement, as related to gastrulation inXenopus laevis. *Wilehm Roux Arch Dev Biol,* 182**,** 165-186.

KIM, J. B., ISLAM, S., KIM, Y. J., PRUDOFF, R. S., SASS, K. M., WHEELOCK, M. J. & JOHNSON, K. R. 2000. N-Cadherin extracellular repeat 4 mediates epithelial to mesenchymal transition and increased motility. *J Cell Biol,* 151**,** 1193-206.

KIYOMITSU, T. & CHEESEMAN, I. M. 2012. Chromosome- and spindle-pole-derived signals generate an intrinsic code for spindle position and orientation. *Nat Cell Biol,* 14**,** 311-7.

KNOBLICH, J. A. 2010. Asymmetric cell division: recent developments and their implications for tumour biology. *Nat Rev Mol Cell Biol,* 11**,** 849-60.

KORNBERG, L., EARP, H. S., PARSONS, J. T., SCHALLER, M. & JULIANO, R. L. 1992. Cell adhesion or integrin clustering increases phosphorylation of a focal adhesion-associated tyrosine kinase. *J Biol Chem,* 267**,** 23439-42.

KOTAK, S., BUSSO, C. & GONCZY, P. 2012. Cortical dynein is critical for proper spindle positioning in human cells. *J Cell Biol,* 199**,** 97-110.

KRAGTORP, K. A. & MILLER, J. R. 2006. Regulation of somitogenesis by Ena/VASP proteins and FAK during Xenopus development. *Development,* 133**,** 685-95.

KWON, M., BAGONIS, M., DANUSER, G. & PELLMAN, D. 2015. Direct Microtubule-Binding by Myosin-10 Orients Centrosomes toward Retraction Fibers and Subcortical Actin Clouds. *Dev Cell,* 34**,** 323-37.

LAMPUGNANI, M. G., CORADA, M., ANDRIOPOULOU, P., ESSER, S., RISAU, W. & DEJANA, E. 1997. Cell confluence regulates tyrosine phosphorylation of adherens junction components in endothelial cells. *J Cell Sci,* 110 (Pt 17)**,** 2065-77.

LAZARO-DIEGUEZ, F., ISPOLATOV, I. & MUSCH, A. 2015. Cell shape impacts on the positioning of the mitotic spindle with respect to the substratum. *Mol Biol Cell,* 26, 1286 – 1295.

LE DUC, Q., SHI, Q., BLONK, I., SONNENBERG, A., WANG, N., LECKBAND, D. & DE ROOIJ, J. 2010. Vinculin potentiates E-cadherin mechanosensing and is recruited to actin-anchored sites within adherens junctions in a myosin II-dependent manner. *J Cell Biol,* 189**,** 1107-15.

LECHLER, T. & FUCHS, E. 2005. Asymmetric cell divisions promote stratification and differentiation of mammalian skin. *Nature,* 437**,** 275-80.

LEE, G., HYNES, R. & KIRSCHNER, M. 1984. Temporal and spatial regulation of fibronectin in early Xenopus development. *Cell,* 36**,** 729-40.

LEGOFF, L., ROUAULT, H. & LECUIT, T. 2013. A global pattern of mechanical stress polarizes cell divisions and cell shape in the growing Drosophila wing disc. *Development,* 140**,** 4051-9.

LEVINE, M. S. & HOLLAND, A. J. 2018. The impact of mitotic errors on cell proliferation and tumorigenesis. *Genes Dev,* 32**,** 620-638.

LI, F., ZHANG, Y. & WU, C. 1999. Integrin-linked kinase is localized to cell-matrix focal adhesions but not cell-cell adhesion sites and the focal adhesion localization of integrin-linked kinase is regulated by the PINCH-binding ANK repeats. *J Cell Sci,* 112 (Pt 24)**,** 4589-99.

LOPEZ-COLOME, A. M., LEE-RIVERA, I., BENAVIDES-HIDALGO, R. & LOPEZ, E. 2017. Paxillin: a crossroad in pathological cell migration. *J Hematol Oncol,* 10**,** 50.

LU, M. S. & JOHNSTON, C. A. 2013. Molecular pathways regulating mitotic spindle orientation in animal cells. *Development,* 140**,** 1843-56.

MAO, Y., TOURNIER, A. L., BATES, P. A., GALE, J. E., TAPON, N. & THOMPSON, B. J. 2011. Planar polarization of the atypical myosin Dachs orients cell divisions in Drosophila. *Genes Dev,* 25**,** 131-6.

MAO, Y., TOURNIER, A. L., HOPPE, A., KESTER, L., THOMPSON, B. J. & TAPON, N. 2013. Differential proliferation rates generate patterns of mechanical tension that orient tissue growth. *EMBO J,* 32**,** 2790-803.

MARSDEN, M. & DESIMONE, D. W. 2001. Regulation of cell polarity, radial intercalation and epiboly in Xenopus: novel roles for integrin and fibronectin. *Development,* 128**,** 3635-47.

MAYER, B. J., HIRAI, H. & SAKAI, R. 1995. Evidence that SH2 domains promote processive phosphorylation by protein-tyrosine kinases. *Curr Biol,* 5**,** 296-305.

MCINTOSH, J., 2016. Mitosis. *Cold Spring Harbor Perspectives in Biology,* 8(9), 1-16.

MIEDLICH, S. U., TAYA, M., YOUNG, M. R. & HAMMES, S. R. 2017. Paxillin and embryonic PolyAdenylation Binding Protein (ePABP) engage to regulate androgen-dependent Xenopus laevis oocyte maturation - A model of kinase-dependent regulation of protein expression. *Mol Cell Endocrinol,* 448**,** 87-97.

MIERKE, C. T., KOLLMANNSBERGER, P., ZITTERBART, D. P., SMITH, J., FABRY, B. & GOLDMANN, W. H. 2008. Mechano-coupling and regulation of contractility by the vinculin tail domain. *Biophys J,* 94**,** 661-70.

MINC, N., BURGESS, D. & CHANG, F. 2011. Influence of cell geometry on division-plane positioning. *Cell,* 144**,** 414-26.

MIRANTI, C. K. & BRUGGE, J. S. 2002. Sensing the environment: a historical perspective on integrin signal transduction. *Nat Cell Biol,* 4**,** E83-90.

MITCHISON, T. & KIRSCHNER, M. 1984. Dynamic instability of microtubule growth. *Nature,* 312**,** 237-42.

MITCHISON, T. J. & SALMON, E. D. 2001. Mitosis: a history of division. *Nat Cell Biol,* 3**,** E17-21.

MITRA, S. K., HANSON, D. A. & SCHLAEPFER, D. D. 2005. Focal adhesion kinase: in command and control of cell motility. *Nat Rev Mol Cell Biol,* 6**,** 56-68.

MIYAMOTO, S., TERAMOTO, H., COSO, O. A., GUTKIND, J. S., BURBELO, P. D., AKIYAMA, S. K. & YAMADA, K. M. 1995. Integrin function: molecular hierarchies of cytoskeletal and signaling molecules. *J Cell Biol,* 131**,** 791-805.

MOGILNER, A. & CRAIG, E. 2010. Towards a quantitative understanding of mitotic spindle assembly and mechanics. *J Cell Sci,* 123**,** 3435-45.

MORIN, X., JAOUEN, F. & DURBEC, P. 2007. Control of planar divisions by the G-protein regulator LGN maintains progenitors in the chick neuroepithelium. *Nat Neurosci,* 10**,** 1440-8.

NAKATSUJI, N. & JOHNSON, K. E. 1983. Comparative study of extracellular fibrils on the ectodermal layer in gastrulae of five amphibian species. *J Cell Sci,* 59**,** 61-70.

NAKATSUJI, N., SMOLIRA, M. A. & WYLIE, C. C. 1985. Fibronectin visualized by scanning electron microscopy immunocytochemistry on the substratum for cell migration in Xenopus laevis gastrulae. *Dev Biol,* 107**,** 264-8.

NESTOR-BERGMANN, A., GODDARD, G. & WOOLNER, S. 2014. Force and the spindle: mechanical cues in mitotic spindle orientation. *Semin Cell Dev Biol,* 34**,** 133-9.

NIKOLOPOULOS, S. N. & TURNER, C. E. 2000. Actopaxin, a new focal adhesion protein that binds paxillin LD motifs and actin and regulates cell adhesion. *J Cell Biol,* 151**,** 1435-48.

NIKOLOPOULOS, S. N. & TURNER, C. E. 2001. Integrin-linked kinase (ILK) binding to paxillin LD1 motif regulates ILK localization to focal adhesions. *J Biol Chem,* 276**,** 23499-505.

NISHIMURA, T. & TAKEICHI, M. 2009. Remodeling of the adherens junctions during morphogenesis. *Curr Top Dev Biol,* 89**,** 33-54.

NOLLET, F., KOOLS, P. & VAN ROY, F. 2000. Phylogenetic analysis of the cadherin superfamily allows identification of six major subfamilies besides several solitary members. *J Mol Biol,* 299**,** 551-72.

NOVAK, A., HSU, S. C., LEUNG-HAGESTEIJN, C., RADEVA, G., PAPKOFF, J., MONTESANO, R., ROSKELLEY, C., GROSSCHEDL, R. & DEDHAR, S. 1998. Cell adhesion and the integrin-linked kinase regulate the LEF-1 and beta-catenin signaling pathways. *Proc Natl Acad Sci U S A,* 95**,** 4374-9.

O'CONNELL, C. B. & WANG, Y. L. 2000. Mammalian spindle orientation and position respond to changes in cell shape in a dynein-dependent fashion. *Mol Biol Cell,* 11**,** 1765-74.

OKTAY, M., WARY, K. K., DANS, M., BIRGE, R. B. & GIANCOTTI, F. G. 1999. Integrin-mediated activation of focal adhesion kinase is required for signaling to Jun NH2-terminal kinase and progression through the G1 phase of the cell cycle. *J Cell Biol,* 145**,** 1461-9.

OSTERHOUT, J. A., JOSTEN, N., YAMADA, J., PAN, F., WU, S. W., NGUYEN, P. L., PANAGIOTAKOS, G., INOUE, Y. U., EGUSA, S. F., VOLGYI, B., INOUE, T., BLOOMFIELD, S. A., BARRES, B. A., BERSON, D. M., FELDHEIM, D. A. & HUBERMAN, A. D. 2011. Cadherin-6 mediates axon-target matching in a non-image-forming visual circuit. *Neuron,* 71**,** 632-9.

PALACIOS, F., SCHWEITZER, J. K., BOSHANS, R. L. & D'SOUZA-SCHOREY, C. 2002. ARF6-GTP recruits Nm23-H1 to facilitate dynamin-mediated endocytosis during adherens junctions disassembly. *Nat Cell Biol,* 4**,** 929-36.

PANKOV, R., CUKIERMAN, E., KATZ, B. Z., MATSUMOTO, K., LIN, D. C., LIN, S., HAHN, C. & YAMADA, K. M. 2000. Integrin dynamics and matrix assembly: tensin-dependent translocation of alpha(5)beta(1) integrins promotes early fibronectin fibrillogenesis. *J Cell Biol,* 148**,** 1075-90.

PARSONS, J. T. 2003. Focal adhesion kinase: the first ten years. *J Cell Sci,* 116**,** 1409-16.

PATEL, S. D., CIATTO, C., CHEN, C. P., BAHNA, F., RAJEBHOSALE, M., ARKUS, N., SCHIEREN, I., JESSELL, T. M., HONIG, B., PRICE, S. R. & SHAPIRO, L. 2006. Type II cadherin ectodomain structures: implications for classical cadherin specificity. *Cell,* 124**,** 1255-68.

PEASE, J. C. & TIRNAUER, J. S. 2011. Mitotic spindle misorientation in cancer--out of alignment and into the fire. *J Cell Sci,* 124**,** 1007-16.

PETIT, V. & THIERY, J. P. 2000. Focal adhesions: structure and dynamics. *Biol Cell,* 92**,** 477-94.

PETRIDOU, N. I. & SKOURIDES, P. A. 2014. FAK transduces extracellular forces that orient the mitotic spindle and control tissue morphogenesis. *Nat Commun,* 5**,** 5240.

PETRIDOU, N. I. & SKOURIDES, P. A. 2016. A ligand-independent integrin beta1 mechanosensory complex guides spindle orientation. *Nat Commun,* 7**,** 10899.

PETRIDOU, N. I., STYLIANOU, P. & SKOURIDES, P. A. 2013. A dominant-negative provides new insights into FAK regulation and function in early embryonic morphogenesis. *Development,* 140**,** 4266-76.

PEYRE, E., SILVA, C. G. & NGUYEN, L. 2015. Crosstalk between intracellular and extracellular signals regulating interneuron production, migration and integration into the cortex. *Front Cell Neurosci,* 9**,** 129.

POKUTTA, S., HERRENKNECHT, K., KEMLER, R. & ENGEL, J. 1994. Conformational changes of the recombinant extracellular domain of E-cadherin upon calcium binding. *Eur J Biochem,* 223**,** 1019-26.

QUESADA-HERNANDEZ, E., CANEPARO, L., SCHNEIDER, S., WINKLER, S., LIEBLING, M., FRASER, S. E. & HEISENBERG, C. P. 2010. Stereotypical cell division orientation controls neural rod midline formation in zebrafish. *Curr Biol,* 20**,** 1966-72.

QUYN, A. J., APPLETON, P. L., CAREY, F. A., STEELE, R. J., BARKER, N., CLEVERS, H., RIDGWAY, R. A., SANSOM, O. J. & NATHKE, I. S. 2010. Spindle orientation bias in gut epithelial stem cell compartments is lost in precancerous tissue. *Cell Stem Cell,* 6**,** 175-81.

REYNOLDS, A. B., DANIEL, J., MCCREA, P. D., WHEELOCK, M. J., WU, J. & ZHANG, Z. 1994. Identification of a new catenin: the tyrosine kinase substrate p120cas associates with E-cadherin complexes. *Mol Cell Biol,* 14**,** 8333-42.

REYNOLDS, A. B., HERBERT, L., CLEVELAND, J. L., BERG, S. T. & GAUT, J. R. 1992. p120, a novel substrate of protein tyrosine kinase receptors and of p60v-src, is related to cadherin-binding factors beta-catenin, plakoglobin and armadillo. *Oncogene,* 7**,** 2439-45.

RIDLEY, A. J. & HALL, A. 1992. The small GTP-binding protein rho regulates the assembly of focal adhesions and actin stress fibers in response to growth factors. *Cell,* 70**,** 389-99.

RIMM, D. L., KOSLOV, E. R., KEBRIAEI, P., CIANCI, C. D. & MORROW, J. S. 1995. Alpha 1(E)-catenin is an actin-binding and -bundling protein mediating the attachment of F-actin to the membrane adhesion complex. *Proc Natl Acad Sci U S A,* 92**,** 8813-7.

SAKAI, R., IWAMATSU, A., HIRANO, N., OGAWA, S., TANAKA, T., MANO, H., YAZAKI, Y. & HIRAI, H. 1994. A novel signaling molecule, p130, forms stable complexes in vivo with v-Crk and v-Src in a tyrosine phosphorylation-dependent manner. *EMBO J,* 13**,** 3748-56.

SAUNDERS, R. M., HOLT, M. R., JENNINGS, L., SUTTON, D. H., BARSUKOV, I. L., BOBKOV, A., LIDDINGTON, R. C., ADAMSON, E. A., DUNN, G. A. & CRITCHLEY, D. R. 2006. Role of vinculin in regulating focal adhesion turnover. *Eur J Cell Biol,* 85**,** 487-500.

SCHAEFER, M., SHEVCHENKO, A., SHEVCHENKO, A. & KNOBLICH, J. A. 2000. A protein complex containing Inscuteable and the Galpha-binding protein Pins orients asymmetric cell divisions in Drosophila. *Curr Biol,* 10**,** 353-62.

SCHALLER, M. D. 2001. Paxillin: a focal adhesion-associated adaptor protein. *Oncogene,* 20**,** 6459-72.

SCHALLER, M. D., HILDEBRAND, J. D., SHANNON, J. D., FOX, J. W., VINES, R. R. & PARSONS, J. T. 1994. Autophosphorylation of the focal adhesion kinase, pp125FAK, directs SH2-dependent binding of pp60src. *Mol Cell Biol,* 14**,** 1680-8.

SCHALLER, M. D., OTEY, C. A., HILDEBRAND, J. D. & PARSONS, J. T. 1995. Focal adhesion kinase and paxillin bind to peptides mimicking beta integrin cytoplasmic domains. *J Cell Biol,* 130**,** 1181-7.

SCHESWOHL, D. M., HARRELL, J. R., RAJFUR, Z., GAO, G., CAMPBELL, S. L. & SCHALLER, M. D. 2008. Multiple paxillin binding sites regulate FAK function. *J Mol Signal,* 3**,** 1.

SCHLAEPFER, D. D., BROOME, M. A. & HUNTER, T. 1997. Fibronectin-stimulated signaling from a focal adhesion kinase-c-Src complex: involvement of the Grb2, p130cas, and Nck adaptor proteins. *Mol Cell Biol,* 17**,** 1702-13.

SCHLAEPFER, D. D., MITRA, S. K. & ILIC, D. 2004. Control of motile and invasive cell phenotypes by focal adhesion kinase. *Biochim Biophys Acta,* 1692**,** 77-102.

SCHWARTZ, M. A., SCHALLER, M. D. & GINSBERG, M. H. 1995. Integrins: emerging paradigms of signal transduction. *Annu Rev Cell Dev Biol,* 11**,** 549-99.

SCHWOCK, J., DHANI, N., CAO, M. P., ZHENG, J., CLARKSON, R., RADULOVICH, N., NAVAB, R., HORN, L. C. & HEDLEY, D. W. 2009. Targeting focal adhesion kinase with dominant-negative FRNK or Hsp90 inhibitor 17-DMAG suppresses tumor growth and metastasis of SiHa cervical xenografts. *Cancer Res,* 69**,** 4750-9.

SHAKIBA, D., ALISAFAEI, F., SAVADIPOUR, A., ROWE, R., LIU, Z., PRYSE, K., SHENOY, V., ELSON, E. & GENIN, G., 2020. The Balance between Actomyosin Contractility and Microtubule Polymerization Regulates Hierarchical Protrusions That Govern Efficient Fibroblast–Collagen Interactions. *ACS Nano,* 345-65

SHAPIRO, L., FANNON, A. M., KWONG, P. D., THOMPSON, A., LEHMANN, M. S., GRUBEL, G., LEGRAND, J. F., ALS-NIELSEN, J., COLMAN, D. R. & HENDRICKSON, W. A. 1995a. Structural basis of cell-cell adhesion by cadherins. *Nature,* 374**,** 327-37.

SHAPIRO, L., KWONG, P. D., FANNON, A. M., COLMAN, D. R. & HENDRICKSON, W. A. 1995b. Considerations on the folding topology and evolutionary origin of cadherin domains. *Proc Natl Acad Sci U S A,* 92**,** 6793-7.

SHAPIRO, L. & WEIS, W. I. 2009. Structure and biochemistry of cadherins and catenins. *Cold Spring Harb Perspect Biol,* 1**,** a003053.

SHEMESH, T., GEIGER, B., BERSHADSKY, A. D. & KOZLOV, M. M. 2005. Focal adhesions as mechanosensors: a physical mechanism. *Proc Natl Acad Sci U S A,* 102**,** 12383-8.

SHEN, Y. & SCHALLER, M. D. 1999. Focal adhesion targeting: the critical determinant of FAK regulation and substrate phosphorylation. *Mol Biol Cell,* 10**,** 2507-18.

SLACK, J., 2013. *Essential Developmental Biology*. Oxford: Wiley-Blackwell, 11-19, 67-71.

SPRINGER, T. A. & WANG, J. H. 2004. The three-dimensional structure of integrins and their ligands, and conformational regulation of cell adhesion. *Adv Protein Chem,* 68**,** 29-63.

STEINBERG, M. S. 1996. Adhesion in development: an historical overview. *Dev Biol,* 180**,** 377-88.

STYLIANOU, P. & SKOURIDES, P. A. 2009. Imaging morphogenesis, in Xenopus with Quantum Dot nanocrystals. *Mech Dev,* 126**,** 828-41.

SZABÓ, A., COBO, I., OMARA, S., MCLACHLAN, S., KELLER, R., & MAYOR, R. 2016. The Molecular Basis of Radial Intercalation during Tissue Spreading in Early Development. *Developmental Cell,* 37(3), 213–225.

TACHIBANA, K., SATO, T., D'AVIRRO, N. & MORIMOTO, C. 1995. Direct association of pp125FAK with paxillin, the focal adhesion-targeting mechanism of pp125FAK. *J Exp Med,* 182**,** 1089-99.

TAKEICHI, M. 1988. The cadherins: cell-cell adhesion molecules controlling animal morphogenesis. *Development,* 102**,** 639-55.

TAKEICHI, M. 1991. Cadherin cell adhesion receptors as a morphogenetic regulator. *Science,* 251**,** 1451-5.

TAKEICHI, M. 1995. Morphogenetic roles of classic cadherins. *Curr Opin Cell Biol,* 7**,** 619-27.

TAME, M. A., RAAIJMAKERS, J. A., VAN DEN BROEK, B., LINDQVIST, A., JALINK, K. & MEDEMA, R. H. 2014. Astral microtubules control redistribution of dynein at the cell cortex to facilitate spindle positioning. *Cell Cycle,* 13**,** 1162-70.

TEPASS, U., GODT, D. & WINKLBAUER, R. 2002. Cell sorting in animal development: signalling and adhesive mechanisms in the formation of tissue boundaries. *Curr Opin Genet Dev,* 12**,** 572-82.

TEPASS, U., TRUONG, K., GODT, D., IKURA, M. & PEIFER, M. 2000. Cadherins in embryonic and neural morphogenesis. *Nat Rev Mol Cell Biol,* 1**,** 91-100.

THEODOSIOU, M., WIDMAIER, M., BÖTTCHER, R., ROGNONI, E., VEELDERS, M., BHARADWAJ, M., LAMBACHER, A., AUSTEN, K., MÜLLER, D., ZENT, R. AND FÄSSLER, R., 2015. Kindlin-2 cooperates with talin to activate integrins and induces cell spreading by directly binding paxillin. *eLife,* 5.

THERY, M., JIMENEZ-DALMARONI, A., RACINE, V., BORNENS, M. & JULICHER, F. 2007. Experimental and theoretical study of mitotic spindle orientation. *Nature,* 447**,** 493-6.

THERY, M., RACINE, V., PEPIN, A., PIEL, M., CHEN, Y., SIBARITA, J. B. & BORNENS, M. 2005. The extracellular matrix guides the orientation of the cell division axis. *Nat Cell Biol,* 7**,** 947-53.

THOMAS, S. M., HAGEL, M. & TURNER, C. E. 1999b. Characterization of a focal adhesion protein, Hic-5, that shares extensive homology with paxillin. *J Cell Sci,* 112 (Pt 2)**,** 181-90.

THORESON, M. A., ANASTASIADIS, P. Z., DANIEL, J. M., IRETON, R. C., WHEELOCK, M. J., JOHNSON, K. R., HUMMINGBIRD, D. K. & REYNOLDS, A. B. 2000. Selective uncoupling of p120(ctn) from E-cadherin disrupts strong adhesion. *J Cell Biol,* 148**,** 189-202.

TOMINAGA, J., FUKUNAGA, Y., ABELARDO, E. & NAGAFUCHI, A. 2008. Defining the function of beta-catenin tyrosine phosphorylation in cadherin-mediated cell-cell adhesion. *Genes Cells,* 13**,** 67-77.

TOYOSHIMA, F. & NISHIDA, E. 2007. Spindle orientation in animal cell mitosis: roles of integrin in the control of spindle axis. *J Cell Physiol,* 213**,** 407-11.

TOWNES, P. AND HOLTFRETER, J., 1955. Directed movements and selective adhesion of embryonic amphibian cells. *Journal of Experimental Zoology*, 128(1), 53-120.

TSUKITA, S., OISHI, K., AKIYAMA, T., YAMANASHI, Y., YAMAMOTO, T. & TSUKITA, S. 1991. Specific proto-oncogenic tyrosine kinases of src family are enriched in cell-to-cell adherens junctions where the level of tyrosine phosphorylation is elevated. *J Cell Biol,* 113**,** 867-79.

TU, Y., HUANG, Y., ZHANG, Y., HUA, Y. & WU, C. 2001. A new focal adhesion protein that interacts with integrin-linked kinase and regulates cell adhesion and spreading. *J Cell Biol,* 153**,** 585-98.

TU, Y., LI, F., GOICOECHEA, S. & WU, C. 1999. The LIM-only protein PINCH directly interacts with integrin-linked kinase and is recruited to integrin-rich sites in spreading cells. *Mol Cell Biol,* 19**,** 2425-34.

TUMBARELLO, D. A., BROWN, M. C. & TURNER, C. E. 2002. The paxillin LD motifs. *FEBS Lett,* 513**,** 114-8.

TURNER, C. E., GLENNEY, J. R., JR. & BURRIDGE, K. 1990. Paxillin: a new vinculin-binding protein present in focal adhesions. *J Cell Biol,* 111**,** 1059-68.

VOGEL, V. & SHEETZ, M. 2006. Local force and geometry sensing regulate cell functions. *Nat Rev Mol Cell Biol,* 7**,** 265-75.

VOGT, W. 1929c. Gestaltungsanalyse am Amphibienkeim mit Örtlicher Vitalfärbung. *Wilhelm Roux' Archiv für Entwicklungsmechanik der Organismen,* 120**,** 384-706.

VOLBERG, T., GEIGER, B., KAM, Z., PANKOV, R., SIMCHA, I., SABANAY, H., COLL, J. L., ADAMSON, E. & BEN-ZE'EV, A. 1995. Focal adhesion formation by F9 embryonal carcinoma cells after vinculin gene disruption. *J Cell Sci,* 108 (Pt 6)**,** 2253-60.

VOURET-CRAVIARI, V., BOULTER, E., GRALL, D., MATTHEWS, C. & VAN OBBERGHEN-SCHILLING, E. 2004. ILK is required for the assembly of matrix-forming adhesions and capillary morphogenesis in endothelial cells. *J Cell Sci,* 117**,** 4559-69.

WALCZAK, C. E. & HEALD, R. 2008. Mechanisms of mitotic spindle assembly and function. *Int Rev Cytol,* 265**,** 111-58.

WATANABE, T., SATO, K. & KAIBUCHI, K. 2009. Cadherin-mediated intercellular adhesion and signaling cascades involving small GTPases. *Cold Spring Harb Perspect Biol,* 1**,** a003020.

WEBB, D. J., PARSONS, J. T. & HORWITZ, A. F. 2002. Adhesion assembly, disassembly and turnover in migrating cells -- over and over and over again. *Nat Cell Biol,* 4**,** E97-100.

WICKSTROM, S. A., LANGE, A., HESS, M. W., POLLEUX, J., SPATZ, J. P., KRUGER, M., PFALLER, K., LAMBACHER, A., BLOCH, W., MANN, M., HUBER, L. A. & FASSLER, R. 2010. Integrin-linked kinase controls microtubule dynamics required for plasma membrane targeting of caveolae. *Dev Cell,* 19**,** 574-88.

WILLARD, F. S., KIMPLE, R. J., KIMPLE, A. J., JOHNSTON, C. A. & SIDEROVSKI, D. P. 2004. Fluorescence-based assays for RGS box function. *Methods Enzymol,* 389**,** 56-71.

WILLIAMS, S. E. & FUCHS, E. 2013. Oriented divisions, fate decisions. *Curr Opin Cell Biol,* 25**,** 749-58.

WINKLBAUER, R. 1990. Mesodermal cell migration during Xenopus gastrulation. *Dev Biol,* 142**,** 155-68.

WINKLBAUER, R. & KELLER, R. E. 1996. Fibronectin, mesoderm migration, and gastrulation in Xenopus. *Dev Biol,* 177**,** 413-26.

WITTMANN, T., HYMAN, A. & DESAI, A. 2001. The spindle: a dynamic assembly of microtubules and motors. *Nat Cell Biol,* 3**,** E28-34.

WU, C. 2007. Focal adhesion: a focal point in current cell biology and molecular medicine. *Cell Adh Migr,* 1**,** 13-8.

WU, C., KEIGHTLEY, S. Y., LEUNG-HAGESTEIJN, C., RADEVA, G., COPPOLINO, M., GOICOECHEA, S., MCDONALD, J. A. & DEDHAR, S. 1998. Integrin-linked protein kinase regulates fibronectin matrix assembly, E-cadherin expression, and tumorigenicity. *J Biol Chem,* 273**,** 528-36.

XIAO, K., ALLISON, D. F., BUCKLEY, K. M., KOTTKE, M. D., VINCENT, P. A., FAUNDEZ, V. & KOWALCZYK, A. P. 2003. Cellular levels of p120 catenin function as a set point for cadherin expression levels in microvascular endothelial cells. *J Cell Biol,* 163**,** 535-45.

XU, W., BARIBAULT, H. & ADAMSON, E. D. 1998a. Vinculin knockout results in heart and brain defects during embryonic development. *Development,* 125**,** 327-37.

XU, W., COLL, J. L. & ADAMSON, E. D. 1998b. Rescue of the mutant phenotype by reexpression of full-length vinculin in null F9 cells; effects on cell locomotion by domain deleted vinculin. *J Cell Sci,* 111 (Pt 11)**,** 1535-44.

YAMADA, S. & NELSON, W. J. 2007. Synapses: sites of cell recognition, adhesion, and functional specification. *Annu Rev Biochem,* 76**,** 267-94.

YAMADA, S., POKUTTA, S., DREES, F., WEIS, W. I. & NELSON, W. J. 2005. Deconstructing the cadherin-catenin-actin complex. *Cell,* 123**,** 889-901.

YAMAMOTO, H., EHLING, M., KATO, K., KANAI, K., VAN LESSEN, M., FRYE, M., ZEUSCHNER, D., NAKAYAMA, M., VESTWEBER, D. & ADAMS, R. H. 2015.

Integrin beta1 controls VE-cadherin localization and blood vessel stability. *Nat Commun,* 6**,** 6429.

YANO, H., MAZAKI, Y., KUROKAWA, K., HANKS, S. K., MATSUDA, M. & SABE, H. 2004. Roles played by a subset of integrin signaling molecules in cadherin-based cell-cell adhesion. *J Cell Biol,* 166**,** 283-95.

YAP, A. S., NIESSEN, C. M. & GUMBINER, B. M. 1998. The juxtamembrane region of the cadherin cytoplasmic tail supports lateral clustering, adhesive strengthening, and interaction with p120ctn. *J Cell Biol,* 141**,** 779-89.

YU, F., MORIN, X., CAI, Y., YANG, X. & CHIA, W. 2000. Analysis of partner of inscuteable, a novel player of Drosophila asymmetric divisions, reveals two distinct steps in inscuteable apical localization. *Cell,* 100**,** 399-409.

ZAIDEL-BAR, R., COHEN, M., ADDADI, L. & GEIGER, B. 2004. Hierarchical assembly of cell-matrix adhesion complexes. *Biochem Soc Trans,* 32**,** 416-20.

ZAIDEL-BAR, R., ITZKOVITZ, S., MA'AYAN, A., IYENGAR, R. & GEIGER, B. 2007. Functional atlas of the integrin adhesome. *Nat Cell Biol,* 9**,** 858-67.

ZHANG, C., MILLER, D. J., GUIBAO, C. D., DONATO, D. M., HANKS, S. K. & ZHENG, J. J. 2017. Structural and functional insights into the interaction between the Cas family scaffolding protein p130Cas and the focal adhesion-associated protein paxillin. *J Biol Chem,* 292**,** 18281-18289.

ZHANG, X., JIANG, G., CAI, Y., MONKLEY, S. J., CRITCHLEY, D. R. & SHEETZ, M. P. 2008. Talin depletion reveals independence of initial cell spreading from integrin activation and traction. *Nat Cell Biol,* 10**,** 1062-8.

ZHENG, Z., WAN, Q., LIU, J., ZHU, H., CHU, X. & DU, Q. 2013. Evidence for dynein and astral microtubule-mediated cortical release and transport of Galphai/LGN/NuMA complex in mitotic cells. *Mol Biol Cell,* 24**,** 901-13.

ZHENG, Z., ZHU, H., WAN, Q., LIU, J., XIAO, Z., SIDEROVSKI, D. P. & DU, Q. 2010. LGN regulates mitotic spindle orientation during epithelial morphogenesis. *J Cell Biol,* 189**,** 275-88.

ZHU, L., LIU, H., LU, F., YANG, J., BYZOVA, T. AND QIN, J., 2019. Structural Basis of Paxillin Recruitment by Kindlin-2 in Regulating Cell Adhesion. *Structure*, 27(11),1686-1697.e5.

ZIEGLER, W. H., LIDDINGTON, R. C. & CRITCHLEY, D. R. 2006. The structure and regulation of vinculin. *Trends Cell Biol,* 16**,** 453-60.